11-30-2011

Balancing Dynamic Strength of Spur Gears Cut by Pinion Cutter Operated at Extended Center Distance

John Benton Wade

BALANCING DYNAMIC STRENGTH OF SPUR GEARS CUT BY PINION CUTTER OPERATED AT EXTENDED CENTER DISTANCE

by

John Benton Wade

A Thesis

Submitted in Partial Fulfillment of the

Requirements for the Degree of

Master of Science

Major: Mechanical Engineering

The University of Memphis

December 2011

Acknowledgements

I would like to thank my advisor, Dr. Hsiang Hsi Lin, for his technical support and guidance throughout the educational and research process. I would also like to thank the faculty of the Mechanical Engineering Department at the University of Memphis for their encouragement of curiosity, learning, and advancement of education at the graduate level.

I would also like to thank my family for their encouragement and support in my academic pursuits, and especially my wife, Kimberly.

Abstract

Wade, John Benton. M.S. The University of Memphis. December/2011. "Balancing Dynamic Strength of Spur Gears Cut by Pinion Cutter Operated at Extended Center Distance." Major Professor: Hsiang H. Lin, Ph.D.

This thesis report presents a design problem on the study of dynamic properties in a spur gear system. The system consists of two in-line spur gears, defined as pinion and gear, both cut by a pinion cutter, operated at a center distance greater than standard. The design problem is based upon the published literature. In this study, the dynamic model is created in the computer program Dynamic Analysis of Spur Gear Transmissions (DANST). The program solution contains several outputs. The primary output of concern is the stress at the root of the tooth due to bending caused by the tangential component of the tooth load. The model is optimized by minimizing the difference in stress between the pinion and gear. This optimization occurs for a pinion offset less than the static optimization of the stress.

Table of Contents

List of Tables

List of Figures

List of Terminology

A_c'.....Point of origin of the radius of the tooth tip curve of the pinion cutter, see figure 11 (Colbourne, 1987, pp. 133-136)

A_{hc} .....Point where pinion cutter involute profile curve meets the tooth tip curve of the pinion cutter, see figure 11 (Colbourne, 1987, pp. 133-136)

A_i .....“Cross sectional area of segment i” (Lin & Liou, 1998, p. 15)

B.....Backlash (Rogers, Mabie, & Reinholtz, 1990, pp. 623-625)

[C] .....“Global damping matrix” (Macdonald, 2007, pp. 73-75)

C.....Standard center distance between gears (Green & Mabie, 1980a, p. 491)

c.....“Tooth clearance” (American Gear Manufacturers Association, 1974; Green & Mabie, 1980a, p. 495; Mabie & Reinholtz, 1987, p. 147)

C' .....Operating center distance between gears (Green & Mabie, 1980a, p. 496)

C_c.....Center distance given by operating cutting pressure angle of pinion cutter (Colbourne, 1987, pp. 120-121)

C_{Gg}.....Damping coefficient of gear tooth mesh, lb-sec (Lin, Huston, & Coy, 1987, p. 2)

CR .....Contact ratio (Lin & Liou, 1998, p. 24)

C_S .....Damping coefficient of shaft, in-lb-sec (Lin et al., 1987, p. 2)

C_{sg} .....Standard center distance between gear and pinion cutter (Green & Mabie, 1980b, p. 507)

d_g .....Vertical height of the gear tooth, see figures 9 and 10 (Green & Mabie, 1980a, p. 499)

D_g .....Diameter of gear (Green & Mabie, 1980b, pp. 507-508)

E .....Young's modulus (Oswald, Lin, & Delgado, 1996b, p. 2)

e_g .....Pinion offset from gear (Green & Mabie, 1980b, pp. 491-492; Mabie & Reinholtz, 1987, pp. 187-188)

$_dE$.....“Deflection of gear teeth at contact point” (Lin & Liou, p. 23)

E_e.....“Effective Young's modulus of elasticity” (Lin & Liou, 1998, p. 14)

E_g.....Young's modulus for a given gear (Lin & Liou, 1998, p. 20)

$_pE$.....“Tooth profile error” (Lin & Liou, 1998, p. 23)

$_sE$ .....“Tooth spacing error” (Lin & Liou, 1998, p. 23)

E_t^k.....Total transmission error (Lin & Liou, 1998, pp. 23-24)

{F} .....“Global load vector” (Macdonald, 2007, pp. 73-75)

f .....“Average coefficient of friction” (Buckingham, 1949)

f_a .....“Average coefficient of friction of approach” (Buckingham, 1949)

F_{ng}.....Load normal to tooth, also defined as “W” (Green & Mabie, 1980a, p. 497)

f_r .....“Average coefficient of recess” (Buckingham, 1949)

F_{tg} .....Horizontal component of load normal to tooth, F_n (Green & Mabie, 1980a, p. 497)

F_w .....Gear face width (Oswald et al., 1996b, p. 2)

G.....Shear modulus (Lin & Liou, 1998, p. 15)

h_g .....Horizontal thickness of the gear tooth, see figures 9 and 10 (Green & Mabie, 1980a, p. 499)

h_t.....Depth of cut (Green & Mabie, 1980b, p. 509)

I_i .....“Moment of inertia of segment I” (Lin & Liou, 1998, p. 14)

J_L .....Polar moment of inertia of load, in-lb-sec^2 (Lin et al., 1987, p. 2)

J_M.....Polar moment of inertia of motor, in-lb-sec^2 (Lin et al., 1987, p. 2)

J_g.....Polar moment of inertia of gear in-lb-sec^2 (Lin et al., 1987 p. 2)

[K].....“Global stiffness matrix” (Macdonald, 2007, pp. 73-75)

$(K_G)_{avg}$ .....Average tooth stiffness, see figure 16 (Lin & Liou, 1998, pp. 20-21)

$(K_G)_i$ .....Stiffness for each segment, see figure 16 (Lin & Liou, 1998, pp. 20-21)

k_t.....Factor for tooth type (Green & Mabie, 1980a, p. 495)

k.....“Mating tooth pairs in sequence” (Lin & Liou, 1998, p. 23)

K_d .....Dynamic factor, also referred to as dynamic load factor (Lin et al., 1987, p. 3)

K_g .....Stiffness of gear tooth, in-lb/rad (Lin et al., 1987, p. 3)

K_s.....Stiffness of shaft, in-lb/rad (Lin et al., 1987, p. 3)

L_{ij}.....“The distance from j to i” (Lin & Liou, 1998, p. 14)

M_{ij} .....Bending moment relating do deflection under applied load (Lin & Liou, 1998, pp. 14-15)

[M] .....“Global mass matrix” (Macdonald, 2007, pp. 73-75)

N.....“Speed of driving gear” in revolutions per unit time (Lin & Liou, 1998, p. 12)

N_c .....Number of teeth of the pinion cutter (Green & Mabie, 1980a, p. 493)

N_g .....Number of teeth of the gear (Green & Mabie, 1980a, p. 493)

P .....P = 0 for k = 1 or P = 1 if $k \neq 1$ (Lin & Liou, 1998, p. 23)

p_b .....“Base pitch” (Green & Mabie, 1980b, p. 508)

P_d.....Diametral pitch (Mabie & Reinholtz, 1987, p. 143)

P_s .....Standard circular pitch (Colbourne, 1987, pp. 39-40)

q_f.....Total deflection of tooth fillet, see figure 16 (Lin & Liou, 1998, p. 18)

q_{fb} .....“Deflection at and in the direction of load due to beam compliance of fillet” (Lin & Liou, 1998, p. 18)

q_{fe} .....“Deflection due to foundation effects” (Lin & Liou, 1998, p. 18)

q_l.....Cumulative deflection due to loading, moment and shear (Lin & Liou, 1998, pp. 15-16)

q_L.....Local deflection due to contact along line of action, see figure 16 (Lin & Liou, 1998, p. 20; Tavakoli & Houser, 1985, pp. 529-535)

q_M .....Deflection due to moment, see figure 16 (Lin & Liou, pp. 14-20)

q_s .....Deflection due to shear, see figure 16 (Lin & Liou, 1998, p. 15)

q_T.....Total deflection due to applied load, bending moment, and contact deflection, see figure 16 (Lin & Liou, 1998, pp. 20-21)

q_W.....Deflection due to applied load, see figure 16 (Lin & Liou, 1998, pp. 14-15)

R.....Polar coordinate where point A_c on the pinion cutter meets the gear, see figure 12 (Colbourne, 1987, p. 223)

R_0.....Length relationship between “two cutting pitch circles” (Colbourne, 1987, p. 237)

R_{0c} .....Outer radius of the pinion cutter (Green & Mabie, 1980a, p. 495)

R_{0g}' .....Operating outside gear radius (Green & Mabie, 1980b, p. 509)

R_a.....Pitch radius at a given tooth thickness, t_a, see figure 3 (Mabie & Reinholtz, 1987, p. 133)

R_{bc} .....Base circle of pinion cutter (Colbourne, 1987, pp. 133-136)

R_{bg} .....Base radius of gear, in (Green & Mabie, 1980b, p. 508)

R_c.....Radius of pinion cutter (Green & Mabie, 1980a, p. 492)

R_c'.....Operating radius of pinion cutter

R_{cc}'.....Radius of cutting pitch circle of pinion cutter relative to gear (Colbourne, 1987, pp. 118-119)

RCEG.....“Cutter edge radius ratio” (Oswald et al., 1996b, p. 2)

R_{Cg}.....“Radius of curvature of gear” at “any radius of gear tooth profile” (Lin & Liou, 1998, p. 11)

r_{cT} .....Radius of curvature of pinion cutter tooth tip (Colbourne, 1987, pp. 133-136)

R_{dg}' .....Operating gear dedendum radius (Green & Mabie, 1980b, p.509)

r_f .....“Fillet radius”, also see ρ_f (Lin & Liou, 1998, p. 45)

r_g.....“Any radius of gear tooth profile” (Lin & Liou, 1998, p. 11)

R_g.....Standard radius of gear (Green & Mabie, 1980a, p. 492)

R_g'.....Operating pitch radius (Green & Mabie, 1980a, p. 496 and Oswald, Lin, & Delgado, 1996a)

R_{gg} .....Gear generating pitch radius (Green & Mabie, 1980b, p. 508)

R_{hc} .....“Polar coordinate of A_{hc},” see figure 11 (Colbourne, 1987, pp. 133-136)

R_{pg} .....Pitch radius of gear, in (Colbourne, 1987, p. 26)

R_{Tc}' .....Polar coordinate of A_c', see figure 11 (Colbourne, 1987, pp. 133-136)

s.....Relationship between points A_c' and A_c, see figure 12 (Colbourne, 1987, pp. 221-222)

s' .....Relationship between points A_c' and A_c, see figure 12 (Colbourne, 1987, pp. 221-222)

S_g .....Stress factor, see figures 9 and 10 (Green & Mabie, 1980a, p. 499)

t_a .....Tooth thickness at a given pitch radius, R_a, see figure 3 (Mabie & Reinholtz, 1987, p. 133)

t_{ag} .....Gear tooth thickness at addendum or top of gear (Green & Mabie, 1980a, p. 496)

t_c .....Tooth thickness of pinion cutter at standard pitch radius (Mabie & Green, 1980a, p. 493)

t_{dg} .....Tooth thickness of gear at dedendum radius (Green & Mabie, 1980a, p. 499)

T_f .....Friction in approach and recess, see figure 5 (Buckingham, 1949; Lin & Liou, 1998, pp. 24-26)

T_{f1} .....Torque on gear 1, or driving pinion, in-lb (Lin et al., 1987, p. 3)

T_{f2} .....Torque on gear 2, or driven gear, in-lb (Lin et al., 1987, p. 3)

t_g' .....Tooth thickness of gear on operating pitch radius (Green & Mabie, 1980a, p. 494)

t_{gg} .....Tooth thickness of gear on gear generating pitch radius (Green & Mabie, p. 509)

T_i .....“Thickness of segment i” (Lin & Liou, 1998, p. 14)

T_L .....Torque on load, in-lb (Lin et al., 1987, p. 3)

T_M .....Torque on motor, in-lb (Lin et al., 1987, p. 3)

t_{sg} .....Tooth thickness of gear at standard pitch radius (Colbourne, 1987, p. 151)

u.....0.25 (Heywood, 1952)

{U}....."Global displacement vector" (Macdonald, 2007, pp. 73-75)

$\{\dot{U}\}$.....Global velocity vector (Macdonald, 2007, pp. 73-75)

$\{\ddot{U}\}$.....Global acceleration vector (Macdonald, 2007, pp. 73-75)

V....."Pitch-line velocity of gears" (Lin & Liou, 1998, p. 12)

V_0 ....."Initial . . . value of angular . . . velocity" in dynamic equations of motion iteration (Lin & Liou, 1998, pp. 38-39)

V_n ....."Calculated value of angular . . . velocity" in dynamic equations of motion iteration (Lin & Liou, 1998, pp. 38-39)

V_s....."Sliding velocity" (Lin & Liou, 1998, p. 12)

W, W_j .....Applied load, lb, also defined as "F_{ng}" (Lin et al., 1987, p. 3; Lin & Liou, 1998, p. 14)

W_{dg}.....Dynamic load on the given gear tooth (Lin & Liou, 1998, pp. 38-40)

X_{ag}.....Vertical length from the gear center to tip of the gear tooth, see figures 9 and 10 (Green & Mabie, 1980a, p. 499)

x_c', y_c'....."Cartesian coordinate . . . of point A_c' ," see figure 11 (Colbourne, 1987, pp. 133-136)

X_0 ....."Initial . . . value of angular displacement" in dynamic equations of motion iteration (Lin & Liou, 1998, pp. 38-39)

X_{dg}.....Vertical length from the gear center to the bottom of the gear tooth, see figures 9 and 10 (Green & Mabie, 1980a, p. 499)

X_n ....."Calculated value of angular displacement" in dynamic equations of motion iteration (Lin & Liou, 1998, pp. 38-39)

α_f.....Angle between A_c' and the "line of centers," see figure 12 (Colbourne, 1987, p. 221).

α_g .....See figure 8 (Green & Mabie, 1980b, p.509)

β_{ct}.....“Angle . . . through which the [pinion cutter] tooth center-line” turns, see figure 12 (Colbourne, 1987, p. 223)

β_g .....“Angle of application . . . of the normal tooth load F_n,” see figure 8 (Green & Mabie, 1980b, p.509)

β_{gt} .....“Angle . . . through which the [gear] tooth center-line” turns, see figure 12 (Colbourne, 1987, p. 223)

β_j.....“Load angle” (Lin & Liou, 1998, p. 45)

γ_a.....Half circular angle of curvature, radians or degrees depending upon use

γ_f.....“The fillet angle” shown in figure 17 (Cornell & Westervelt, 1978, pp. 69-76; Lin & Liou, 1998, p.)

γ_{hc} .....“Angle . . . with the tooth center-line . . . tangent to the tooth profile at A_{hc},” see figure 11 (Colbourne, 1987, pp. 133-136)

γ_s.....See figure 19 (Lin & Liou, 1998, pp. 43-46)

ζ, η.....Coordinates of point A_c, see figure 12 (Colbourne, 1987, pp. 221-222)

ζ', η' .....Coordinates of point A_c', see figure 12 (Colbourne, 1987, pp. 221-222)

θ.....Angular displacement, rad (Lin et al., 1987, p. 3)

$\dot{\theta}$ .....Angular velocity, rad/sec (Lin et al., 1987, p. 3)

$\ddot{\theta}$ .....Angular acceleration, rad/sec^2 (Lin et al., 1987, p. 3)

θ_a .....Circular angle of curvature, radians

θ_c'.....Polar coordinate of x_c', y_c', see figure 11 (Colbourne, 1987, pp. 133-136)

θ_g .....Angle relating to base of the gear tooth, see figures 9 and 10 (Green & Mabie, 1980a, p. 499)

θ_{hc} .....“Polar coordinate of A_{hc},” see figure 11 (Colbourne, 1987, pp. 133-136)

θ_R.....Polar coordinate where point A_c on the pinion cutter meets the gear, see figure 12 (Colbourne, 1987, p. 223)

ν.....Poisson’s ratio (Oswald et al., 1996b, p. 2)

ξ_{Gg} .....Gear damping ratio (Lin & Liou, 1998, p. 41)

ξ_S .....Shaft damping ratio (Lin & Liou, 1998, p. 41)

π.....Pi

ρ_f.....“Magnitude . . . of the radius of curvature,” also see r_f (Colbourne, 1987, p. 237)

σ_j.....Dynamic stress as calculated in equation 117, see figure 19 (Cornell, 1981, pp. 447-459; Heywood, 1952; Lin & Liou, 1998, pp. 43-46)

σ_{sg}.....Static stress due to bending at the base of the gear tooth (Green & Mabie, 1980a, pp. 497-499)

φ_c.....Standard cutting pressure angle of pinion cutter, or general cutting pressure angle (Green & Mabie, 1980a, pp. 491-492)

φ_c' .....Operating cutting pressure angle of pinion cutter (Colbourne, 1987, p. 120)

φ_{dg}.....See figure 9 (Green & Mabie, 1980a, p. 499)

φ_{hc}.....“Profile angle of A_{hc},” see figure 11 (Colbourne, 1987, pp. 133-136)

φ_g' .....Operating pressure angle between gears (Green & Mabie, 1980a, p. 506; Oswald et al., 1996a)

φ_{gg}.....Gear generating pressure angle (Green & Mabie, 1980b, 508)

φ_{m} .....Angle pertinent to cutting of gear, see figure 12 (Colbourne, 1987, pp. 222, 235)

ψ_{g}.....See figure 8 (Green & Mabie, 1980b, p.509)

ω_{g}.....Speed of gear or angular velocity of the gear in radians per unit time (Lin & Liou, 1998, p. 12)

Chapter 1

Introduction

1.1. Background and Motivation

Standardization of gear design and components allow for ease of mass production, use, and service. Having standard dimensions and designs of gears simplifies the engineering and allows the production of a key component of society to be produced on a massive scale. However, components which are standardized sacrifice optimization gained through individual component customization. Aerospace and automotive industries require large numbers of nonstandard gear designs optimized for specific uses, which in turn makes mass production of nonstandard gear designs a necessity. Conversely, the process of design customization of nonstandard designs increases the cost of manufacture, use, and serviceability. Thus, it is important that the engineer weigh the necessity of the design optimization with the cost of the customization.

For example, a gear pair could be required to operate at a center-to-center distance greater than the standard design establishes. Dynamic affects can also necessitate nonstandard gear designs. Oswald, Townsend, Rebbechi, and Lin (1996) explain that dynamic affects generate helicopter cabin noise known to "exceed 100 decibels." In addition to causing excessive cabin noise, these dynamic effects also cause fatigue and wear and have resulted in relative overdesign of parts and components. Such overdesigns, disadvantages, and dynamic effects can negatively impact use (p. 1).

There are several types of nonstandard gear designs, depending upon the type of gear. As shown by Dudley (1984), there are many techniques for making gears: shaping with a cutter, hobbing, milling, shaving, grinding, broaching, punching, casting, and

forming. In this study, shaping with a pinion cutter is the method used (pp. 5.1-5.4). As explained by Mabie and Reinholtz (1987), using a pinion cutter to create nonstandard designs has the effect of changing certain key dimensions such as the pressure angle, center distance, and tooth profile. The nonstandard design used in this study is the modification of the center distance by withdrawing the pinion cutter a distance, e_g, from the pinion or gear (referred to as pinion offset, e_1, or gear offset, e_2, for the remainder of this study). This design is called the "extended center distance" method (pp. 171-172, 188).

As Lin, Liou, Oswald, and Townsend (1996) explain, the dynamic effects should be accounted for, especially in "the design of high speed gears." Their study of nonstandard gear designs cut by a hob cutter is carried to this study in the use of the pinion cutter (p. 2). As part of quantifying the dynamic effects, this study also explores the static effects, theories, designs, and limitations. According to several recently published works as reviewed by Lin and Liou (1998), the assumptions made for a static analysis are ideal conditions, and do not take into account dynamic affects which amplify the stress at the root of the tooth (p. 1).

A nonstandard design can also be used to balance the dynamic stresses in a gear assembly. Though different stress categories exist, it is the stress at the root of the tooth that is balanced in the study that follows. As explained by Mabie, Walsh, and Bateman (1983), this dynamic stress considered is due to the moment caused by the tangential component of the normal load (p. 188). Balancing the dynamic stress at the root of the tooth optimizes the life and service of the gear assembly.

1.2. Literature Review

The following timeline of dynamic gear design development was provided by Lin and Liou (1998). Under the auspices of the American Society of Mechanical Engineers (ASME), dynamic gear studies began in the early 20th century with Lewis and Buckingham, investigating the dynamic effects caused by teeth of gears in mesh and associated meshing errors (Buckingham, 1931). As dynamic modeling and studies progressed, models were developed involving simplifying the gear teeth into spring and mass models with "constant stiffness" and "time varying stiffness" (Cloutier & Tordion, 1962; Gregory, Harris, & Munro, 1964; Lin & Liou, 1998, pp. 1-3; Tupin, 1953). Dynamic studies involving the effects of contact, tooth motion, and the "nonlinearity of the tooth pair stiffness" were developed in the third quarter of the 20th century (Cornell & Westervelt, 1978; Lin & Liou, 1998, pp. 1-3; Richardson, 1958). With the development of finite element analysis, "lumped mass models," and the "transfer matrix method," additional dynamic model types became available. The next steps in dynamic study of the gear system involved separate components such as the shaft (Hamad & Seireg, 1980; Lin & Liou, 1998, pp. 1-3), dynamic vibrational effects (Iida, Tamura, Kikuchi, & Agata, 1980; Lin & Liou, 1998, pp. 1-3), "mass unbalance," and "periodic variation of mesh stiffness and profile errors" (Iwatsubo, Arii, & Kawai, 1984a; Iwatsubo et al., 1984b; Lin & Liou, 1998, pp. 1-3). With the advent of the computer in the late twentieth century, complex calculations could be carried out in computing facilities, allowing the expansion of the separate modeling types (Lin & Liou, 1998).

The study that follows incorporates a dynamic model utilized by Oswald, Lin, and Delgado (1996b). The dynamic model is part of a computer program called the Dynamic

Analysis of Spur Gear Transmissions (referred to as DANST in the report that follows) (p. 1). The DANST program was coded and written for FORTRAN-90 for this study (Microsoft, 1995, computer software). The DANST program was one of a set of computer programs including the Gear Dynamic Analysis Program (GEARDYN) (Boyd & Pike, 1987) and GRD (Kahraman et al., 1990) that model dynamic effects within the spur gear system (Lim & Singh, 1989). The dynamic concepts and theory used within DANST were developed from static design theory of gears cut by a pinion cutter (Green & Mabie, 1980a; Green & Mabie, 1980b; Rogers, Mabie, & Reinholtz, 1990). Several published works exist upon the DANST program and its applications. A series of studies were successfully performed to compare the DANST modeling capabilities to an experimental testing rig developed by the National Aeronautics and Space Administration (NASA) and U.S. Army Research Laboratory (Oswald & Townsend et al., 1996; Oswald, Rebbechi, Zakrajsek, Townsend, & Lin, 1991). A finite element model was developed for comparison to the DANST program using load factoring (Oswald, Lin, Liou, & Valco, 1993). Other published works cover dynamic effects including contact ratio, profile modification, and bearing and shaft connections (Lin, Huston, & Coy, 1987; Lin & Liou, 1998).

1.3. Purpose and Objective

The primary objective of this study is to create a dynamic model of spur gears cut by pinion cutter where the stress at the root of the tooth is equalized. The design problem is based upon on a set of published design examples (Green & Mabie, 1980a; Green & Mabie, 1980b; Lin et al., 1996; Oswald et al., 1996b; Rogers et al., 1990). As stated in the literature review, this dynamic model makes use of the DANST program as

developed by Oswald, Lin, and Delgado (1996a). A comparative static model is written in FORTRAN-90 code (Microsoft, 1995, computer software). The static model program is based upon the works of Green and Mabie (1980b) through a published design example and static stress optimization solution (pp. 507-514). In addition, the works of Colbourne (1987) are incorporated in a concurrent study and assumption of tooth fillet radii (pp. 39-40, 120-121, 133-136, 151, 221-223, 235-237). The study that follows is meant to directly compare with the work of Lin, Liou, Oswald, and Townsend (1996) who performed a dynamic study of a gear pair cut by hob cutters (p. 1). By optimization of the offset to produce equal dynamic stress at the root of the tooth, a gear system cut by pinion cutter can be chosen which balances a series of parameters for increased service life and use.

Chapter 2

Gear Design

2.1. Review of Gear Fundamentals

Mabie and Reinholtz (1987) summarize that a set of gears is roughly equivalent to two pulleys connected by a belt. Two pulleys will operate at the same constant velocity relative to their dimensions, so long as the belt does not slip. Gears, which operate on a similar principle, are subject to the same relationship, see equation 1. Figure 1 shows the dimensions of this gear system, which includes the pitch point, P, base circle, and involute pressure angle, φ. The forces between the gears are also related as they are equal and opposite as shown in figure 2 (pp. 128-131).

$$\frac{\omega_1}{\omega_2} = \frac{D_1}{D_2} = \frac{N_1}{N_2} \qquad \text{EQ. 1}$$

As shown by Mabie and Reinholtz (1987), the shape of a gear tooth is subject to certain base equations. Using figure 3 and figure 4 as guides it is possible to determine "the involute pressure angle at any . . . radius on the involute," as seen in equation 2. Moreover, by the same figure, "it is possible to calculate the tooth thickness at any point on the involute, given the thickness at some other point" as seen in equation 3 (pp. 132-134).

$$\mathrm{COS}\ \varphi_B = \frac{R_A}{R_B} * \mathrm{COS}\ \varphi_A \qquad \text{EQ. 2}$$

$$t_B = 2 * R_B * \left[\frac{t_A}{2 * R_A} + \text{INV}\,\varphi_A - \text{INV}\,\varphi_B\right] \quad \text{EQ. 3}$$

In equation 3, the involute function, or "INV," is as follows in equation 4, where φ must be in radians (Mabie & Reinholtz, 1987, p. 134).

$$\text{INV}\,\varphi = \text{TAN}\,\varphi - \varphi \quad \text{EQ. 4}$$

As explained by Mabie and Reinholtz (1987), a gear pair meshes along the "line of action." During the course of this movement, between points A and B as seen on figure 5, there may be one, or more than one, tooth pair in contact. In terms of gear design, the contact ratio is the "the ratio of the arc of action to the circular pitch." This contact ratio is commonly defined as the "average number of teeth in contact" (pp. 135-137), or "the angle through which a gear rotates during one mesh cycle" divided by "the angle subtended at the gear center by one tooth" (Colbourne, 1987, p. 83).

Also as seen in figure 5, the pressure angle is known as the "pressure angle of the two gears in mesh" as it is where the "pressure angle of the gears in mesh and the involute pressure angles of the two involutes in contact at the pitch point [P are] equal" (Mabie & Reinholtz, 1987, p, 137).

Dudley (1984) defines shaping as "a gear-cutting method in which the cutting tool is shaped like a pinion. The shaper cuts while traversing across the face width and rolling with the gear blank at the same time," see figure 6 as a reference. Though generating a gear with a pinion cutter can result in a nonstandard design, it is a fairly common type of "rotating and reciprocating tool" (pp. 5.1-5.4).

As introduced in the previous chapter, Mabie and Reinholtz (1987), describe the "extended center distance" method as withdrawing the pinion cutter a distance, e_g, from the gear blank. This has the general effect of changing the shape of the tooth and increasing the gear body as shown in figure 7 (pp. 171-172).

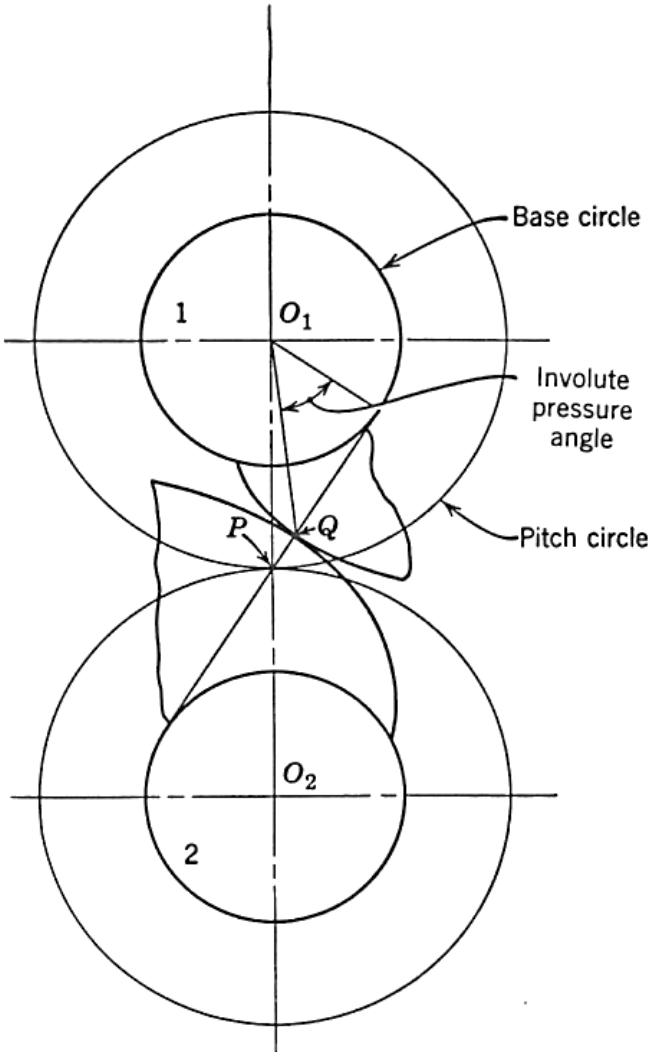

Figure 1. Base dimensions of a gear assembly (Mabie & Reinholtz, 1987, p. 131).

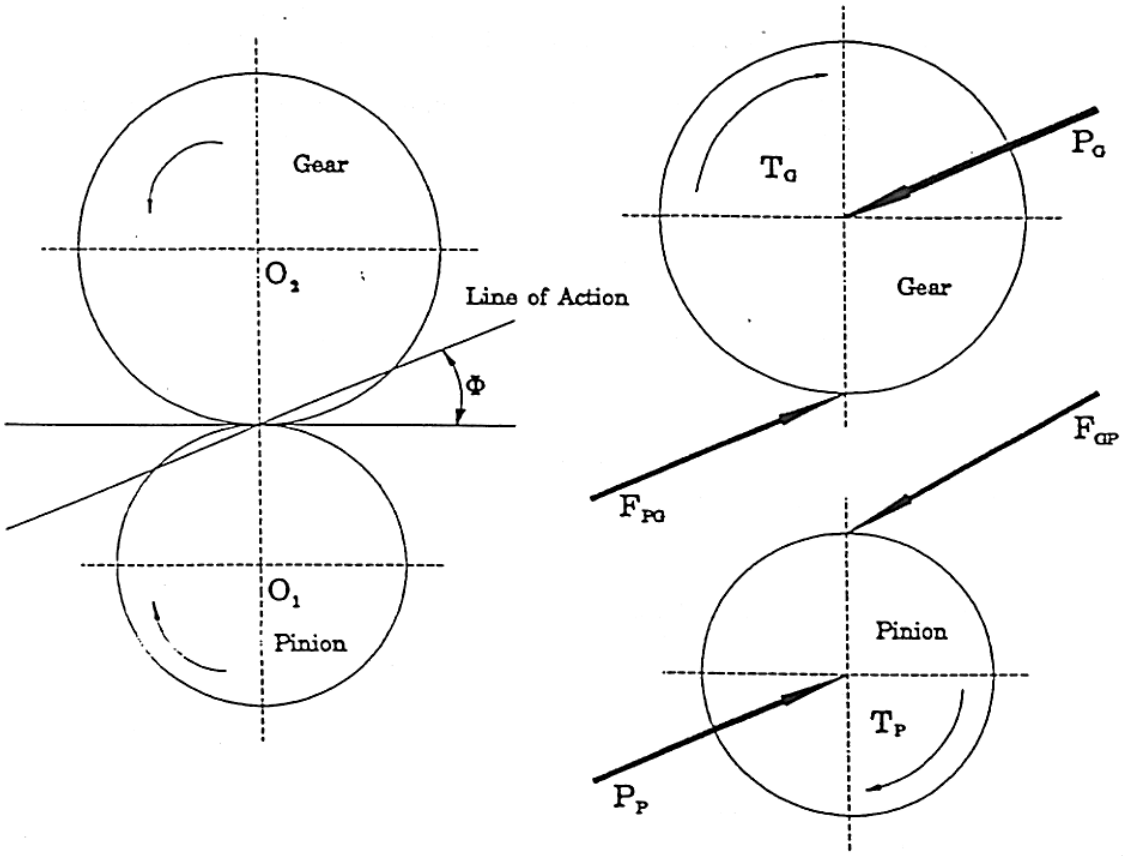

Figure 2. Force body diagram of the gear assembly (Lin & Liou, 1998, p. 29).

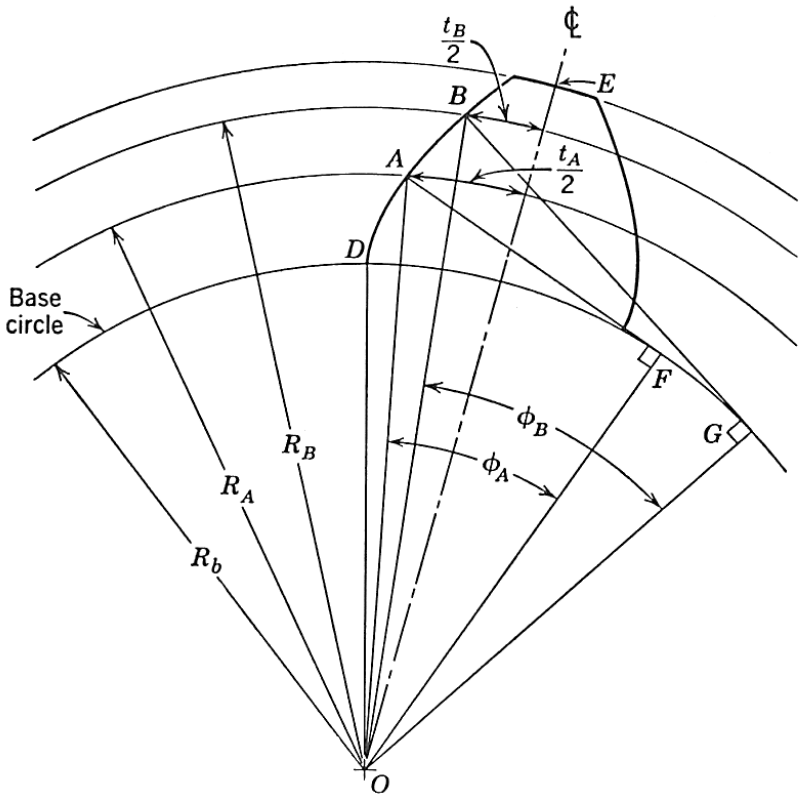

Figure 3. Involute relationships (Mabie & Reinholtz, 1987, p. 133). In this figure, ϕ represents φ.

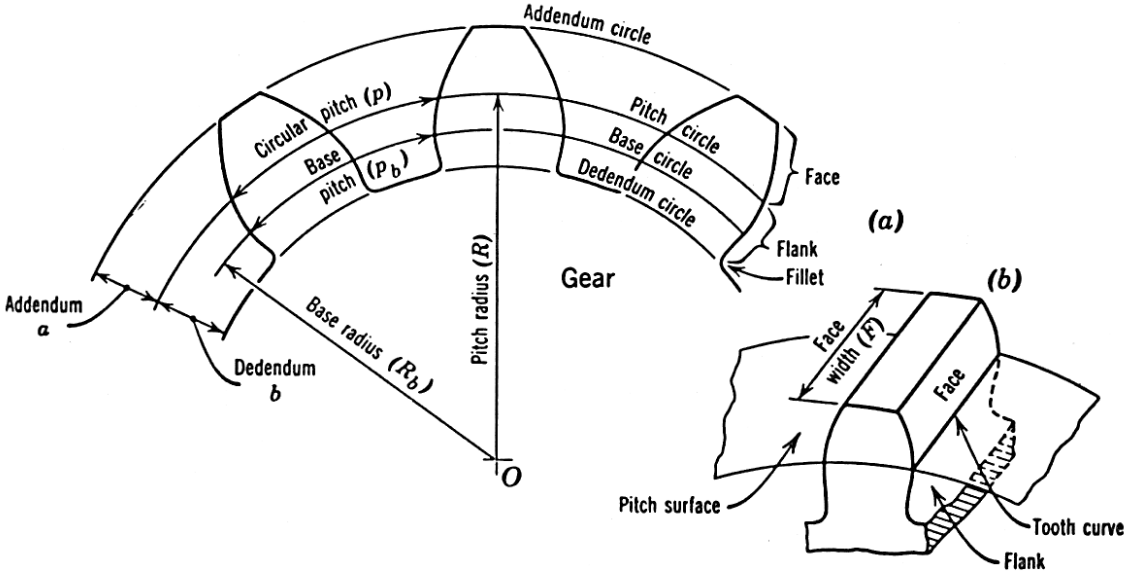

Figure 4. Base gear dimensions (Mabie & Reinholtz, 1987, p. 135).

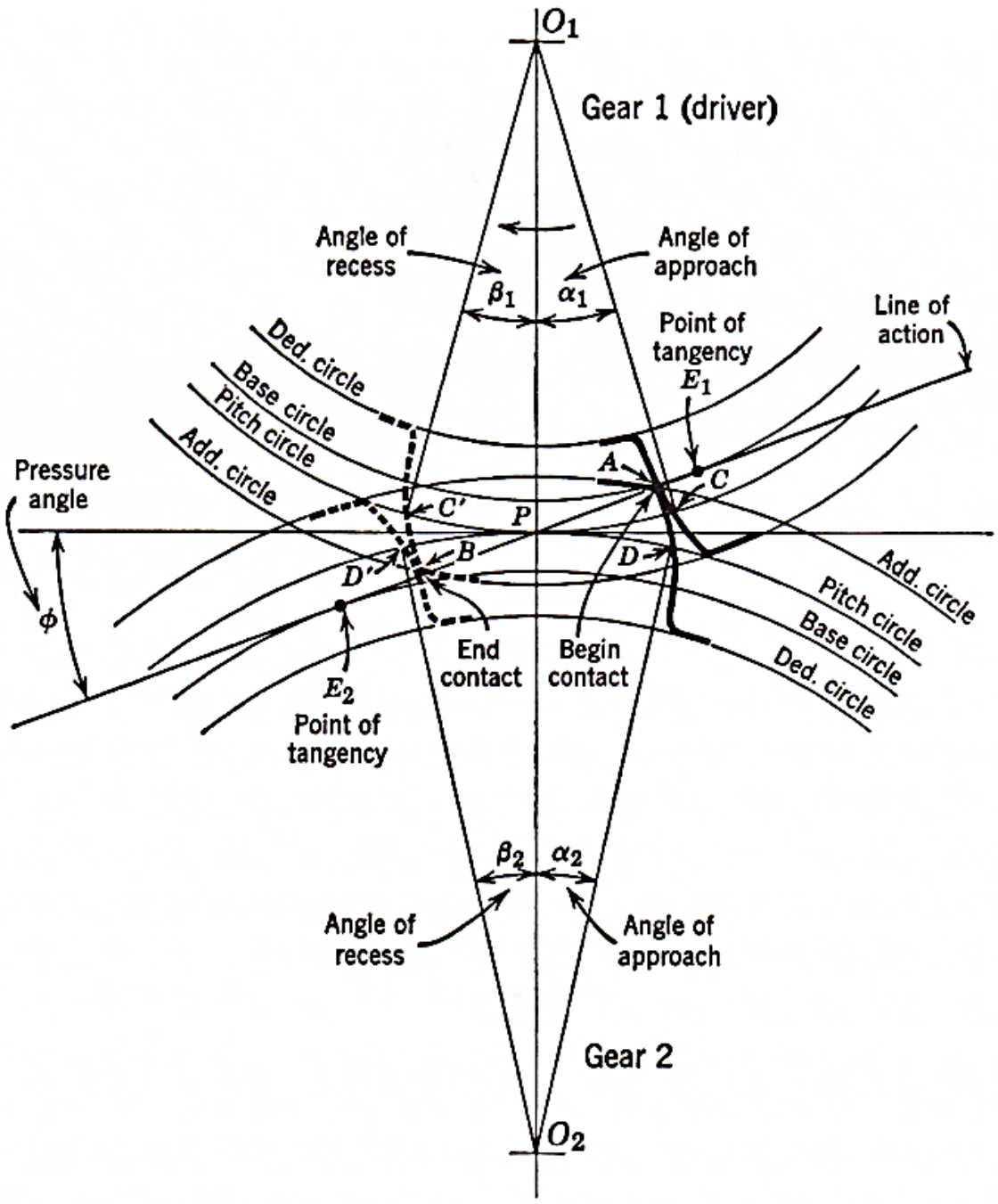

Figure 5. Dimensions of the gear mesh (Mabie & Reinholtz, 1987, p. 136).

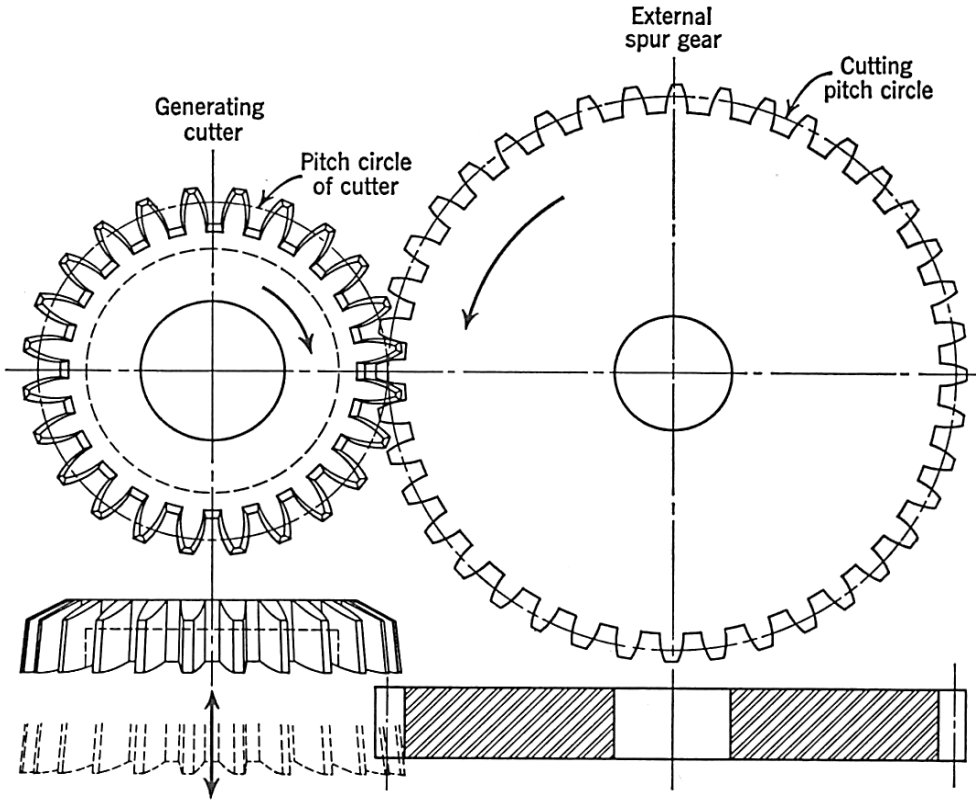

Figure 6. Cutting with a pinion cutter (Mabie & Reinholtz, 1987, p. 144).

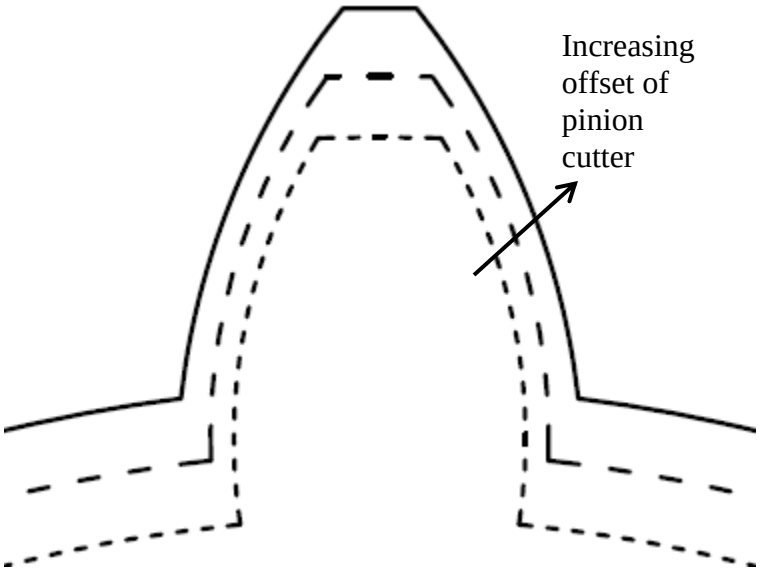

Figure 7. Shape of gear tooth and body shown for increasing pinion offset. This image does not include the fillet.

2.2. Static Model

Design Assumptions and Dimensions. As outlined in the introduction, the concepts underlying the dynamic model are built upon static design concepts and assumptions. According to Rogers, Mabie, and Reinholtz (1990), tooth stress at the root of the teeth in a gear pair are equalized through the following dimensional conditions: "a specific minimum contact ratio, . . . the pinion and gear must not be undercut, . . . the pinion and gear are to have equal strengths, and . . . the maximum possible depth of cut must not be exceeded." In order to optimize the design statically, the following assumptions are made: "the gear tooth is treated as a cantilever beam with the load applied at the tip . . . [and] . . . the entire load is carried by a single pair of teeth" (p. 629). Furthermore, Green and Mabie (1980a) explain that the type of pinion cutter and the amount of backlash is important in the static model. As chapter 3 section 2 will show, the pinion cutter is a Fellows-type and the backlash is 0.0 inches (p. 491). Performing both a static and dynamic analysis allows for proper comparison and testing between both models. The following equations and relationships provide the means to create a static model. The program created in FORTRAN-90 (Microsoft, 1995, computer software) that performs these calculations is shown in appendix A.

According to Mabie and Reinholtz (1987), the challenges to the spur gear design cut by pinion cutter involve modified pitch circles and pressure angles. Thus, it is necessary to perform several calculations that are important for both a static and dynamic design (pp. 187-188). In order to find the static stress due to bending caused by the tangential component of the tooth load at the base of the gear (Mabie et al., 1983, p. 188), Green and Mabie (1980a and 1980b) developed the following relationships. A further

description can be found in their works, which can be found in the bibliography. First, a series of dimensions are found, which are shown primarily in figure 8 but also figures 9 and 10.

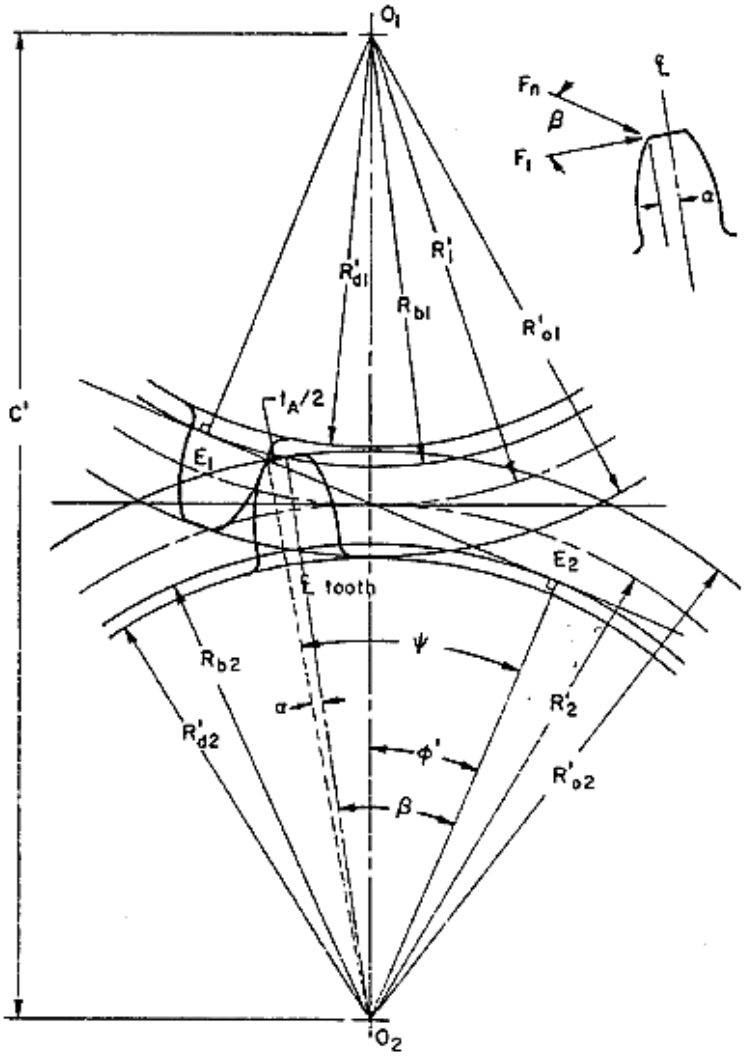

Figure 8. Dimensions between gears. In this figure, ϕ represents φ (Green & Mabie, 1980a, p. 497).

$$\varphi'_g = \mathrm{ACOS}\left(\frac{C * \mathrm{COS}\,\varphi_c}{C'}\right) \qquad \text{EQ. 5}$$

φ_g' is the operating pressure angle between gears (Green & Mabie, 1980a; Oswald, Lin, & Delgado, 1996a). In this equation, φ_c is the standard cutting pressure angle of pinion cutter, C is the standard center distance between gears, and C' is the operating center distance between gears (Green & Mabie, 1980a).

$$C_{sg} = \frac{N_g + N_c}{2 * P_d} \quad \text{EQ. 6}$$

C_{sg} is the standard center distance between gear and pinion cutter (Green & Mabie, 1980b). In this equation, N_c is the number of teeth of the pinion cutter, N_g is the number of teeth in the appropriate gear (Green & Mabie, 1980a), and P_d is the diametral pitch (Mabie & Reinholtz, 1987).

$$p_b = \frac{\pi}{P_d} * \text{COS}\ \varphi_c \quad \text{EQ. 7}$$

p_b is the "base pitch" (Green & Mabie, 1980b, p. 508).

$$\varphi_{gg} = \text{ACOS}\left[\frac{(N_g + N_c) * p_b}{2 * \pi * (C_{sg} + e_g)}\right] \quad \text{EQ. 8}$$

φ_{gg} is the gear generating pressure angle (Green & Mabie, 1980b).

$$R_{gg} = \frac{N_g}{N_g + N_c} * (C_{sg} + e_g) \quad \text{EQ. 9}$$

R_{gg} is the gear generating pitch radius (Green & Mabie, 1980b).

$$t_c = \frac{\pi}{2 * P_d} \quad \text{EQ. 10}$$

t_c is the tooth thickness of pinion cutter at the standard pitch radius (Mabie & Green, 1980a).

$$R_{bg} = R_g * \text{COS}\ \varphi_c \quad \text{EQ. 11}$$

In this equation, R_{bg} is the base circle of pinion cutter. R_{bc} can be found in a similar manner (Green & Mabie, 1980b). In this equation, R_g is the standard radius of the respective gear (Green & Mabie, 1980a).

$$t_{gg} = \frac{p_b - t_c * \text{COS}\ \varphi_c - 2 * R_{bc} * \left(\text{INV}\ \varphi_c - \text{INV}\ \varphi_{gg}\right)}{\text{COS}\ \varphi_{gg}} \quad \text{EQ. 12}$$

t_{gg} is the tooth thickness of gear on the gear generating pitch radius (Green & Mabie).

$$t'_g = \frac{p_b - t_c * \text{COS}\ \varphi_c - 2 * R_{bc} * \left(\text{INV}\ \varphi_c - \text{INV}\ \varphi_{gg}\right)}{\text{COS}\ \varphi'_g} + \frac{2 * R_{bg} * \left(\text{INV}\ \varphi_{gg} - \text{INV}\ \varphi'_g\right)}{\text{COS}\ \varphi'_g} \quad \text{EQ. 13}$$

t_g' is the tooth thickness of gear on operating pitch radius (Green & Mabie, 1980a).

$$R'_g = \frac{R_{bg}}{COS\ \varphi'_g} \qquad \text{EQ. 14}$$

R_g' is the operating pitch radius (Green & Mabie, 1980a; Oswald et al., 1996a).

$$R'_{0g} = C' - R_g - e_g + \frac{k_t}{P_d} \qquad \text{EQ. 15}$$

R_{0g}' is the operating outside gear radius (Green & Mabie, 1980b). In this equation, k_t is the factor for tooth type. For the study that follows, k_t is 1.0 (Green & Mabie, 1980a, p. 495).

$$c = \frac{0.250}{P_d} \qquad \text{EQ. 16}$$

For "coarse pitch gears," the clearance, c, is given in accordance with AGMA 201.02 (American Gear Manufacturers Association, 1974; Green & Mabie, 1980a, p. 495; Mabie & Reinholtz, 1987, p. 147). The numerator value, 0.250, is the "tooth clearance ratio." This ratio is used in the input for the DANST program (Oswald et al., 1996b, p. 2).

The input for the DANST program also requires the "cutter addendum ratio" (Oswald et al., 1996b, p. 2). As the pinion cutter is a gear with standard proportions,

Mabie and Reinholtz suggest the use of AGMA 201.02 for the determination of this ratio, 1.00 (American Gear Manufacturers Association, 1974; Mabie & Reinholtz, 1987, p. 147).

$$h_t = R'_{01} + R'_{02} - C' + c \qquad \text{EQ. 17}$$

h_t is the depth of cut (Green & Mabie, 1980b).

$$R'_{dg} = R'_{0g} - h_t \qquad \text{EQ. 18}$$

R_{dg}' is the operating gear dedendum radius (Green & Mabie, 1980b).

$$\psi_g = \text{ACOS}\left(\frac{R_{bg}}{R'_{0g}}\right) \qquad \text{EQ. 19}$$

ψ_g is shown in figure 8 (Green & Mabie, 1980b).

$$\alpha_g = \frac{t_{gg}}{2 * R_{gg}} + \text{INV}\,\varphi_{gg} - \text{INV}\psi_g = \frac{t_{ag}}{2 * R'_{0g}} \qquad \text{EQ. 20}$$

α_g is shown in figure 8 (Green & Mabie, 1980b), and 't_{ag},' which is the gear tooth thickness at addendum or top of gear (Green & Mabie, 1980a, p. 496), can be found by means of equation 21.

$$t_{ag} = 2 * \alpha_g * R'_{0g} \quad \text{EQ. 21}$$

$$\beta_g = \psi_g - \alpha_g \quad \text{EQ. 22}$$

β_g is the angle of application . . . of the normal tooth load F_n" as is shown in figure 8 (Green & Mabie, 1980b, p.509).

As explained by Green and Mabie (1980a) the following dimension, θ_g, is defined by whether the base radius of the gear is less than or equal to the operating dedendum radius of the gear, or if the base radius of the gear is greater than the operating dedendum radius. Figures 9 and 10 highlight the following dimensions that are to be found (pp. 497-499).

According to Green and Mabie (1980a), for the case where the base radius of the gear is less than or equal to the operating dedendum radius of the gear, the following dimensional calculations apply (pp. 497-499).

$$\theta_g = \frac{t_{dg}}{2 * R'_{dg}} = \frac{t_{gg}}{2 * R_{gg}} + \text{INV}\ \varphi_{gg} - \text{INV}\ \varphi_{dg} \quad \text{EQ. 23}$$

$$\varphi_{dg} = \text{ACOS}\left(\frac{R_g}{R'_{dg}} * \text{COS}\ \varphi_{gg}\right) \quad \text{EQ. 24}$$

The dimension φ_{dg} is shown in figure 9 (Green & Mabie, 1980a).

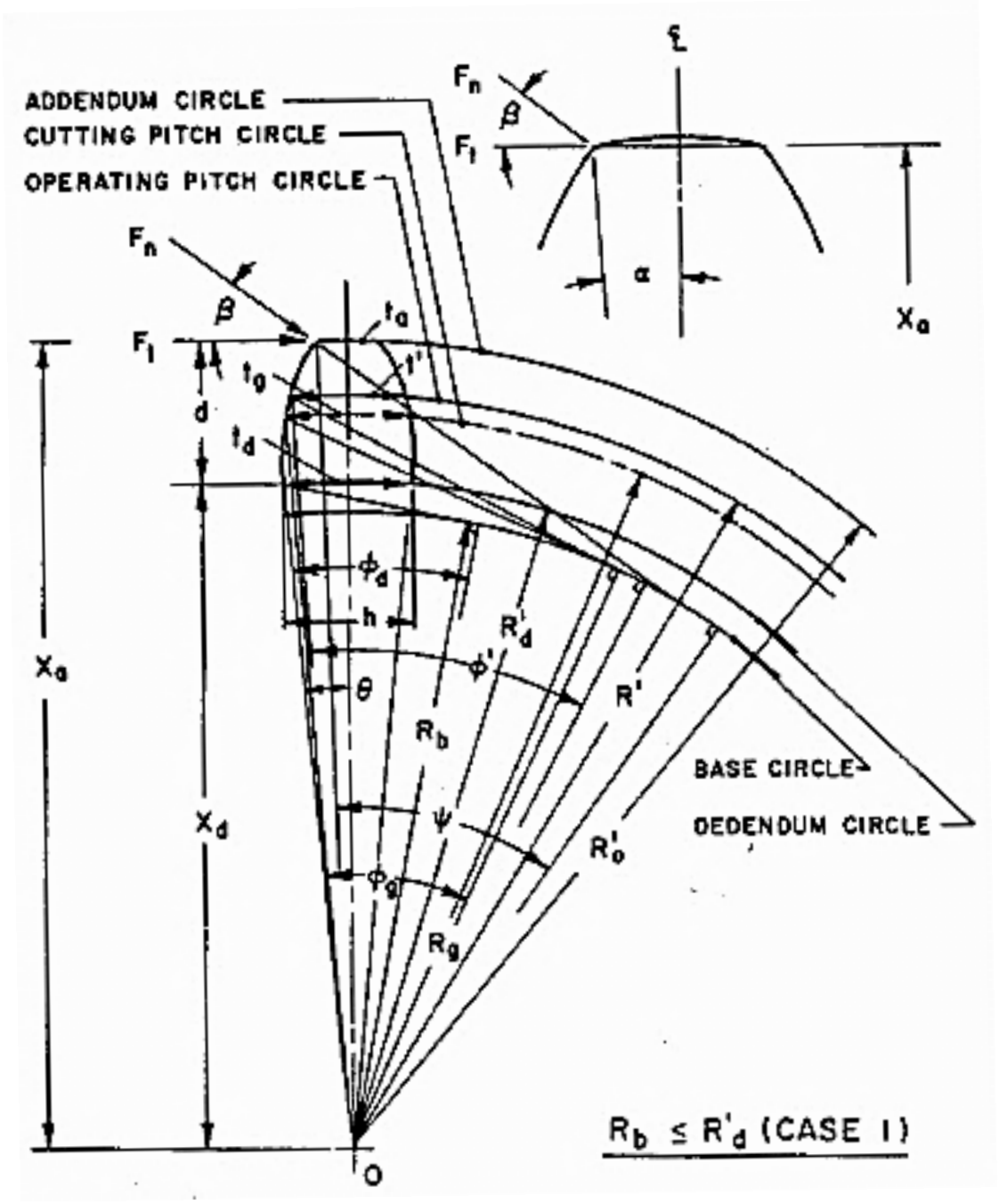

Figure 9. Case used when the base radius of the gear is less than or equal to the operating dedendum radius of the gear. The image is magnified for clarity. In this figure, ϕ represents φ (Green & Mabie, 1980a, p. 498).

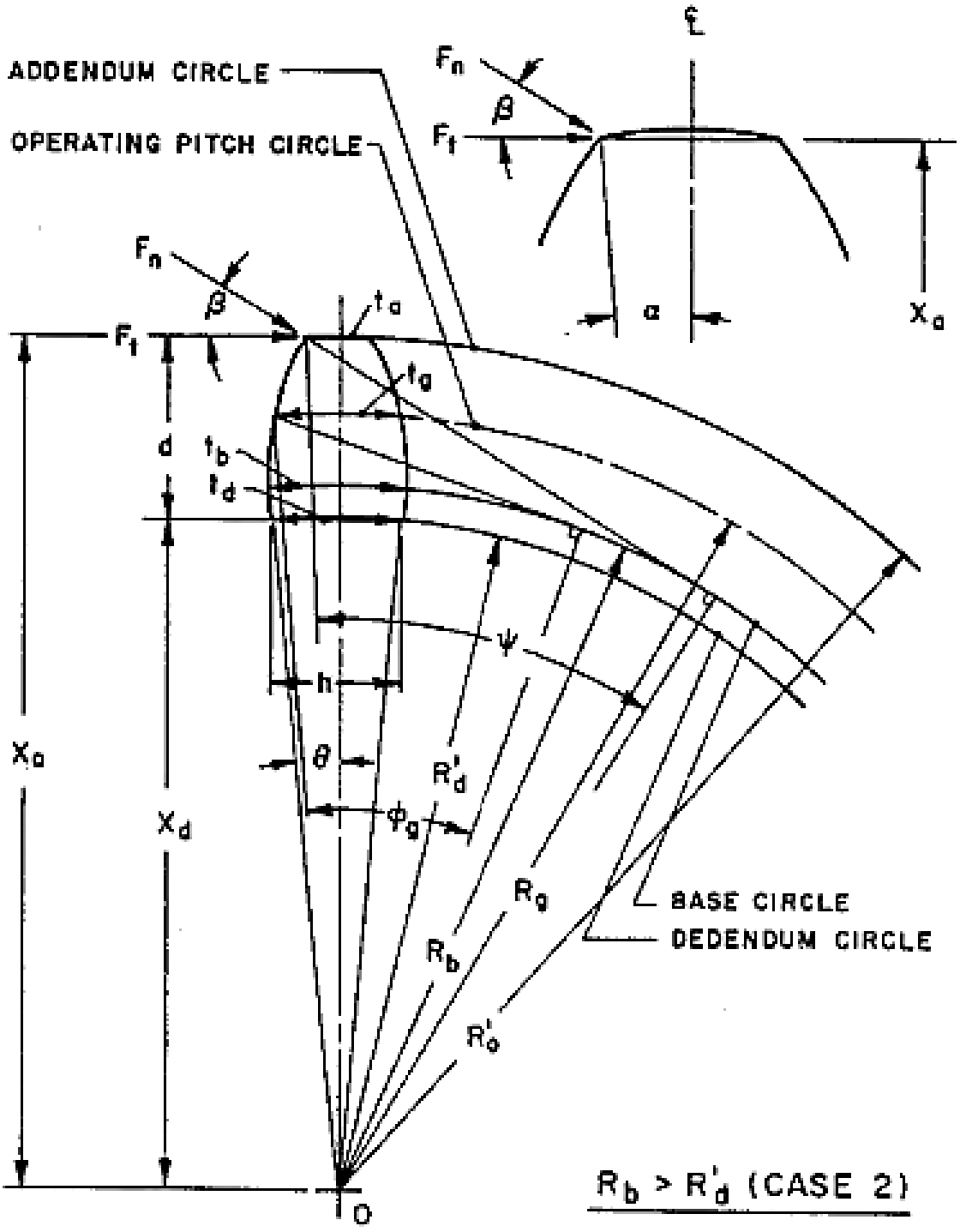

Figure 10. The case used when the base radius of the gear is greater than the operating dedendum radius. The image is magnified for clarity. In this figure, Φ represents φ (Green & Mabie, 1980a, p. 498).

For the case where the base radius of the gear is greater than the operating dedendum radius, the following dimensional calculation applies (Green & Mabie, 1980a).

$$\theta_g = \frac{t_{gg}}{2 * R_{gg}} + \text{INV}\ \varphi_{gg} \qquad \text{EQ. 25}$$

$$t_{dg} = 2 * R'_{dg} * \theta_g \qquad \text{EQ. 26}$$

The dimension t_{dg} is the tooth thickness of gear at the dedendum radius (Green & Mabie, 1980a), and can be found by means of equation 23, or approximated by the combination of equations 23 and 25.

Once θ_g is found, the following dimensions, from figures 9 and 10, are used to find the stress factor, S_g, which Mabie and Green (1980a and 1980b) use to establish a balanced system in terms of static stress at the root of the tooth (p. 497-505).

$$X_{ag} = R'_{0g} * \text{COS}\ \alpha_g \qquad \text{EQ. 27}$$

X_{ag} is the vertical length from the gear center to tip of the gear tooth, for clarity see figures 9 and 10 (Green & Mabie, 1980a).

$$X_{dg} = R'_{dg} * \text{COS}\ \theta_g \qquad \text{EQ. 28}$$

X_{dg} is the vertical length from the gear center to the bottom of the gear tooth, for clarity see figures 9 and 10 (Green & Mabie, 1980a).

$$h_g = 2 * R'_{dg} * \text{SIN}\ \theta_g \qquad \text{EQ. 29}$$

h_g is the horizontal thickness of the gear tooth, for clarity see figures 9 and 10 (Green & Mabie, 1980a).

$$d_g = X_{ag} - X_{dg} \qquad \text{EQ. 30}$$

d_g is the vertical height of the gear tooth as is shown in figures 9 and 10 (Green & Mabie, 1980a).

$$S_g = \frac{6 * d_g * \text{COS}\ \beta_g}{(h_g)^2} \qquad \text{EQ. 31}$$

Backlash Dimension. As explained by Green and Mabie (1980a) the preceding calculations balance stress while assuming that backlash is zero. However, in a successive works by Rogers et al. (1990) the authors developed an equation that involves backlash, B, with the following variables: N_c, N_g, φ_c, P_d, C, C', B, and e_g (p. 625). The definitions of these variables can be found in the previous sections or the list of terminology.

$$0 = 2 * N_c * \text{INV}\ \varphi_c - (N_c + N_1) * \text{INV}\ \varphi_{g1} \qquad \text{EQ. 32}$$
$$-(N_c + N_2) * \text{INV}\ \varphi_{g2} + (N_1 + N_2) * \text{INV}\ \varphi'_g - \frac{B * P_d * C}{C'}$$

This equation provided by the authors Rogers et al. (1990) is essentially a function of several dependent gear dimensions, including offset and backlash (p. 625). For example, if N_c, N_1, N_2, φ_c, φ_{g1}, φ_g', P_d, C, C', B, and e_1 are known, e_2, the distance the pinion cutter is offset from gear 2, can be solved for.

$$\text{INV}\,\varphi_{g2} = \frac{1}{(N_c + N_2)} * \left[2 * N_c * \text{INV}\,\varphi_c - (N_c + N_1) * \text{INV}\,\varphi_{g1} + (N_1 + N_2) * \text{INV}\,\varphi_g' - \frac{B * P_d * C}{C'}\right] \quad \text{EQ. 33}$$

Using equation 33 and solving the involute function, results in φ_{g2}. Once φ_{g2} is known, e_2 can be found from equation 8.

Static Tooth Stress. In the previous sections, a stress factor was found that represented the stress at the root of the tooth due to bending caused by the tangential component of the tooth load, σ_{sg} (Green & Mabie, 1980a; Mabie et al., 1983).

$$\sigma_{sg} = \frac{6 * F_{ng} * \text{COS}\,\beta_g * d_g}{F_W * (h_g)^2} \quad \text{EQ. 34}$$

This relationship is further explained through DANST program (Oswald et al., 1996) and by Mabie and Reinholtz (1987). Knowing equation 31 and 34 and understanding the angle of the load, β_g, between F_n and F_t as seen in figures 9 and 10 allows calculation of the stress from an applied input torque, T_{f1} (p. 179).

$$F_{t1} = \frac{T_{f1}}{R_{b1}}$$ EQ. 35

F_{tg} is the horizontal component of load normal to tooth, F_n (Green & Mabie, 1980a).

$$F_{ng} = \frac{F_{tg}}{COS\ \beta_g}$$ EQ. 36

F_{ng} is the load normal to tooth and is also defined as W (Green & Mabie, 1980a).

$$\sigma_{sg} = \frac{S_g * F_{ng}}{F_W}$$ EQ. 37

σ_{sg} is the resulting stress (Green & Mabie, 1980a).

2.3. Gear Tooth Fillet Dimensions

Pinion Cutter Tooth Tip Dimensions. One of the primary differences between the static and dynamic model is the inclusion of geometry at the root of the tooth. This location is where the stress under consideration occurs. This geometrical dimension is the fillet radius of curvature, ρ_f. Essentially, this radius of curvature acts as a stress riser or reducer.

Colbourne (1987) formulates the cutter tooth tip geometry in the following manner. The following dimensions are directly related to the following schematic (pp. 133-136).

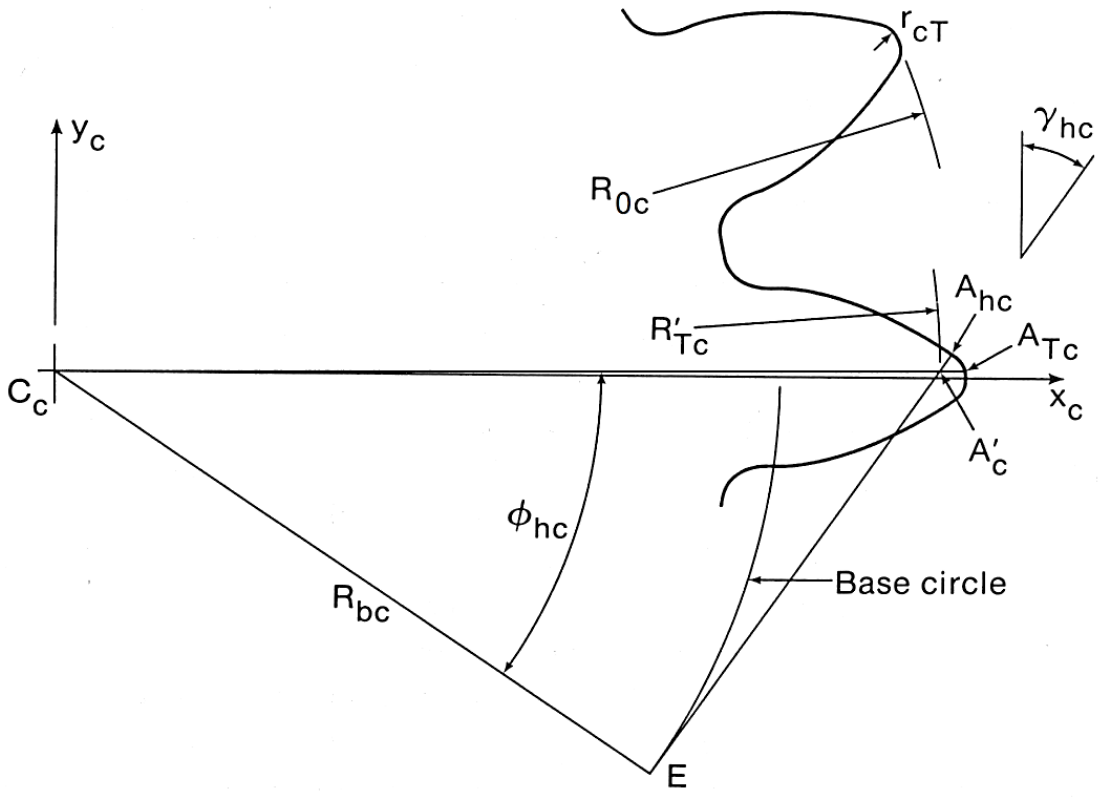

Figure 11. "Pinion cutter tooth tip geometry." In this figure, ϕ represents φ (modified from Colbourne, 1987, p. 134).

$$R_{0c} = R_c + \frac{k_t}{P_d} + c \qquad \text{EQ. 38}$$

R_{0c} is the outer radius of the pinion cutter (Green & Mabie, 1980a), where R_c is the radius of pinion cutter (Green & Mabie, 1980a).

$$R'_{Tc} = R_{0c} - r_{cT} \qquad \text{EQ. 39}$$

R_{Tc}' is the polar coordinate of A_c' as seen in figure 11, where r_{cT} is the radius of curvature of pinion cutter tooth tip. The optimization of r_{cT} is discussed at the end of this

section. The value chosen for the study that follows is 0.0, which is discussed in further detail in chapter 3, section 2 (Colbourne, 1987, pp. 133-136).

$$\mathrm{RCEG} = r_{cT} * P_d \qquad \text{EQ. 40}$$

The DANST program requires the "cutter edge radius ratio," RCEG, which takes into account the r_{cT} value (Oswald et al., 1996b, p. 2).

$$\varphi_{hc} = \mathrm{ATAN}\left(\frac{\sqrt{(R'_{Tc})^2 - (R_{bc})^2} + r_{cT}}{R_{bc}}\right) \qquad \text{EQ. 41}$$

φ_{hc} is the "profile angle of A_{hc}" as seen in figure 11 (Colbourne, 1987, pp. 133-136).

$$R_{hc} = \frac{R_{bc}}{\mathrm{COS}\ \varphi_{hc}} \qquad \text{EQ. 42}$$

R_{hc} is the "polar coordinate of A_{hc}" as seen in figure 11 (Colbourne, 1987, pp. 133-136).

$$\theta_{hc} = \frac{t_c}{2 * R_c} + \mathrm{INV}\ \varphi_c - \mathrm{INV}\ \varphi_{hc} \qquad \text{EQ. 43}$$

θ_{hc} is the "polar coordinate of A_{hc}" as seen in figure 11 (Colbourne, 1987, pp. 133-136).

$$\gamma_{hc} = \varphi_{hc} - \theta_{hc} \quad \text{EQ. 44}$$

γ_{hc} is the "angle . . . with the tooth center-line . . . tangent to the tooth profile at A_{hc}" as seen in figure 11 (Colbourne, 1987, pp. 133-136).

$$x_c' = R_{hc} * \text{COS}\,\theta_{hc} - r_{cT} * \text{SIN}\,\gamma_{hc} \quad \text{EQ. 45}$$

$$y_c' = R_{hc} * \text{SIN}\,\theta_{hc} - r_{cT} * \text{COS}\,\gamma_{hc} \quad \text{EQ. 46}$$

x_c' and y_c' are the "Cartesian coordinate[s] . . . of point A_c' " as seen in figure 11 (Colbourne, 1987, pp. 133-136). Moreover, according to Colbourne (1987) the above relationships can determine the maximum pinion cutter tooth tip radius, r_{cT}, by determining where y_c' is negligibly positive or zero (pp. 133 – 136).

$$\theta_c' = \text{ATAN}\left(\frac{y_c'}{x_c'}\right) \quad \text{EQ. 47}$$

θ_c' is the polar coordinate of x_c', y_c' as seen in figure 11 (Colbourne, 1987, pp. 133-136).

Gear Fillet Dimensions. In order to transition from the pinion cutter tooth tip that cuts the gear to the cut fillet of the gear, a series of initial dimensions are needed. The first dimension needed is the standard circular pitch, P_s (Colbourne, 1987, pp. 39-40).

$$P_s = \frac{\pi}{P_d} \quad \text{EQ. 48}$$

$$t_{sg} = \frac{\pi}{2 * P_d} + 2 * e_g * \text{TAN } \varphi_c \quad \text{EQ. 49}$$

t_{sg} is the tooth thickness of a gear at the standard pitch circle (Colbourne, 1987, p. 151).

$$\text{INV } \varphi_c' = \text{INV } \varphi_c - \frac{1}{2 * C_{sg}} * \left(P_s - t_{sg} - t_c\right) \quad \text{EQ. 50}$$

φ_c' is the operating cutting pressure angle between pinion cutter and gear. According to Colbourne (1987), once INV φ_c' is known, φ_c' can be found (p. 120).

$$C_c = \frac{R_{bg} + R_{bc}}{\text{COS } \varphi_c'} \quad \text{EQ. 51}$$

C_c is the appropriate center distance between gear and cutting pinion (Colbourne, 1987, pp. 120-121).

$$R_{cc}' = \frac{N_c + C_c}{N_g + N_c} \quad \text{EQ. 52}$$

R_{cc}' is the radius of the cutting pitch circle of the pinion cutter relative to the gear (Colbourne, 1987, pp. 120-121).

$$R_0 = \frac{N_g * N_c * C_c}{(N_g + N_c)^2} \qquad \text{EQ. 53}$$

R_0 is the length relationship between "two cutting pitch circles" (Colbourne, 1987, p. 237).

In order to complete the dimensions of the gear fillet, Colbourne (1987) outlines the following steps corresponding to figure 12. Additionally, the following dimensions can represent any point along the fillet. The bottom and top of the fillet dimensions of each gear when cut by pinion cutter are found during the static analysis (pp. 221, 235-237).

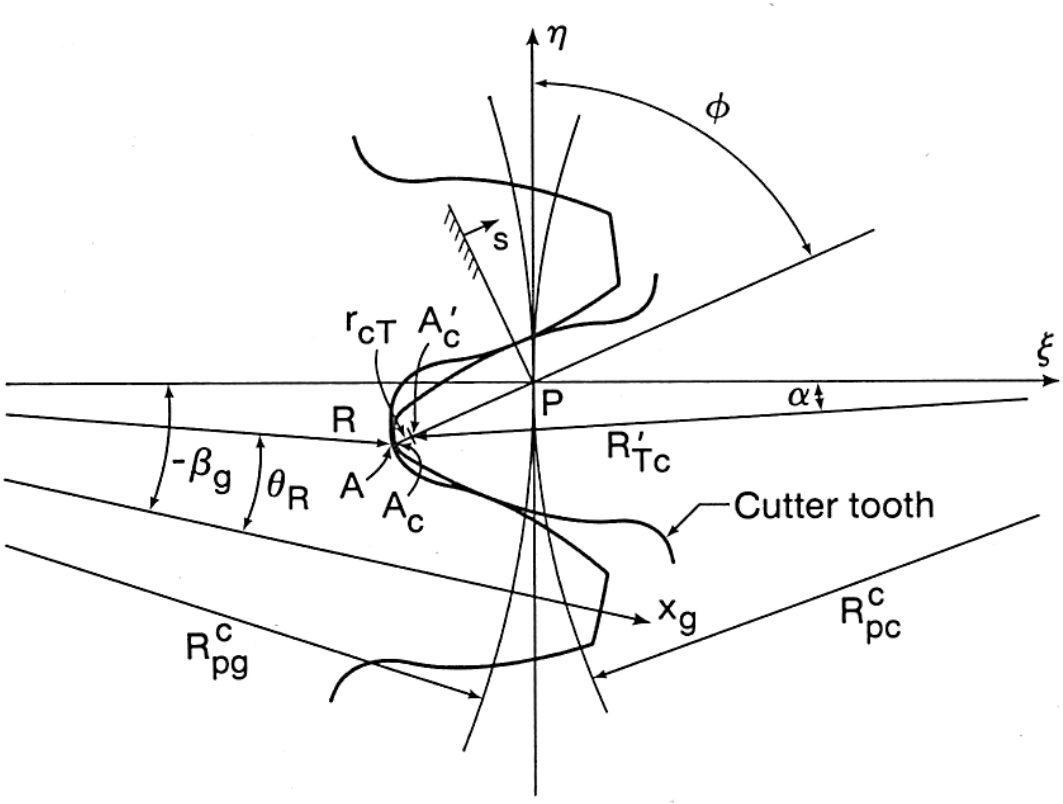

Figure 12. Cutting of the gear by pinion cutter. In this figure, ϕ represents φ (modified from Colbourne, 1987, p. 222).

$$\alpha_f = \text{ACOS}\left(\frac{R_{bc}}{R'_{Tc}}\right) - \varphi'_c \qquad \text{EQ. 54}$$

As explained by Colbourne (1987), α_f is the angle between A_c' and the "line of centers" (p. 221). The maximum and minimum angle value of α_f corresponds to the top and bottom of the fillet. According to standard gear theory, the minimum angle, α_f, is 0.0, which corresponds to the bottom of the fillet. Also, φ_c' must be in radians in this relationship (pp. 221-224).

$$\zeta' = R'_{cc} - R'_{Tc} * \text{COS}\ \alpha_f \qquad \text{EQ. 55}$$

$$\eta' = -R'_{Tc} * \text{SIN}\ \alpha_f \qquad \text{EQ. 56}$$

ζ' and η' represent the coordinates of point A_c' (Colbourne, 1987, pp. 221-222).

$$s' = -\sqrt{(\zeta')^2 + (\eta')^2} \qquad \text{EQ. 57}$$

$$s = s' - r_{cT} \qquad \text{EQ. 58}$$

Once A_c' is found, s and s' establish the relationship between points A_c' and A_c. Using s and s', the coordinates of A_c can be found: ζ and η (Colbourne, 1987, pp. 221-222).

$$\zeta = \frac{s}{s'} * \zeta' \qquad \text{EQ. 59}$$

$$\eta = \frac{s}{s'} * \eta' \qquad \text{EQ. 60}$$

$$\beta_{ct} = \alpha_f - \theta'_c \qquad \text{EQ. 61}$$

$$\beta_{gt} = -\frac{1}{R_g} * \left(r_{ct} * \beta_{ct} + \frac{P_s}{2}\right) \qquad \text{EQ. 62}$$

β_{ct} is the "angle . . . through which the [pinion cutter] tooth center-line" turns, and β_{gt} is the "angle . . . through which the [cut gear] tooth center-line" turns (Colbourne, 1987, p. 223).

$$R = \sqrt{\left(R_g + \zeta\right)^2 + \eta^2} \qquad \text{EQ. 63}$$

$$\theta_R = \text{ATAN}\left(\frac{\eta}{R_g + \zeta}\right) - \beta_{gt} \qquad \text{EQ. 64}$$

R and θ_R represent the polar coordinate where point A_c on the pinion cutter meets the gear (Colbourne, 1987, p. 223).

$$\varphi_m = \text{ATAN}\left(\frac{\zeta}{\eta}\right) \qquad \text{EQ. 65}$$

As shown by Colbourne (1987), φ_m is a particular angle relevant to the mesh. This dimension is required to find the radius of curvature of the gear fillet, ρ_f, at any point along the fillet. At the bottom of the gear tooth fillet, the angle, φ_m, corresponds to an angle of 90˚, a value not within the domain of the basic tangent function (pp. 222, 235-236).

Finally, the magnitude of the fillet radius of curvature, ρ_f, can be obtained (Colbourne, 1987, p. 237).

$$\rho_f = r_{cT} + \frac{(r_{cT} + s)^2}{R_0 * \text{SIN}\,\varphi_m - (r_{cT} + s)} \qquad \text{EQ. 66}$$

2.4. Transition from Static to Dynamic Model

The next step in the modeling process is to transition from the static to the dynamic model. The static model input is done interactively, before and during the operation of the program. In order to facilitate the transition, the static model outputs two separate files in a .txt format. One file is for comparison with the DANST program and its output, and an example of this output can be found in appendix B. The other file output by the static model is meant as an input to the DANST program. An example of the input files can be found in appendix C, which is modeled on and explained by Oswald et al. (1996b, pp. 1-3, 5-6). With the appropriate input file, and certain interactive input from the user, the DANST program can be run. Once the DANST program outputs the appropriate file, this can be compared to the static model output. Figure 13 outlines the process in a simple flow chart. As stated previously, both programs are meant to be run in FORTRAN-90 (Microsoft, 1995, computer software).

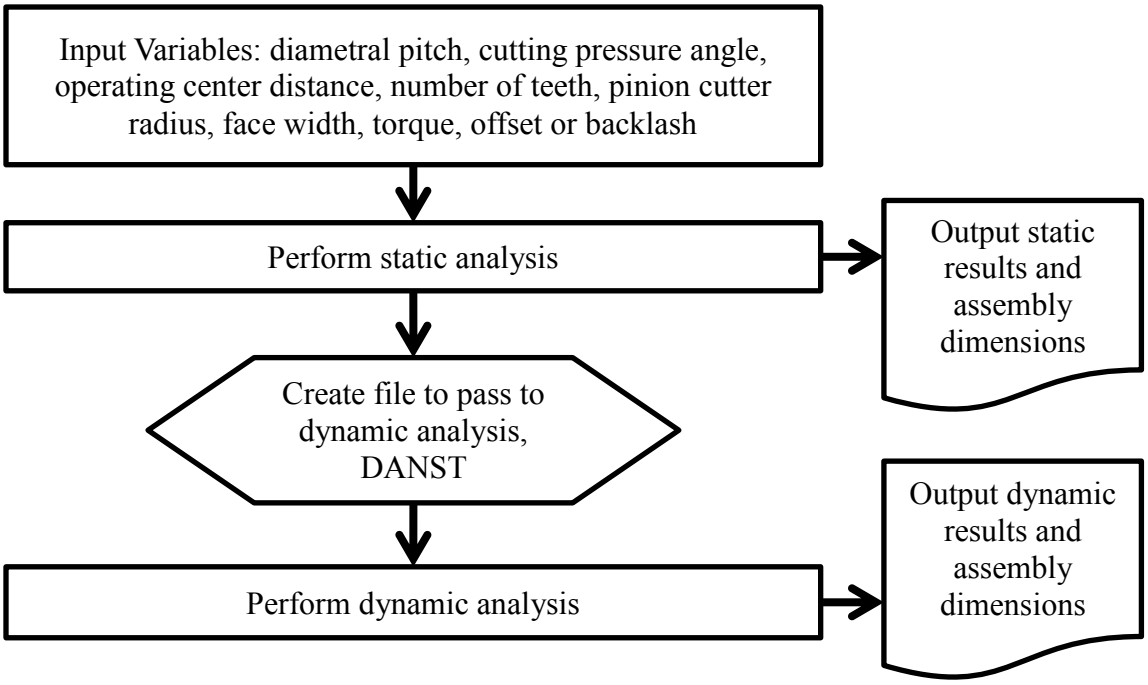

Figure 13. Flow chart of calculations steps for optimization study

2.5. Dynamic Model

Design Assumptions and Dimensions. As introduced in chapter 1, a static analysis is an ideal model that does not account for several dynamic factors. As explained by Dudley (1984), the tooth load can be shared by pairs of gear teeth, and does not always occur at the tip of the tooth (p. 2.10). Several published works explain that the dynamic effects occur due to differences in stiffness as the teeth of the gear assembly enter and leave mesh. This variable stiffness causes and is caused by variations in dimensions, load, deflection, and transmission error. In addition to stiffness, the dynamic model incorporates damping, friction, and deflection within the gear assembly. The resulting dynamic effects occur locally on the teeth and globally within the gear system, and have the general effect of amplifying tooth stress (Lin & Liou, 1998; Oswald & Townsend et al., 1996).

For these reasons, the DANST program developed by Oswald, Lin, and Delgado (1996b) is employed for the dynamic model (p. 1). The dynamic model in the DANST program is shown in figure 14, and is defined by Oswald et al. (1996b) as follows:

> DANST is a FORTRAN computer program for static and dynamic analysis of spur gear systems. The program can be used for parametric studies to predict the static transmission error, dynamic load, tooth bending stress and other properties of spur gears as they are influenced by operating speed, torque, stiffness, damping, inertia, and tooth profile. (p. 1)

Lin and Liou (1998) explain that the "model has four degrees of freedom and consists of gears, input device, output device, and two . . . shafts as shown in figure 14. The dynamic behavior of meshing gears could be considered as a periodic forced function." The variation of the torque, stiffness, and damping during the time interval of the teeth mesh pair act as "excitation terms to the equation of motion" (pp. 34-40).

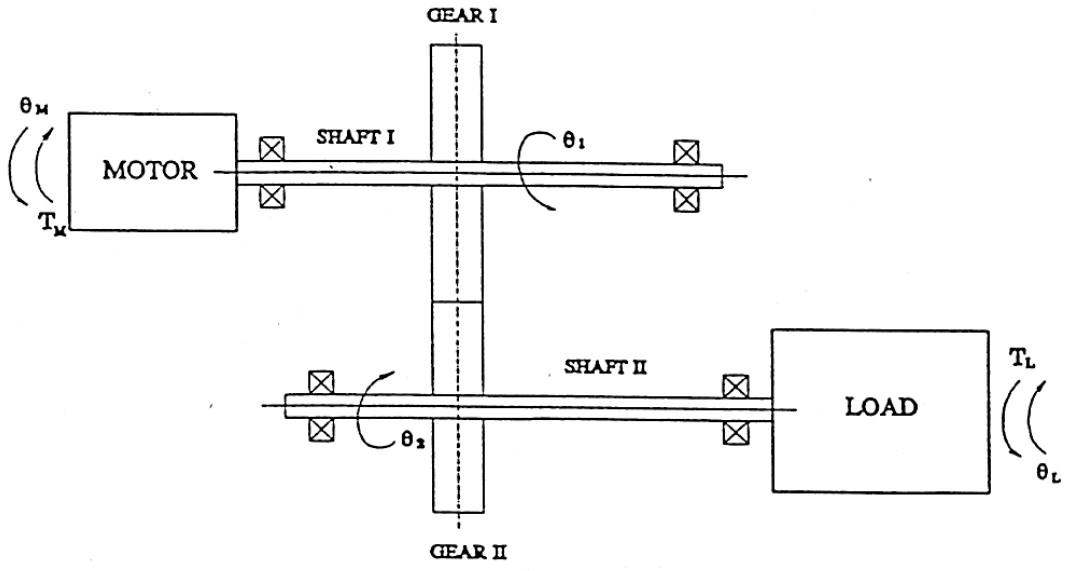

Figure 14. Physical dynamic model (Lin & Liou, 1998, p. 5).

As explained by Lin and Liou (1998), "pure rolling occurs if two friction disks rotate in contact without slipping. However, for the case of two involute gear teeth

meshing with each other, the meshing action is a combination of rolling and sliding" (p. 8).

As can be seen in figure 15 from the Lin and Liou (1998), arc XY on gear two and arc AB on gear must both move over each other and slide to maintain the same position in mesh. This relationship results in equation 67, and with the supplementary equations and relationships, equation 74 can be derived (pp. 8-12).

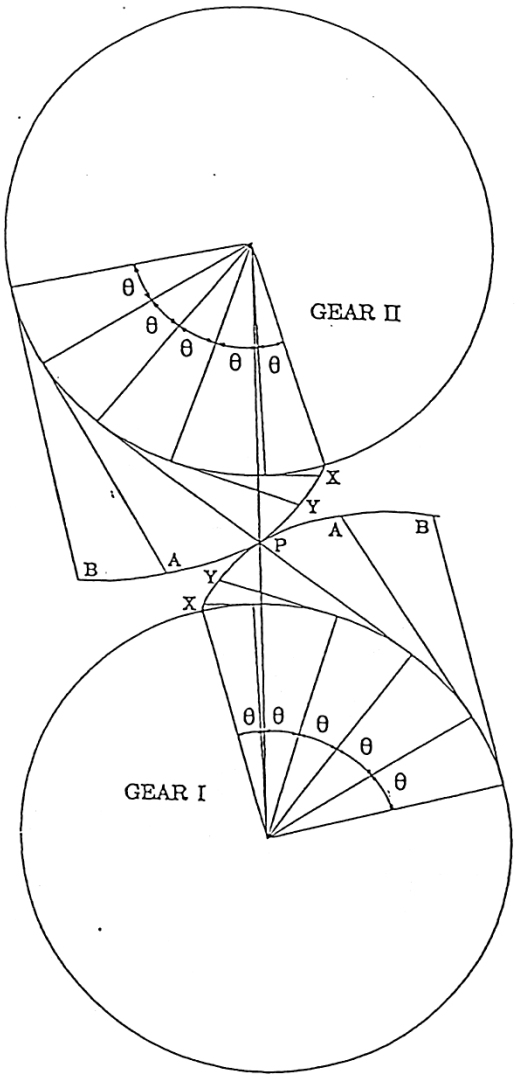

Figure 15. Combination of rolling and sliding (Lin & Liou, 1998, p. 10).

$$V_s = \frac{R_{C1} * \omega_1 - R_{C2} * \omega_2}{12}$$ EQ. 67

$$\omega_1 = \frac{12 * V}{R_{p1}}$$ EQ. 68

$$\omega_2 = \frac{R_{p1} * \omega_1}{R_{p2}}$$ EQ. 69

ω_g is the angular velocity of the appropriate gear in radians per unit time, where V is the "pitch-line velocity of gears" (Lin & Liou, 1998, p. 12) and R_{pg} is the pitch radius of the appropriate gear (Colbourne, 1987, p. 26).

$$V = \frac{2 * \pi * R_{p1} * N}{12} = \frac{R_{p1} * \omega_1}{12}$$ EQ. 70

N is the speed of driving gear in revolutions per unit time (Lin & Liou, 1998).

$$R_{C1} = \sqrt{(r_1)^2 - (R_{b1})}$$ EQ. 71

$$R_{C2} = \sqrt{(r_2)^2 - (R_{b2})} = C * SIN - \sqrt{(r_1)^2 - (R_{b1})}$$ EQ. 72

R_{Cg} is the "radius of curvature of [the] gear" at "any radius of gear tooth profile," where r_g is "any radius of gear tooth profile" (Lin & Liou, 1998, p. 11) and R_{bg} is the base radius of gear (Green & Mabie, 1980b).

$$R_{C1} + R_{C2} = C * \text{SIN}\ \varphi_c \qquad \text{EQ. 73}$$

φ_c is the standard cutting pressure angle of pinion cutter, or general cutting pressure angle (Green & Mabie, 1980a).

Using the following relationships derived by the authors (Lin & Liou, 1998), equation 67 becomes equation 74 (pp. 8-12).

$$V_s = \left[\frac{V * \left(R_{p1} + R_{p2}\right)}{R_{p1} * R_{p2}}\right] * \left(\sqrt{(r_1)^2 - (R_{b1})} - R_{p1} * \text{SIN}\ \varphi_c\right) \qquad \text{EQ. 74}$$

Deflection of the Gears and Gear Teeth. In the static analysis, deflection is not taken into account. As stated by Lin and Liou (1998, p. 12), in the dynamic analysis, the dynamic model takes into account deflection due to the applied load from the pinion torque. From Cornell and Westervelt (1978, pp. 69-76), Lin and Liou (1998) utilized the following relationship. The "deflection is based on a combination of the deflection of the tooth as a cantilever beam, local contact compression, and fillet and tooth foundation flexibility effects" (p. 12). Of these, contact is nonlinear. In order to quantify the cumulative deflection, the dynamic model assumes the gear tooth as a "non-uniform cantilever beam" and the tooth is broken into a series of elements along an "effective length," l_0 located by subscripts "i" and "j." Each of these segments is then subject to basic principles of mechanics (Lin & Liou, 1998, pp. 12-13).

In the dynamic model, a choice must be made between plane stress, a wide gear and tooth, or plane strain, a narrow gear and tooth. For the dynamic study that follows, the face width of the model is 1.0 inch. Equation 75 shoes that the face width dimension

is much greater than dimensions perpendicular to the plane. Because of this reasoning, the gear is considered to be a wide gear and the assumption is made that the dynamic model is held under plane strain conditions. In equation 75, F_w is the face width, and ν is Poisson's ratio (Cornell & Westervelt, 1978; Lin & Liou; MacDonald, 2007). Other dimensions will be defined in chapter 3.

For plane strain, $\frac{F_w}{Y} > 5$ which means $E_e = \frac{E}{1-\nu^2}$ EQ. 75

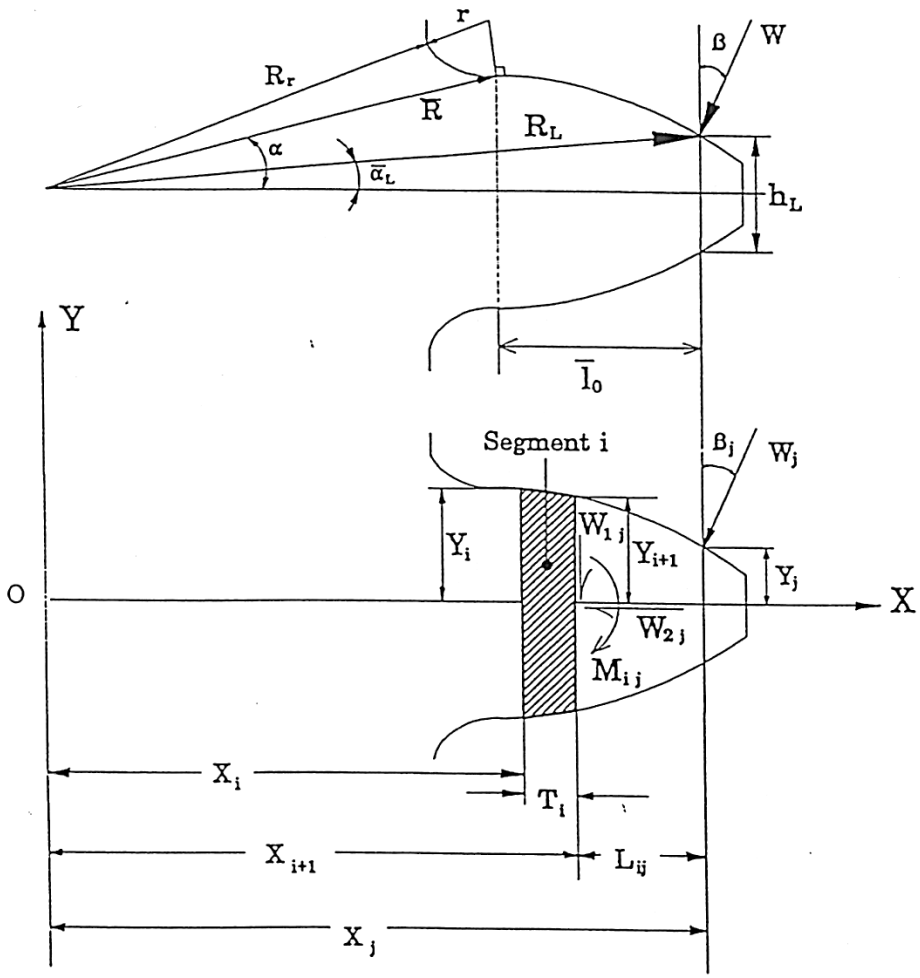

Figure 16. A graphical depiction of the dynamic deflection model (Lin & Liou, 1998, p. 13).

According to Lin and Liou (1998), the following equation is for deflection caused by the horizontal component of the applied load between the teeth, W_j COS β_j (pp. 14-15).

$$(q_w)_{ij} = \frac{W_j * \text{COS}\,\beta_j}{3 * E_e * I_i} * (T_i^3) + \frac{W_j * \text{COS}\,\beta_j}{2 * E_e * I_i} * \left(T_i^2 * L_{ij}\right) \qquad \text{EQ. 76}$$

For equation 76 and those that follow, T_i is the "thickness of segment I," E_e is the "effective Young's modulus of elasticity," L_{ij} is "the distance from j to i," W_j is the applied load, and I_i is the "moment of inertia of segment I" (Lin & Liou, 1998, p. 14). For a reference of these and related dimensions, refer to figure 16.

The following equation is for deflection caused by the bending moment, M_{ij} (Lin & Liou, 1998).

$$(q_M)_{ij} = \frac{W_j * \left(L_{ij} * \text{COS}\,\beta_j - Y_j * \text{SIN}\,\beta_j\right)}{2 * E_e * I_i} * (T_i^2) + \frac{W_j * \left(L_{ij} * \text{COS}\,\beta_j - Y_j * \text{SIN}\,\beta_j\right)}{E_e * I_i} * \left(T_i^2 * L_{ij}\right) \qquad \text{EQ. 77}$$

Deflection caused by shear is defined in the following manner (Lin & Liou, 1998).

$$(q_s)_{ij} = \frac{1.2 * W_j * T_i * \text{COS}\,\beta_j}{G * A_i} = \frac{2.4 * (1 + \nu) * W_j * T_i * \text{COS}\,\beta_j}{E_e * A_i} \qquad \text{EQ. 78}$$

G is the shear modulus and A_i is the "cross sectional area of segment i" (Lin & Liou, 1998, p. 15).

The next relationship is for deflection caused by axial loading of W_j SIN β_j (Lin & Liou, 1998).

$$(q_C)_{ij} = \frac{W_j * T_i * \text{SIN}\,\beta_j}{E * A_i} \qquad \text{EQ. 79}$$

The cumulative deflection and deformation for a segment due to loading with the plane strain assumption is as follows (Lin & Liou, 1998).

$$(q_I)_{ij} = (q_W + q_M + q_S)_{ij} * \text{COS}\,\beta_j + (q_C)_{ij} * \text{SIN}\,\beta_j \qquad \text{EQ. 80}$$

Expanded, equation 80 becomes equation 81 (Lin & Liou).

$$(q_I)_{ij} = W_j * \left\{ \frac{\text{COS}^2\,\beta_j}{E_e} * \left[\frac{T_i^3}{3 * I_i} + \frac{T_i^2 * L_{ij} + T_i * L_{ij}^2}{I_i} \right] \right. \qquad \text{EQ. 81}$$

$$- \frac{\text{COS}\,\beta_j * \text{SIN}\,\beta_j}{E_e} * \left[\frac{T_i^2 * Y_j}{2 * I_i} + \frac{T_i * Y_j * L_{ij}}{I_i} \right]$$

$$\left. + \frac{\text{COS}^2\,\beta_j}{E_e} * \left[\frac{2.4 * (1 + \nu) * T_i}{A_i} \right] + \frac{\text{SIN}^2\,\beta_j}{E_e} * \left[\frac{T_i}{A_i} \right] \right\}$$

As described by Lin and Liou (1998), deflection at the "fillet and tooth foundation flexibility" (pp. 16-19) depends greatly upon the dimensions of the fillet and the application of the load. Furthermore, Cornell and Westervelt (1978) state that "the fillet

angle," γ_f, should be 55 degrees for a low contact ratio, which is the case with this dynamic model (pp. 69-76).

As shown by Lin and Liou (1998), for a plane strain model, or a gear with a large face width, the following deflections of the fillet and foundation, q_f, can be added directly due to the "superposition principle" as shown in equations 82 to 84. The following detail, figure 17, describes the dimensions of the following deflection equations (pp. 18-19).

$$(q_f)_{ij} = (q_{fb})_{ij} + (q_{fe})_{ij} \qquad \text{EQ. 82}$$

q_f is the total deflection of tooth fillet, where q_{fb} is the "deflection at and in the direction of load due to beam compliance of fillet" and q_{fe} is the "deflection due to foundation effects" (Lin & Liou, 1998, p. 18).

$$(q_{fb})_{ij} = W_j * \left\{ \frac{COS^2\,\beta_j}{E_e} \right. \qquad \text{EQ. 83}$$

$$* \left[\frac{(T_{fb})_i^3}{3} + (T_{fb})_i^2 + (T_{fb})_i * (L_{fb})_{ij} \over (I_{fb})_i * \frac{2.4 * (1+\nu) * (T_{fb})}{(A_{fb})_i} \right]$$

$$- \frac{COS\,\beta_j * SIN\,\beta_j}{E_e} * \left[\frac{(T_{fb})_i^2 * Y_j}{2} + (T_{fb})_i * Y_j * (L_{fb})_{ij} \over (I_{fb})_i \right]$$

$$\left. + \frac{SIN^2\,\beta_j}{E_e} * \left[\frac{(T_{fb})_i}{(A_{fb})_i} \right] \right\}$$

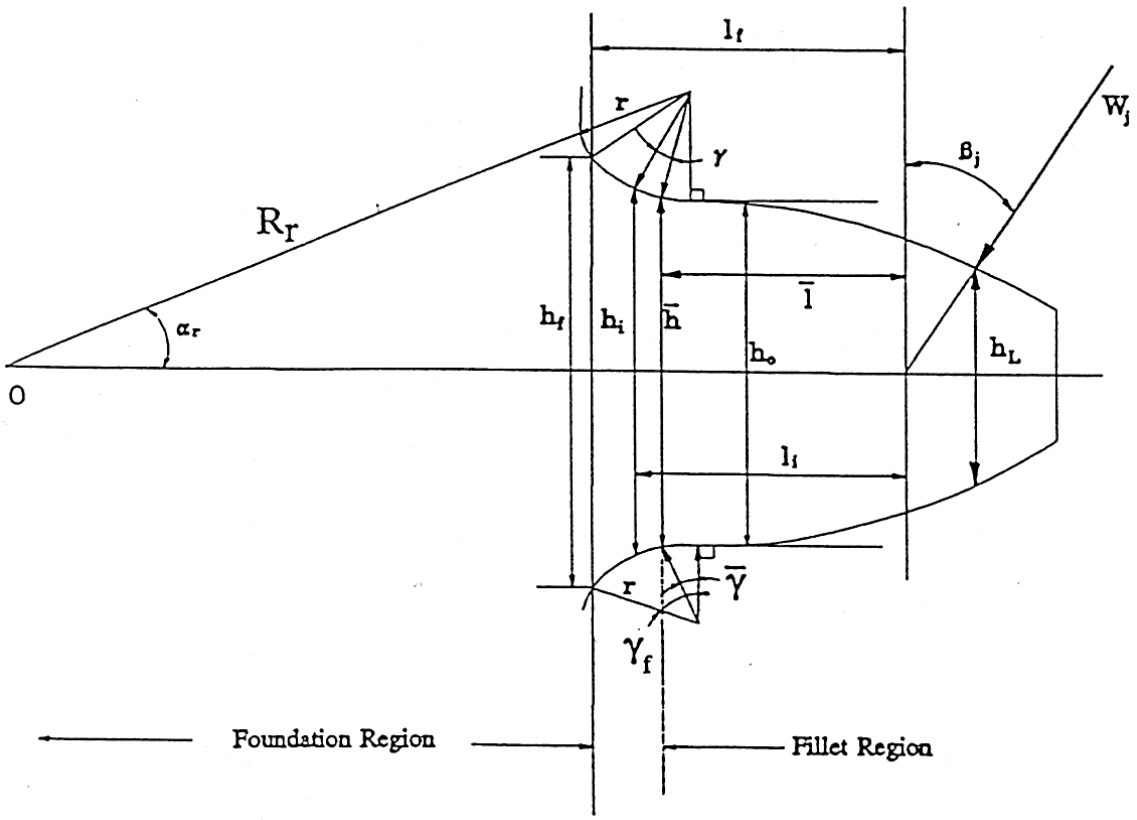

Figure 17. Schematic relating to "fillet and tooth foundation flexibility" (Lin & Liou, 1998, p. 19).

$$(q_{fe})_{ij} = \frac{W_j * COS^2\,\beta_j}{E_e * F_W} * (1-\nu^2) * \left\{ \frac{16.67}{\pi} * \left[\frac{(l_f)_i}{h_f} \right]^2 \right.$$

$$+2 * \left(\frac{1-\nu-2*\nu^2}{1-\nu^2} \right) * \left[\frac{(l_f)_i}{h_f} \right]$$

$$\left. + 1.534 * \left[1 + \frac{TAN^2\,\beta_j}{2.4*(1+\nu)} \right] \right\} \qquad \text{EQ. 84}$$

According to Lin and Liou (1998, p. 20) and Tavakoli and Houser (1985, pp. 529-535) contact between gear teeth can be modeled under the same assumption as two cylinders. The work by Tavakoli and Houser (1985) shows that $(q_L)_{ij}$ or the contact

"deflection is caused by line-contact and compression deformation." Equation 85 is the result of this author's work, where E_g is Young's Modulus for the given gear (pp. 529-535).

$$(q_L)_{ij} = \frac{1.275}{\left(\frac{2 * E_1 * E_2}{E_1 + E_2}\right)^{0.9} * F_w^{0.8} * W_j^{0.1}} \quad \text{EQ. 85}$$

As explained by Lin and Liou (1998) The cumulative deflection of each segment is defined as $(q_T)_j$, which is the summation of deflection caused by the applied load, $(q_W)_{ij}$, bending moment, $(q_M)_{ij}$, and contact deflection, $(q_L)_{ij}$, is shown as equation 86 (pp. 20-21).

$$(q_T)_j = \sum_{i=1}^{n} \left[(q_W)_{ij} + (q_M)_{ij} + (q_L)_{ij}\right] \quad \text{EQ. 86}$$

Lin and Liou then explain that the load, W_j, divided by the deflection, $(q_T)_j$, provides the stiffness for each segment, $(K_G)_J$. Moreover, the "total stiffness can be summed to determine the average tooth meshing stiffness, $(K_G)_{avg}$ (pp. 20-21).

$$(K_G)_i = \frac{W_J}{(q_T)_j} \quad \text{EQ. 87}$$

$$(K_G)_{avg} = \frac{1}{n} * \sum_{i=1}^{n} (K_G)_i \quad \text{EQ. 88}$$

Lin and Liou (1998) provide the following relationship:

> Because the mass of a rotating gear body is theoretically concentrated at the radius of gyration, the deflection reference used in this study is assumed to be at this radius. The theoretical deflection and stiffness of the gear teeth will be affected by changing the mass moment of inertia and the geometry of the gear body. (p. 21)

Transmission Error and Load Sharing. Lin and Liou (1998) define transmission error "as the departure of a meshed gear pair from a constant angular motion. Transmission error may [also] be defined as the [instantaneous] deviation of the following gear from an ideal nominal value." The authors proceed to state the main causes for transmission error: "tooth spacing error, ${}_{s}E$; tooth profile error, ${}_{p}E$, and run out error and combined deflection of meshing teeth, ${}_{d}E$" (Lin & Liou, 1998, pp. 23-24).

$$\left(E_T^k\right)_j = \left(\sum_{r=1}^{2} {}_{d}E_g^k\right)_j + \left(\sum_{r=1}^{2} {}_{p}E_g^k\right)_j + [P] * \left(\sum_{r=1}^{2} {}_{s}E_g^k\right)_j \qquad \text{EQ. 89}$$

Furthermore, k is the "mating tooth pairs in sequence," and P = 0 for k = 1 or P = 1 if $k \neq 1$. Subscript represents the appropriate gear (Lin & Liou, 1998, p. 23).

As the mating of each tooth pair as a patterned relationship, the load is shared among each pattern of mated teeth, as seen in the following equation described by the authors (Lin & Liou, 1998).

$$\left(E_T^k\right)_j = (E_T^1)_j = (E_T^2)_j = \cdots \qquad \text{EQ. 90}$$

$$W = \sum_{n=1}^{(CR)+1} W_j^n \qquad \text{EQ. 91}$$

For equation 91, CR represents the contact ratio (Lin & Liou, 1998).

The load applied to each tooth can be solved, simultaneously, by equations 89, 90, and 91, and which "tooth pairs are still in contact" (Lin & Liou, 1998, p. 24).

Friction between Gear Teeth. According to Oswald et al. (1996b, p. 3), the primary friction method used by the authors is the relationship derived by Buckingham (1949). The following formulas are based upon "empirical" methods, similar to methods developed by Buckingham. Once found, the friction, T_f, in approach and recess, as seen in figure 5, can be added to the dynamic system (Buckingham, 1949; Lin & Liou, 1998, pp. 24-26).

$$f = \frac{0.05}{e^{0.125*V_s}} + 0.002 * \sqrt{V_s} \qquad \text{EQ. 92}$$

And:

$$f_a = \frac{4 * f}{3} \qquad \text{EQ. 93}$$

$$f_r = \frac{2 * f}{3} \qquad \text{EQ. 94}$$

In equation 92, 93, and 94, f is the "average coefficient of friction," f_a is the "average coefficient of friction of approach," and f_r is the "average coefficient of recess" (Buckingham, 1949). V_s is the "sliding velocity" (Lin & Liou, 1998, p. 12).

Inertia and Stiffness Effects. As summarized by Lin and Liou (1998), the "polar mass moment of inertia, stiffness of shaft, and stiffness of connected masses" are part of the governing, dynamic equations (p. 31). Oswald et al. (1993) used the following assumption: "The gears [were assumed] to be solid steel disks equal to the pitch diameter. . . . No allowance for gear shaft inertia [was made]." This assumption allows the derivation of J_g, the polar mass moment of inertia of the gears (p. 5). Values for the input inertia, output inertia, input shaft torsional stiffness, and output shaft torsional stiffness used by Oswald et al. (1996b) are also used for this study (p. 4).

$$J_g = 0.00147 * \pi * R'_g * F_W \qquad \text{EQ. 95}$$

Damping Effects. The damping model of the gears used in the dynamic study is described by Lin and Liou (1998). "The mathematical description of damping is . . . complicated," so equations 96 and 97 approximate the "damping factor" (pp. 40-41). For the dynamic analysis, a gear damping ratio, ξ_{Gg}, of 0.10, is used. The damping ratios are "expressed as a fraction of critical damping." This value was stated by the authors as an average of the range of the range 0.03 to 0.17 found by Kasuba and Evans (1981, pp. 398-409) and Wang and Cheng (1981, pp. 177-187). In combination with the gear damping ratio, and stiffness, base radius, and polar moment of inertia for each gear tooth, the damping coefficient of gear tooth mesh, C_{Gg}, can be found (Lin & Liou, 1998, p. 41).

$$C_{G1} = 2 * \xi_{G1} * \sqrt{\frac{K_{G1}}{\left[\frac{(R_{b1})^2}{J_1} + \frac{(R_{b2})^2}{J_2}\right]}}$$ EQ. 96

$$C_{G2} = 2 * \xi_{G2} * \sqrt{\frac{K_{G2}}{\left[\frac{(R_{b1})^2}{J_1} + \frac{(R_{b2})^2}{J_2}\right]}}$$ EQ. 97

Damping of the shafts is described by Lin and Liou (1998) in equations 98 and 99. For the dynamic analysis, a shaft damping ratio, ξ_S, of 0.005 is used, which Lin and Liou (1998) established from Hahn (1969). In combination with the shaft damping ratio, shaft stiffness, and polar moment of inertia for the gear tooth, motor, and load, the shaft damping coefficient, C_S, can be found (Lin & Liou, 1998, pp. 40-41).

$$C_{S1} = 2 * \xi_{S1} * \sqrt{\frac{K_{S1}}{\left(\frac{1}{J_M} + \frac{1}{J_1}\right)}}$$ EQ. 98

$$C_{S2} = 2 * \xi_{S2} * \sqrt{\frac{K_{S2}}{\left(\frac{1}{J_D} + \frac{1}{J_1}\right)}}$$ EQ. 99

Dynamic Equations of Motion. The dimensions and conditions put forth by the static analysis and Lin and Liou (1998) display the complexity of the gear system, which involves inertia, stiffness, damping, friction, torque, deflection, and load transmission

error across various elements of the system. In order to reduce the complexity, the system is broken up into a "number of lumped masses connected elastically." Moreover, the following assumptions are made in the dynamic model employed within DANST. First, "damping . . . due to material . . . and . . . lubrication . . . is expressed as a constant damping coefficient." Second, "the differential equations of motion are expressed along the theoretical line of action. Third, "the reference point for tooth deflection is assumed to be located along the tooth centerline at the radius gyration of the gear body." The equation model can be graphically described by figure 14 and figure 18 (pp. 34-40).

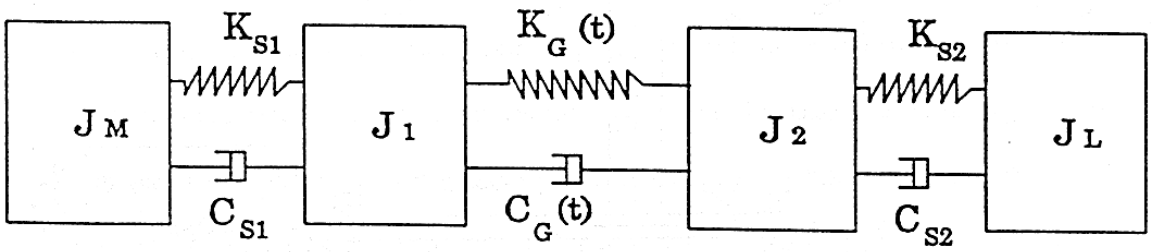

Figure 18. Dynamic model and specific variables (Lin & Liou, 1998, p. 36).

According to Lin and Liou (1998), the governing equations are as follows (p. 37).

$$J_M\ddot{\theta}_M + C_{s1}(\dot{\theta}_M - \dot{\theta}_1) + K_{s1}(\theta_M - \theta_1) = T_M \qquad \text{EQ. 100}$$

$$J_1\ddot{\theta}_1 + C_{s1}(\dot{\theta}_1 - \dot{\theta}_M) + K_{s1}(\theta_1 - \theta_M) + C_g(t)[R_{b1}(R_{b1}\dot{\theta}_1 - R_{b2}\dot{\theta}_2)] \qquad \text{EQ. 101}$$
$$+K_g(t)[R_{b1}(R_{b1}\theta_1 - R_{b2}\theta_2)] = T_{f1}(t)$$

$$J_2\ddot{\theta}_2 + C_{s2}\left(\dot{\theta}_2 - \dot{\theta}_1\right) + K_{s2}(\theta_2 - \theta_1) + C_g(t)\left[R_{b2}\left(R_{b2}\dot{\theta}_2 - R_{b1}\dot{\theta}_1\right)\right] \quad \text{EQ. 102}$$

$$+K_g(t)[R_{b2}(R_{b2}\theta_2 - R_{b1}\theta_1)] = T_{f2}(t)$$

$$J_L\ddot{\theta}_L + C_{s2}\left(\dot{\theta}_L - \dot{\theta}_2\right) + K_{s2}(\theta_L - \theta_2) = -T_L \quad \text{EQ. 103}$$

In general, J represents the "mass moments of inertia" of the gears, motor, or load. C represents the "damping coefficients" of the gears or shafts. K represents the stiffness of the gears or shafts. T represents the torque of the motor, the load, or the friction between the gears. The subscript refers to the appropriate gear, shaft, or module (Lin & Liou, 1998, pp. 35-38). θ, $\dot{\theta}$, and $\ddot{\theta}$ are the angular displacement, velocity, and acceleration, respectively (Lin et al., 1987, p. 3). For a list of terms of these equations and those that follow, refer to chapter 2 or the list of terminology.

According to Lin and Liou (1998), the equations of motion also require convergence relationships and conditions relating to tooth location. Since the governing equations of motion are nonlinear, they are solved simultaneously by numerical methods. In order to begin the first step of the numerical process, initial conditions of angular displacement and velocity are required (pp. 34-40). Lin and Liou (1998) explain the initial values as follows:

> Starting values are obtained through preloading the input shaft with the output shaft fixed. The preload torque is the static design torque carried by the system. The equations of motion are linearized by dividing the mesh into many equal intervals. Those equations are solved by an iteration technique incorporating the nominal initial values. At each step X_n and V_n need to be compared respectively with the initial value X_0 and V_0 to confirm the iteration convergence. . . . The same steps are repeated by averaging the initial and calculated values of angular displacement X_n, and angular velocity V_n, as the new initial values of [the] next period, respectively. (pp. 38-39)

The convergence relationships described Lin and Liou (1998) are shown in equations 104 and 105 (pp. 38-39).

$$|X_n - X_0| \leq 0.05 * X_0 \quad \text{EQ. 104}$$

$$|V_n - V_0| \leq 0.05 * V_0 \quad \text{EQ. 105}$$

In order to solve the equations of motion, the following conditions exist, each of which results in a "specific dynamic condition." When the gears are in contact, the following equation 106 exists which represents the "relative dynamic displacement between gear one and gear two." This results in equation 107 and 108, since the load is equally shared among the tooth pair (Lin & Liou, 1998, p. 39).

$$R_{b1} * \theta_1 - R_{b2} * \theta_2 > 0 \quad \text{EQ. 106}$$

$$W_{d1} = K_G(t) * (R_{b1} * \theta_1 - R_{b2} * \theta_2) + C_g(t) * \left(R_{b1} * \dot{\theta}_1 - R_{b2} * \dot{\theta}_2\right) \quad \text{EQ. 107}$$

$$W_{d2} = W_{d1} \quad \text{EQ. 108}$$

W_{dg} is the dynamic load on the given gear tooth (Lin & Liou, 1998).

When the gears loose contact, the following conditions 109 and 110 exist. This results in equation 111, since the load is lost (Lin & Liou, 1998).

$$R_{b1} * \theta_1 - R_{b2} * \theta_2 \leq 0 \qquad \text{EQ. 109}$$

$$|R_{b1} * \theta_1 - R_{b2} * \theta_2| \leq B \qquad \text{EQ. 110}$$

$$W_{dg} = 0 \qquad \text{EQ. 111}$$

When the gears are in contact on the non-load side, the following conditions 112 and 113 exist. This results in equation 114 and 115, since the load is equally shared among the tooth pair (Lin & Liou, 1998).

$$R_{b1} * \theta_1 - R_{b2} * \theta_2 \leq 0 \qquad \text{EQ. 112}$$

$$|R_{b1} * \theta_1 - R_{b2} * \theta_2| > B \qquad \text{EQ. 113}$$

$$W_{d1} = K_G(t) * [(R_{b1} * \theta_1 - R_{b2} * \theta_2) - B] + C_g(t) * \left(R_{b1} * \dot{\theta}_1 - R_{b2} * \dot{\theta}_2\right) \qquad \text{EQ. 114}$$

$$W_{d2} = W_{d1} \qquad \text{EQ. 115}$$

Lin and Liou (1998) also describe how the dynamic equations of motion, equations 100 to 103, can be used to find the "undamped natural frequencies" of the system. This is done by removing the "damping and excitation terms" from the system. In order to "facilitate the solution [of] eigenvalues," $(K_G)_{avg}$, which is defined in

equations 87 to 88, is used in the undamped equations of motion. Once the matrix is set, as shown in equation 116, it can be solved numerically (pp. 41-42).

$$\begin{bmatrix} J_M & 0 & 0 & 0 \\ 0 & J_1 & 0 & 0 \\ 0 & 0 & J_2 & 0 \\ 0 & 0 & 0 & J_L \end{bmatrix} \begin{bmatrix} \ddot{\theta}_M \\ \ddot{\theta}_1 \\ \ddot{\theta}_2 \\ \ddot{\theta}_L \end{bmatrix} + \begin{bmatrix} k_{S1} & -k_{S1} & 0 & 0 \\ -k_{S1} & k_{S1} + (k_G)_{avg} R_{b1}^2 & -(k_G)_{avg} R_{b1} R_{b2} & 0 \\ 0 & -(k_G)_{avg} R_{b1} R_{b2} & k_{S2} + (k_G)_{avg} R_{b2}^2 & -k_{S2} \\ 0 & 0 & -k_{S2} & k_{S2} \end{bmatrix} \begin{bmatrix} \dot{\theta}_M \\ \dot{\theta}_1 \\ \dot{\theta}_2 \\ \dot{\theta}_L \end{bmatrix} = [0]$$

EQ. 116

Dynamic Stress. For the dynamic analysis, the stress at the fillet can be found from equation 117, as described by Lin and Liou (1998, pp. 43-46) and found by Heywood (1952) and continued by Cornell (1981, pp. 447-459). Equation 117 combines the tooth dimensions, deformations, and relevant characteristics found by solution of the equations of motion. Moreover, σ_j is the stress used in this study. In equation 117, ν is 1/4 and r_f is the fillet radius. Moreover, γ_s is 30 degrees for this study. For a further description of the dimensions and variables in equation 117, see the nomenclature and figure 19 (Lin & Liou, 1998, pp. 43-46).

$$\sigma_j = \frac{W_j * \mathrm{COS}\,\beta_j}{F_W} * \left[1 + 0.26 * \left(\frac{h_s}{2 * r_f}\right)^{0.7}\right] \qquad \text{EQ. 117}$$

$$* \left\{ \frac{6 * l_s - \left(\frac{h_L * \mathrm{TAN}\,\beta_j}{2}\right)}{(h_s)^2} + \left(\frac{0.72}{h_s * l_s}\right)^{0.5} \right.$$

$$\left. * \left(1 - \frac{h_L}{h_s} * \nu * \mathrm{TAN}\,\beta_j\right) * \frac{\mathrm{TAN}\,\beta_j}{h_s} \right\}$$

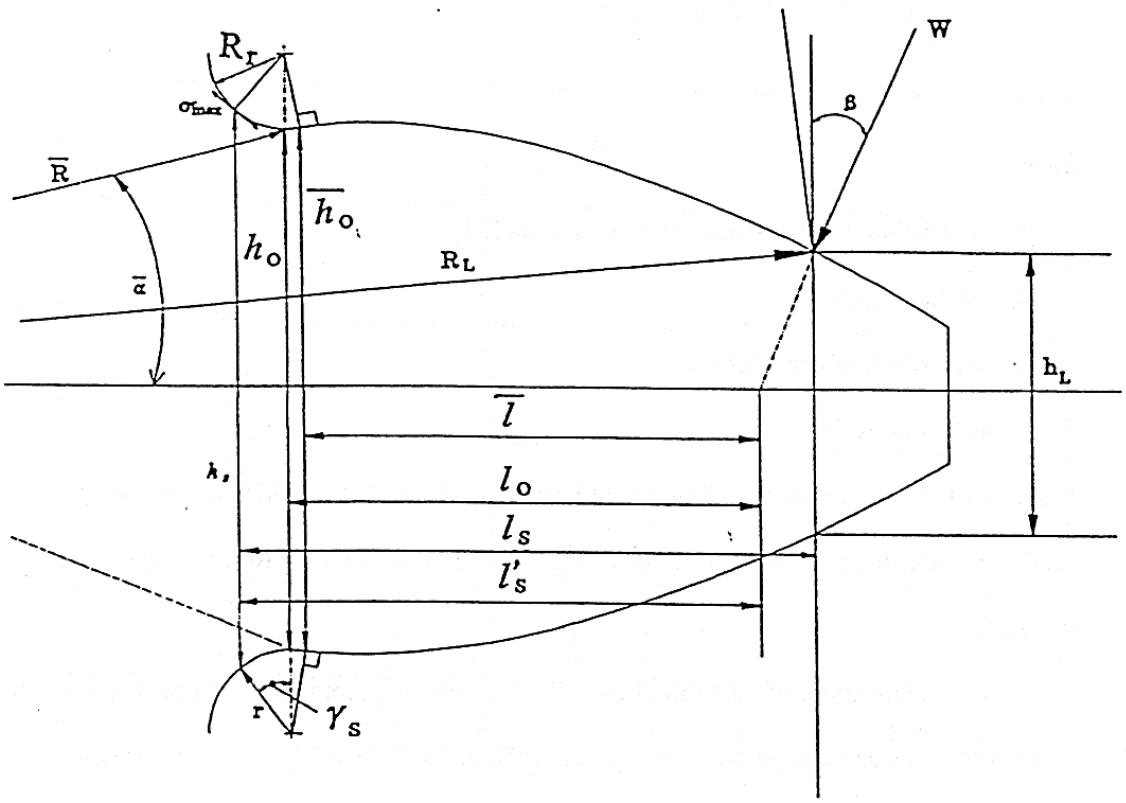

Figure 19. Dimensions relating to dynamic stress from studies by Heywood (1952) and Cornell (1981, pp. 447-459).

Dynamic Factoring. Lin and Liou (1998) stated that as part of the dynamic analysis, the DANST program presents a "non-dimensional" dynamic factor. The

dynamic load factor is a “ratio of maximum dynamic load to total applied load, and the dynamic stress factor, which is the ratio of maximum dynamic stress to maximum static stress” (pp. 45-48).

Chapter 3

Results and Discussion

3.1. Overview of the Parametric Study

As stated in previous chapters, the introduction, dynamic effects in a spur gear assembly become increasingly important as the speed within the system increases. These dynamic affects often exceed the static affects, and are the source of gear wear, noise, and vibration (Lin et al., 1996). Using the DANST program, a parametric study can be performed whereby certain dimensions and values are held constant, while other parameters are varied, and certain output is measured.

The design of both the static and dynamic model is shown in chapter 2. According to Lin et al. (1996), and Green and Mabie (1980a), an increase in the standard center distance does not directly equal the total pinion and gear offset, as e_1 and e_2 are independently related but cannot be found separately. Often, e_1 is set as a known variable and e_2 is found from e_1. It follows that the difference in stress cannot be directly equalized by any direct equation. By a parametric study, with certain dimensions set, the static or dynamic stress difference can be minimized for both pinion and gear.

The following gear design problem follows dimensions and methods developed by Lin et al. (1996) and Green and Mabie (1980b).

3.2. Design Dimensions and Variables

Green and Mabie (1980b) define the base variables used in study. The diametral pitch, P_d, is 10.0 (p. 507). As explained by Mabie and Reinholtz (1987), the diametral pitch is found by dividing the number of teeth by the pitch diameter. Though this results in dimensions of teeth per inch, it is standard gear design practice that units are not

assigned (p. 143). Set by Green and Mabie (1980b), the pressure angle, φ, is taken to be 20.0 degrees. This is also the pressure angle cut by the pinion cutter, φ_c. In certain steps, the two are the same and interchangeable during the study. The center distance extension above standard is 0.10 inches, which results in an operating center distance, C', of 3.100 inches. The number of teeth of the pinion and gear, N_1 and N_2, are 20 and 40 teeth, respectively. The pitch radius of the pinion cutter, R_c, is 2.0 inches. The backlash, B, is set as 0.0 (p. 507). Though the DANST program (Oswald et al., 1996b) has the capability of modeling "various combinations of tooth profiles" (p. 1), in this study, the teeth are of a "standard, full depth" dimension, where k = 1 (Green & Mabie, 1980a, p. 495) and are of a coarse pitch (Rogers et al., 1990, p. 633).

The dimensions relating to the dynamic affects are set by Lin, Liou, Oswald, and Townsend (1996). In this model, the input torque is set as 480 inch-pounds (p. 3).

The face width is chosen to be 1.0 inch. This is set to make a plain strain model, and to provide a simple load per inch calculation within the model. The rotational speed is set between 1000 and 30,000 revolutions per minute to provide a range which covers two of the system natural frequencies of the design as is described in table 2 and table 3. An increment of 146.0 rpm provides 199 data points in this range. The radius at the tip of the pinion cutter, r_{cT}, is set at 0.0. As shown by equation 40, this results in a RCEG value of 0.0. From information deduced from Colbourne (1987), a small value for r_{cT} results in a small radius of curvature for the cut gear fillet. Correspondingly, this results in a large stress concentration at the root of the tooth. The value, r_{cT}, set to 0.0 results in a conservative or maximum stress design (pp. 133-136).

In this parametric study, e_1 is set in a range from 0.0 to 0.077 inches. An increment of 0.001 inches provides 77 data points for this range. Similar to Lin, Liou, Oswald, and Townsend (1996) this range of e_1 is predefined so that no undercutting occurs and the teeth do not end in a point at the tip (p. 3).

Table 1. Design dimensions and variables

Tooth type: Coarse pitch, full depth, involute tooth	
Pinion cutter type: Fellows-type cutter	
Diametral pitch	10.0
Pressure angle [degree]	20.0
Center distance extension [inch]	0.100
Number of teeth, (pinion/gear)	20/40
Backlash [inch]	0.0
Pinion cutter radius [inch]	2.0
Face width [inch]	1.0
Input torque [inch-pound]	480.0
Radius at tip of pinion cutter tooth [inch]	0.0
Young's modulus [psi]	30000000
Input and output inertia [lb-in-s^2]	0.100/0.124
Input and output shaft torsional stiffness [lb-in-s^2]	150000.0
Pinion offset range [inch]	0.000 to 0.077
Rotational speed range [rpm]	1000 to 30000
Static tooth load [pound/inch]	510.8

(Green & Mabie, 1980a, p. 491; Green & Mabie, 1980b, pp. 507-508; Lin et al., 1996, p. 3; Oswald et al., 1996b, pp. 4-6; Rogers et al., 1990, p. 633).

As explained by Lin et al. (1996), the following equation, given in terms of number of teeth of gears, operating and cutting pressure angles, and diametral pitch, was used to obtain the offset for the driven gear, e_2, for gears cut by a hob cutter (p. 2).

$$e_1 + e_2 = \frac{(N_1 + N_2) * (\text{INV}\ \varphi_c' - \text{INV}\ \varphi_c)}{2 * P_d * \text{TAN}\ \varphi_c} \qquad \text{EQ. 118}$$

To change the design from a hob cutter to a pinion cutter complicates the design. In order to find the offset of the driven gear cut by a pinion cutter, e_2, equation 33, shown in chapter 2 (Rogers et al., 1990), is used, incorporating the dimensions and variables shown previously and in table 1.

With these design dimensions and variables set, according to table 1 and equation 33, a relationship can be established between pinion offset [inch], e_1, and gear offset [inch], e_2. This relationship is shown in equation 119, with a correlation, or r^2 value, of approximately 1.0.

$$e_2 = -1.7097 * (e_1)^2 - 0.8473 * e_1 + 0.1022 \qquad \text{EQ. 119}$$

For a backlash of 0.0 inches and the dimensions provided in table 1, the gear assembly is statically balanced when the pinion offset, e_1, is 0.0631 inches and the gear offset, e_2, is 0.0419 inches. These values result in a stress at the root of the tooth due to bending caused by the tangential component of the tooth load that is closely equal in both pinion and gear, approximately 14,000 psi (Green & Mabie, 1980b; Mabie et al., 1983).

3.3. Dynamic Stress and System Resonance

The following results from the DANST program are shown in figures 20 through 27. The data comprises of more than 15,000 data points: 77 increments in the pinion offset range and 199 in the gear assembly rotating speed range as described in chapter 3 section 2. This data is shown as one-dimensional plots as stress versus the pinion offset or rotating speed axes, and a two-dimensional and three-dimensional contour plot with all three axes: stress, pinion offset, and rotating speed.

Each of the figures shows an important aspect of the dynamic design. As developed by Lin et al. (1987), the system as a whole contains certain natural frequencies, also called critical speeds or resonances that work to excite the system and produce amplified stress conditions. The analytical experimentation of the authors showed that the dynamic amplification caused near these critical speeds produced "tooth separation." The resulting dynamic loads produced at these speeds result in greater gear wear and damage. The findings by the authors are further supported by the literature (p. 5).

Furthermore, analytical experimentation performed by the Lin, Huston, and Coy (1987) revealed the existence of secondary dynamic effects, "a nonlinear effect of the time varying tooth stiffness" called "parametric resonance" (p. 5). These secondary effects were further defined in Nafeh and Mook (1987). Finally, as the speed increases past the critical speeds, the dynamic effects smooth and diminish (Lin et al., 1987).

From the figures, the system resonances are seen, as is the general trend as the pinion offset increases. High ridges and valleys can be seen in the contour plots. Figures 20, 21, 22, and 23 show the maximum dynamic stress and system resonances experienced by the pinion during rotation and contact.

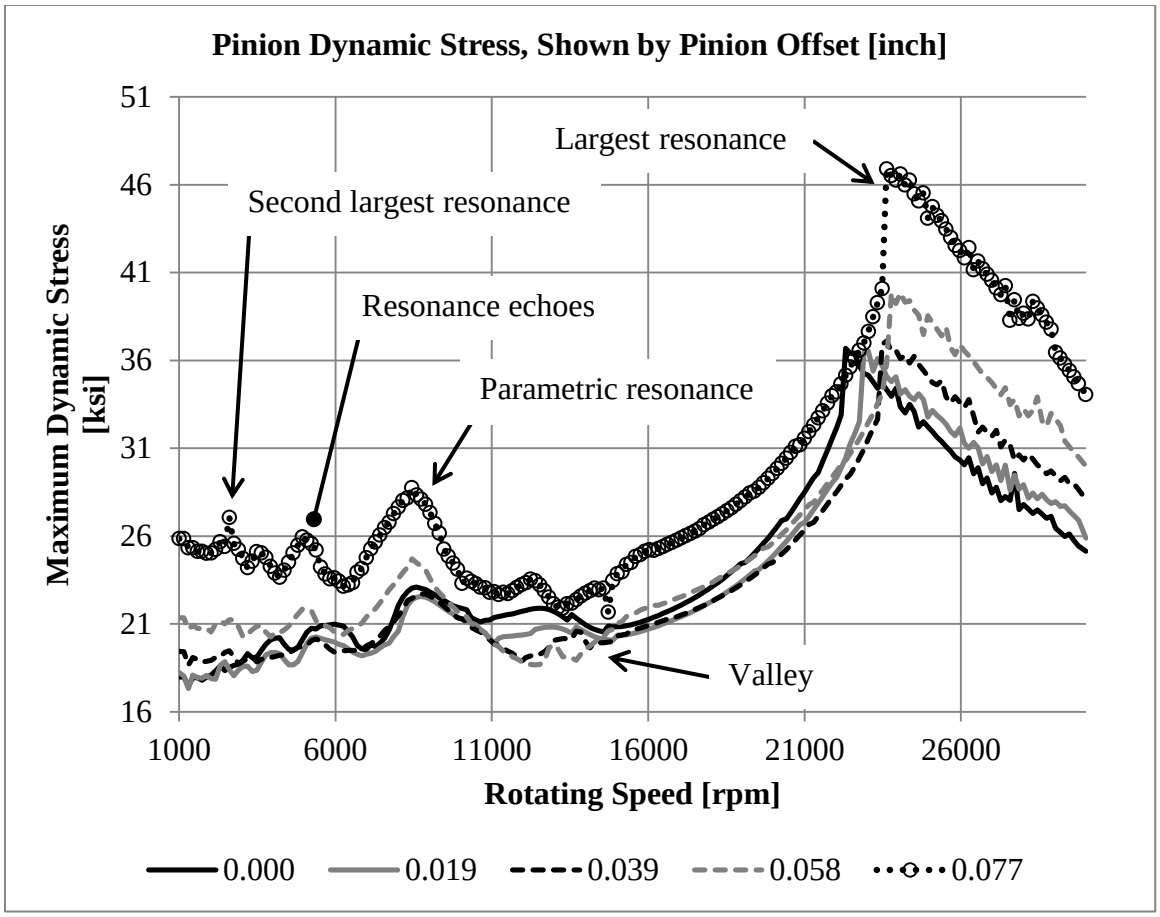

Figure 20. Pinion dynamic stress, shown by pinion offset [inch], e_1, with maximum dynamic stress [ksi] versus gear assembly rotating speed [rpm]. Offset for e_1, 0.077 inches, shows the number of data points.

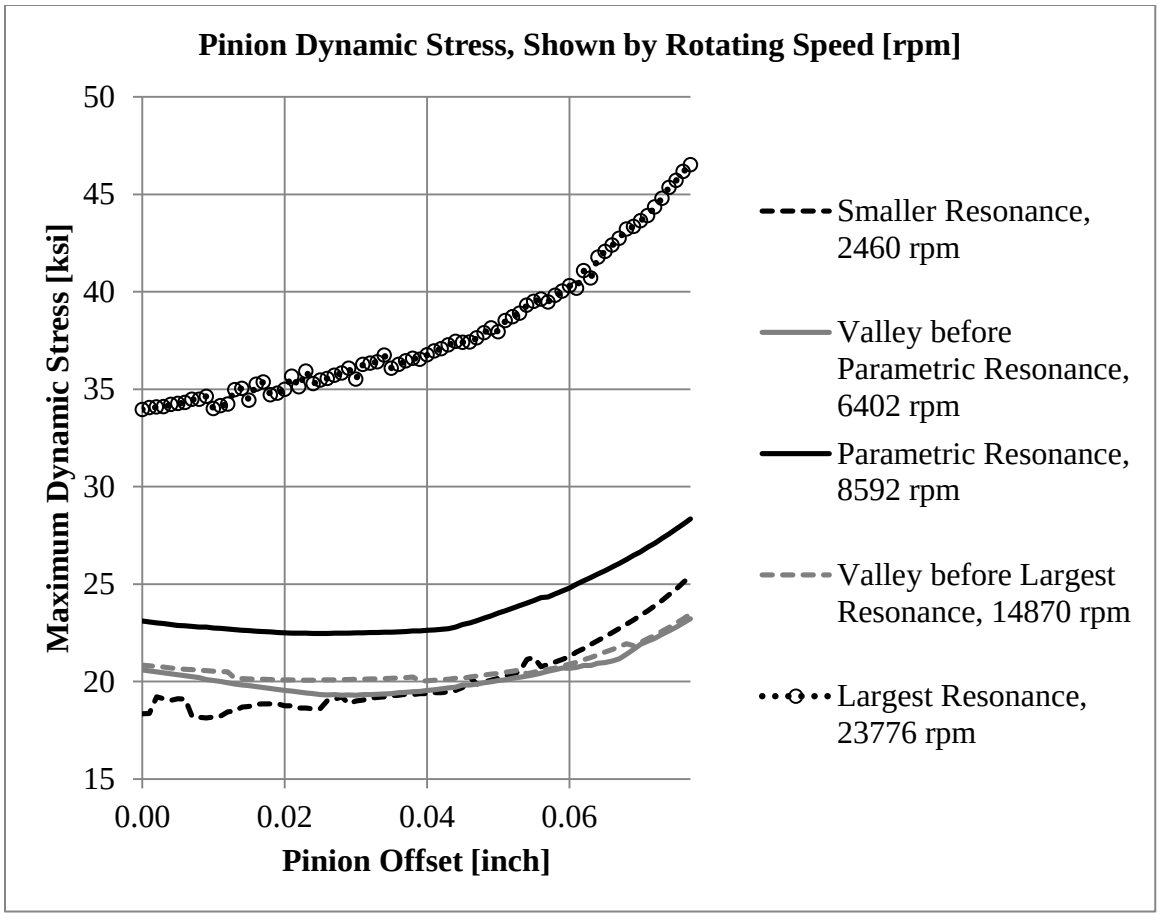

Figure 21. Pinion dynamic stress, shown by gear assembly rotating speed [rpm], with maximum dynamic stress [ksi] versus pinion offset [inch], e_1. Rotating speed 23776 rpm shows the number of data points.

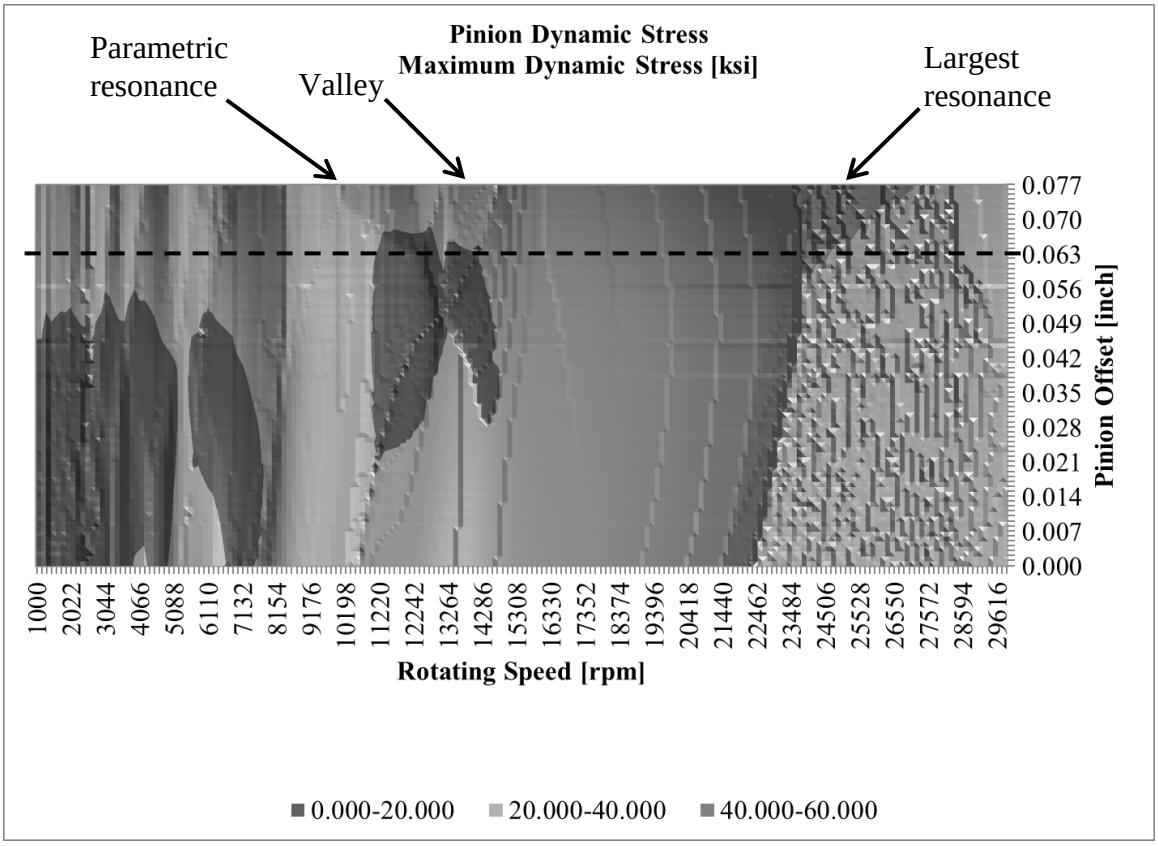

Figure 22. Two-dimensional plot of pinion dynamic stress [ksi] on gear assembly rotating speed [rpm] and pinion offset [inch], e_1, a dashed line shows where the stress at the root of the pinion and gear tooth is statically balanced.

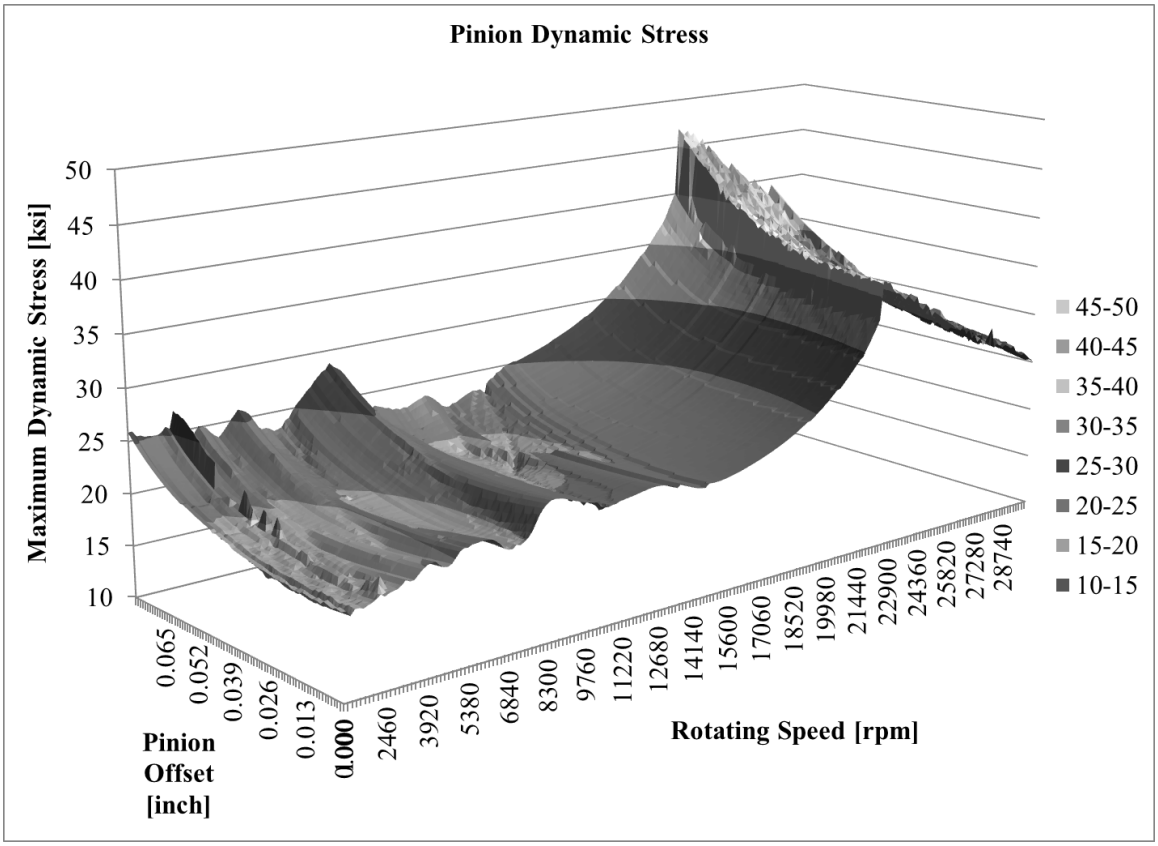

Figure 23. Three-dimensional plot of pinion dynamic stress [ksi] on gear assembly rotating speed [rpm] and pinion offset [inch], e_1.

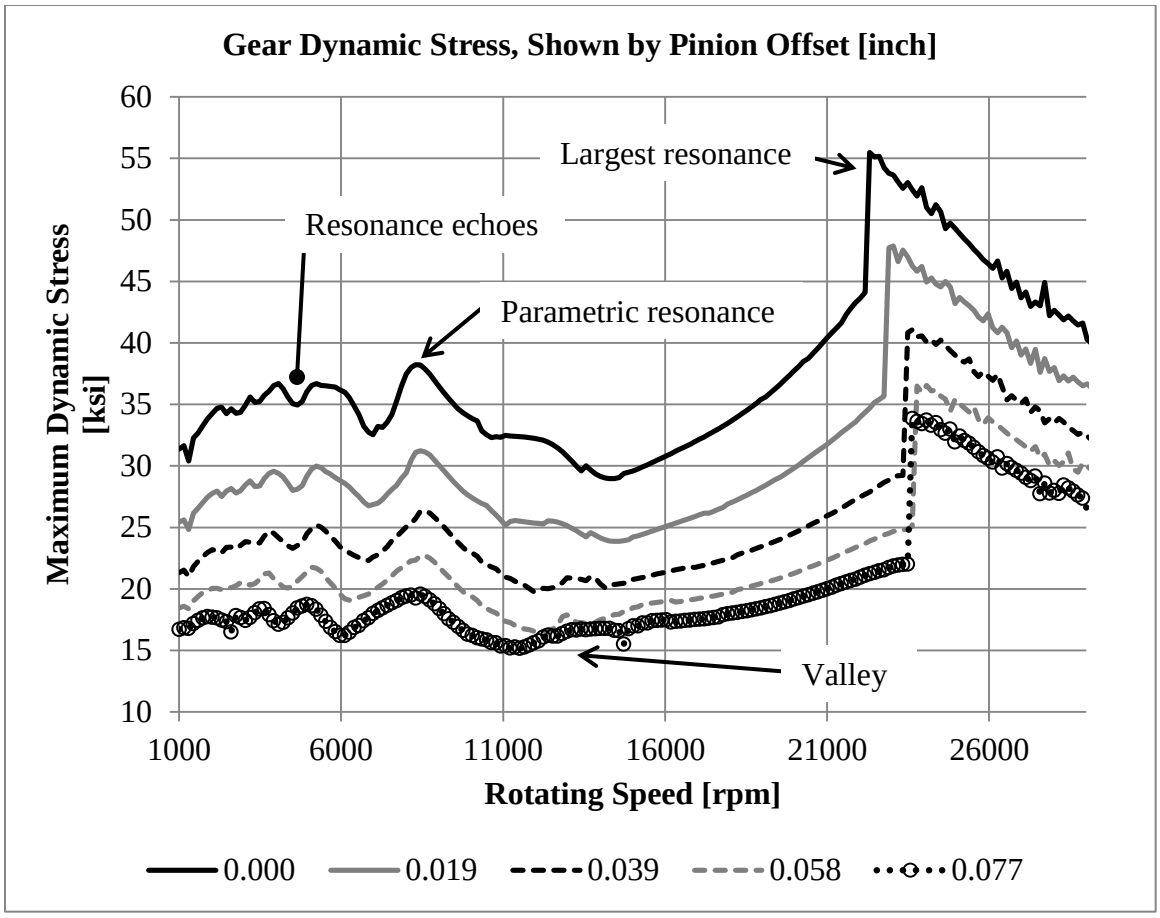

Figure 24. Gear dynamic stress, shown by pinion offset [inch], e_1, with maximum dynamic stress [ksi] versus gear assembly rotating speed [rpm]. Offset for e_1, 0.077 inches, shows the number of data points.

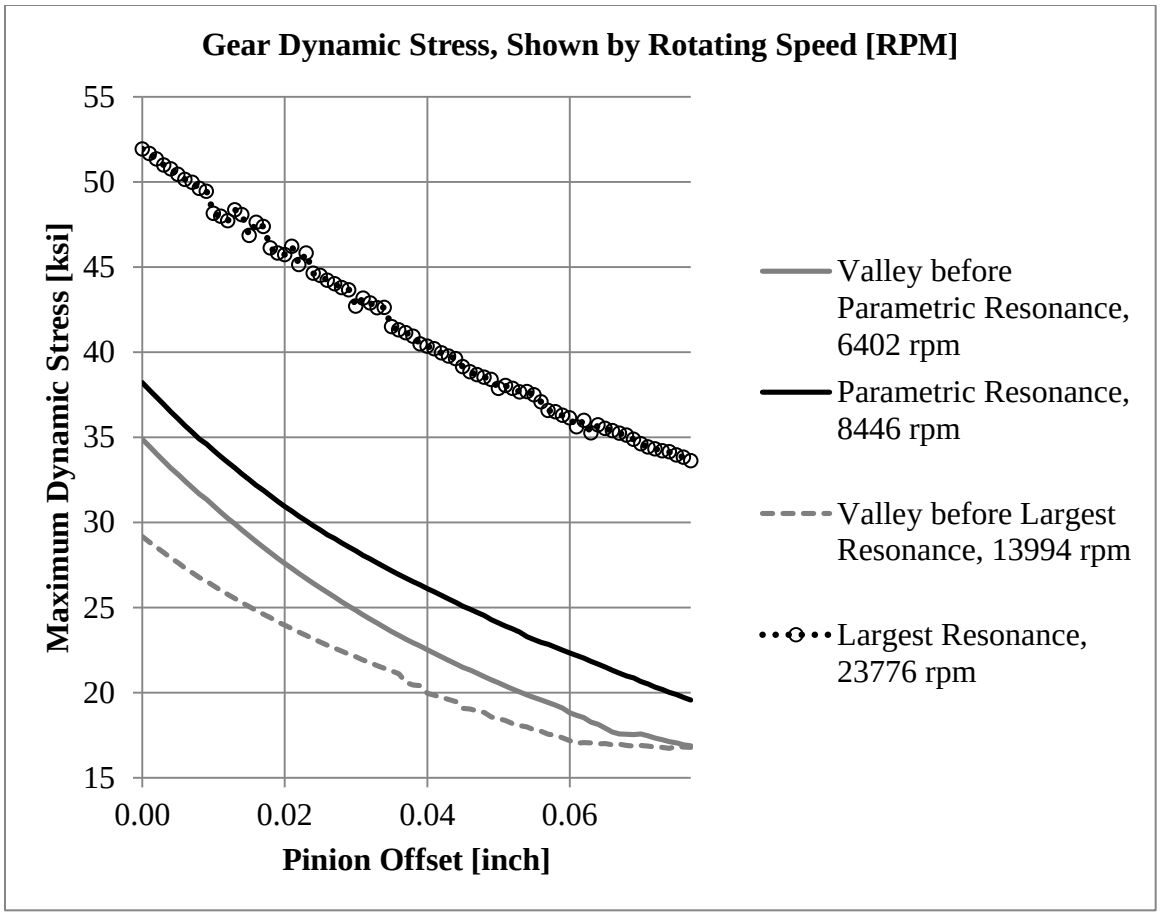

Figure 25. Gear dynamic stress, shown by gear assembly rotating speed [rpm], with maximum dynamic stress [ksi] versus pinion offset [inch], e_1. Rotating speed 23776 rpm shows the number of data points.

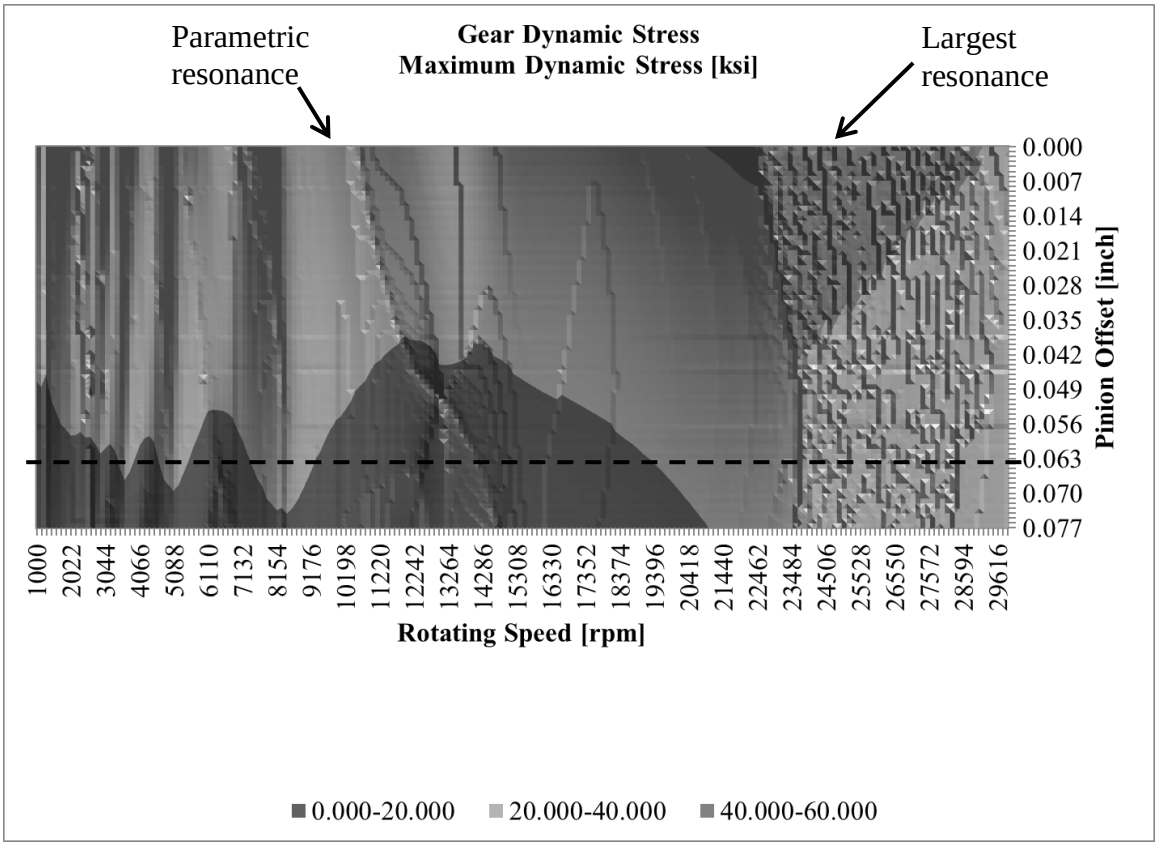

Figure 26. Two-dimensional plot of gear dynamic stress [ksi] on gear assembly rotating speed [rpm] and pinion offset [inch], e_1, a dashed line shows where the stress at the root of the pinion and gear tooth is statically balanced.

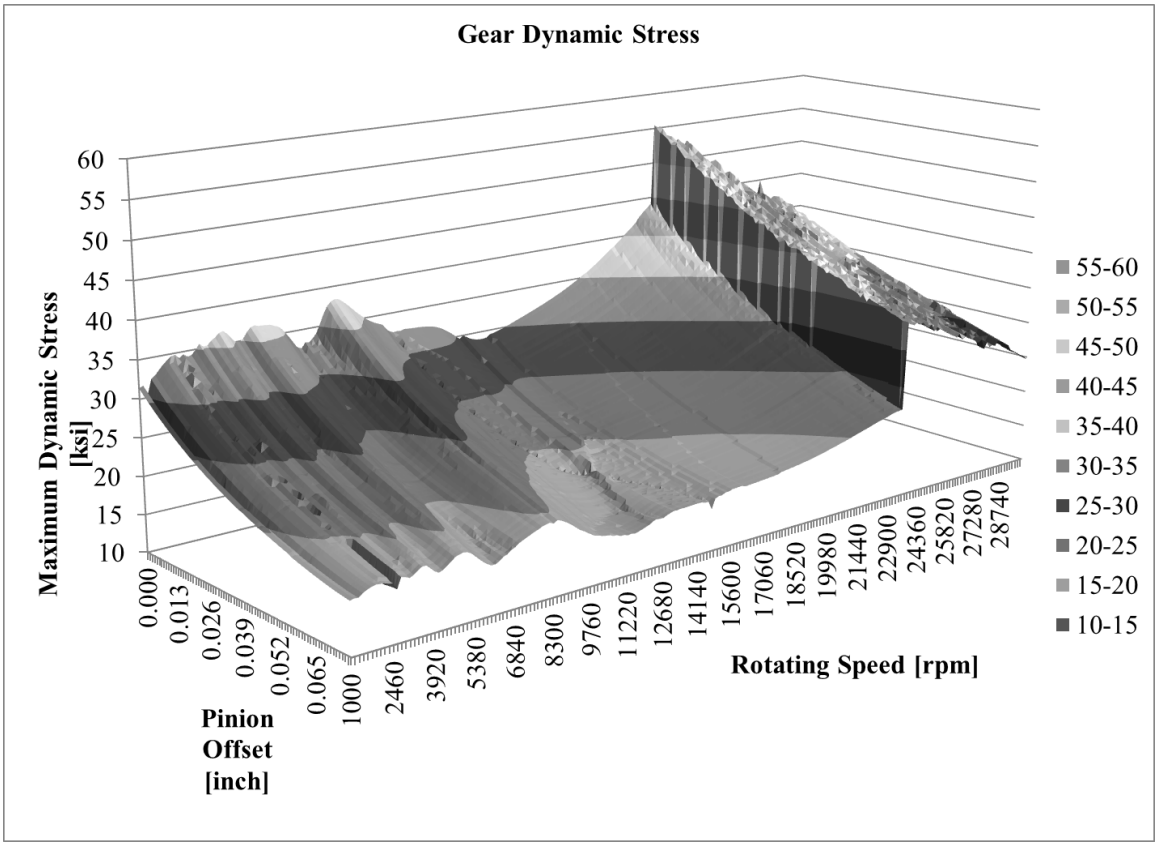

Figure 27. Three-dimensional plot of gear dynamic stress [ksi] on gear assembly rotating speed [rpm] and pinion offset [inch], e_1.

Table 2. Natural frequency and prediction of system resonance of pinion

Pinion - Driver - Gear-1								
Natural Frequency of Pinion			System Resonance					
Pinion Offset	Index F_n		Index	Percen-tage of Index F_n	Index	Percen-tage of Index F_n	Parametric of Index	Percen-tage of Index F_n
	3	4	3	3	4	4	Para-4	4
[inch]	[rpm]	[rpm]	[rpm]	[%]	[rpm]	[%]	[rpm]	[%]
0.000	2580	24828	2314	89.7%	22316	89.9%	8952	36.1%
0.010	2581	25095	2314	89.7%	22754	90.7%	8592	34.2%
0.019	2581	25364	2460	95.3%	23046	90.9%	8738	34.4%
0.029	2582	25500	2460	95.3%	23192	90.9%	8738	34.3%
0.039	2582	25666	2606	100.9%	23630	92.1%	8738	34.0%
0.048	2582	25650	2606	100.9%	23776	92.7%	8446	32.9%
0.058	2582	25669	2606	100.9%	24068	93.8%	8446	32.9%
0.067	2582	25486	2752	106.6%	23776	93.3%	8446	33.1%
0.077	2581	25273	2606	101.0%	23630	93.5%	8446	33.4%

Table 3. Natural frequency and prediction of system resonance of gear

Gear - Driven - Gear 2					
Natural Frequency of Pinion		System Resonance			
Pinion Offset	Index	Index	Percentage of Index F_n	Parametric of Index	Percentage of Index F_n
	4	4	4	Para-4	Para-4
[inch]	[rpm]	[rpm]	[%]	[rpm]	[%]
0.000	24828	22316	89.9%	8300	33.4%
0.010	25095	22754	90.7%	8446	33.7%
0.019	25364	23046	90.9%	8446	33.3%
0.029	25500	23192	90.9%	8446	33.1%
0.039	25666	23630	92.1%	8592	33.5%
0.048	25650	23776	92.7%	8446	32.9%
0.058	25669	24068	93.8%	8592	33.5%
0.067	25486	23776	93.3%	8446	33.1%
0.077	25273	23630	93.5%	8446	33.4%

Figure 20 directly shows the resonance and excitation experienced by the pinion throughout the speed range. The largest resonance is shown as a high ridge, and the accompanying parametric resonance which precedes it is seen as the next highest point. At lower speeds, below 7,000 rpm, minor resonance echoes exist, as well as the second resonance of the system as seen with the small spikes in stress seen at about 2,500 rpm. As is expected, the dynamic affects begin to decrease after resonance, followed by a valley of low stress.

Figure 21 shows the same dynamic stress of the pinion from the perspective of the pinion offset. This figure shows the general trend of an increase in stress for an increase in pinion offset. Once again, the system resonances and valleys are seen. The resonances are shown as black lines and the valleys are shown as gray lines. For low values of pinion offset, the smaller resonance is at a lower stress than the valleys preceding other resonance peaks. As can be seen in figure 20, there are a series of peaks and valleys between the smaller resonance and the parametric resonance. This is because the effects of resonance echoes interfere with and surpass primary resonances.

Figure 22 is a contour plot of figures 20 and 21, showing the maximum pinion dynamic stress plotted against pinion offset and rotational speed. In this figure, the decrease in stress for a decrease in pinion offset can be seen. An area of low dynamic effects, or valley, also exists after the parametric resonance. A dashed line indicates the location of statically balanced gear system by stress at the root of the pinion and gear tooth as found by Mabie and Green (1980b).

Figure 23 is a three-dimensional contour plot of figure 22. Many of the trends discussed in figures 20, 21, and 22 are shown in general in this figure.

Next, maximum dynamic stress plots relating to the gear are presented. Figure 24 directly shows the resonance and excitation experienced by the gear throughout the speed range. The largest resonance is shown as a high ridge, and the accompanying parametric resonance which precedes it is seen as the next highest point. Again, below 7,000 rpm, minor resonance echoes exist. However, the second resonance of the system is completely surpassed by the largest resonance and preceding echoes. Once again, the dynamic affects begin to decrease and smooth after resonance, followed by a valley of low stress.

Figure 25 shows the same dynamic stress as figure 24 of the gear from the perspective of the pinion offset, with system resonances and valleys. The resonances are shown as black lines and the valleys are shown as gray lines. Opposite to the general trend of the pinion in figure 21, the stress decreases with increasing pinion offset. Also, the trend in stress of the gear is approximately 1.5 times greater than that of the pinion.

Figure 26, which is similar to figure 22, is a contour plot of figures 24 and 25, showing the maximum gear dynamic stress plotted against pinion offset and rotational speed. The greater stress trend seen in figure 25 has the effect of reducing the appearance of valleys that are seen in figure 22. A dashed line indicates the location of statically balanced gear system as found by Mabie and Green (1980b).

Figure 27 is a three-dimensional contour plot of figure 26. Many of the trends discussed in figures 24, 25, and 26 are shown in general in this figure.

Figures 20 through 27 show the resonance of the gear system for both pinion and gear. The general shape and trend of the stress patterns agree with results obtained by Lin et al. (1996) for spur gears cut by hob cutter operated at an extended center distance

(pp. 3-5). As stated for the figures, the actual resonance for each offset of the pinion can vary by more than 1,000 rpm. From the data, with the aid of the figures, tables 2 and 3 are developed for the pinion and gear. These tables show the calculated natural frequencies by index, based upon the eigenvalues of the dynamic equations of motion, as calculated by equation 116. Against this is shown the actual system resonance by index, with a fractional percentage, of the relevant system resonance. The natural frequency and system resonance indexes begin at three. Though the DANST program indicates natural frequencies occurring at 0.0 and 535 rpm, indexes one and two respectively, the chosen range of rpm for the design omits these indexes. The range is chosen in part because numerical error, or noise, is created by two natural frequency indexes set close together. Table 2 shows the system resonance for index three, but table 3 does not show system resonance for index three. This is due to the fact that the preceding echoes for the largest system resonance, index four, overshadow that of index three. This noise created by index four makes it difficult to obtain index three.

The system resonance for index four of both pinion and gear, the largest resonance, occurs just above 90% of the natural frequency of the system. The system resonance for index three for the pinion occurs from 90% to above 100% of the natural frequency of the system. The larger variance in index three for the pinion is due to the noise created by index four. Lin et al. (1987) also found that the dynamic effects did not occur directly at critical speeds (p. 5). This finding agrees with Kubo (1981), which found the maximum dynamic effects occur at 90% (pp. 201-206).

Parametric resonance exists for index four of the pinion and gear, which agrees with findings by Lin et al. (1987, p. 5) and Nafeh and Mook (1987) that also verifies their

existence. According to Nafeh and Mook (1987, ch. 5), the secondary effects occur "at about one-half of the critical speed." However, for this design, the parametric resonance for pinion and gear occurs at approximately 34% of index four. The difference between these findings may be attributed to dimensions and variables within the system (Lin et al., 1987, p. 5).

As explained in chapter 2 section 5, a dynamic factor can be applied between the dynamic and static output. In this study, the dynamic factor for the load is between 1.822 and 0.978. For the majority of the pinion offset and rotational speed considered, the dynamic effects amplify the maximum load the teeth experience. The marginal reduction occurs at high pinion offset, 0.074 to 0.077 inches, in the valley preceding the largest resonance, 11,512 to 12,096 rpm.

3.4 Dynamic Stress Optimization

It is the primary objective of this report to show the optimum pinion offset for a dynamic model where tooth stress is balanced between gear and pinion. The static model is based upon the works of Green and Mabie (1980a; 1980b). According to Green and Mabie, the static stress of each tooth is balanced at a pinion offset of 0.0631 inches and gear offset of 0.0419 inches.

In order to find the optimum pinion offset, and gear offset chosen by equation 33, the minimum difference in maximum dynamic stress at the root of the tooth between pinion and gear is found. This is done by subtracting the maximum dynamic stress of the gear from that of the pinion and taking the absolute of this difference. Figure 28 shows the absolute difference between the pinion and gear, where the valley represents the optimum pinion offset value. Figure 28 also shows the pinion offset where the stress at

the root of the tooth of pinion and gear is statically balanced. Figure 29 shows the pinion offset where the stress at the root of the teeth is balanced statically and dynamically. Essentially, the valley in figure 28 is the pinion offset optimization line shown in figure 29. This pinion offset optimization in figure 29 is best represented by data points showing the amount of pinion offset required for a given rotational speed. However, considering the volume of data available in this study, data points are shown at a reduced interval of 438 rpm with a line connecting the reduced number of data points.

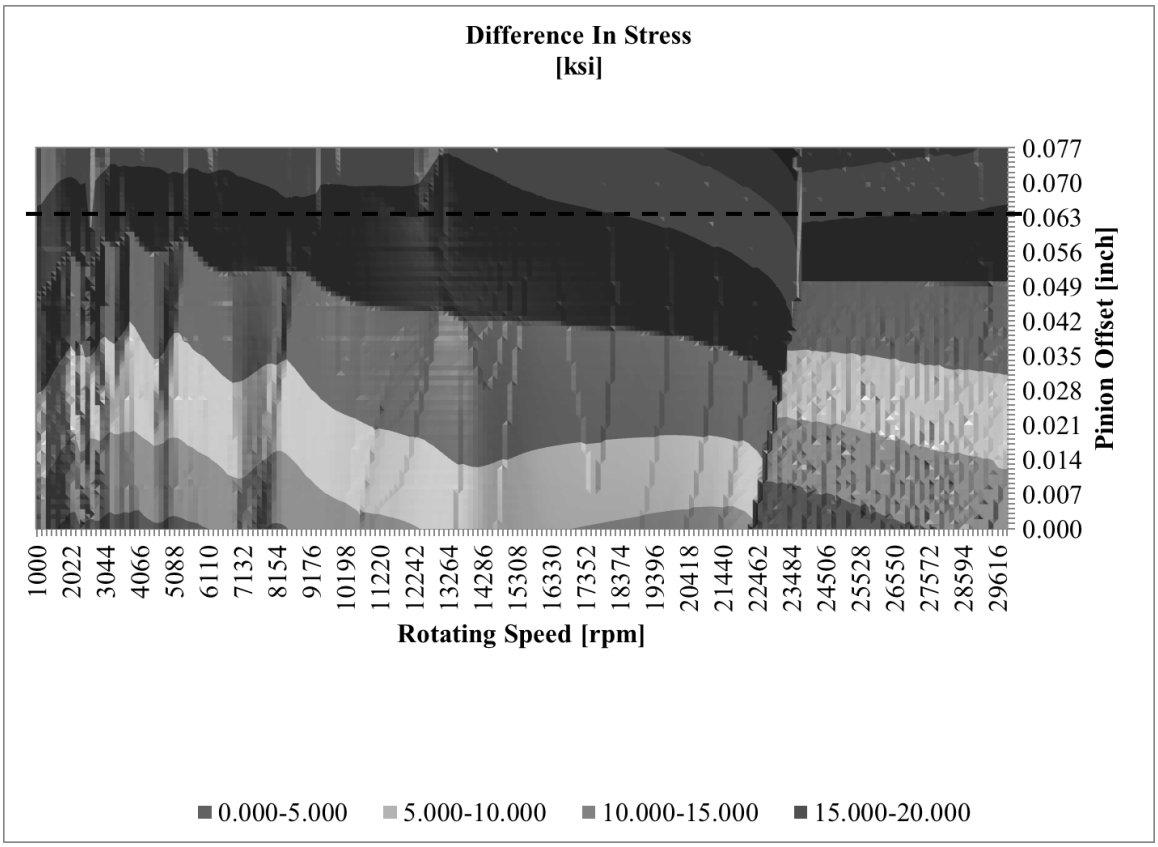

Figure 28. Flat contour plot of absolute stress difference [ksi] between pinion and gear, against pinion offset [inch], e_1 and rotating speed [rpm], a dashed line represents where the tooth root stresses are statically balanced.

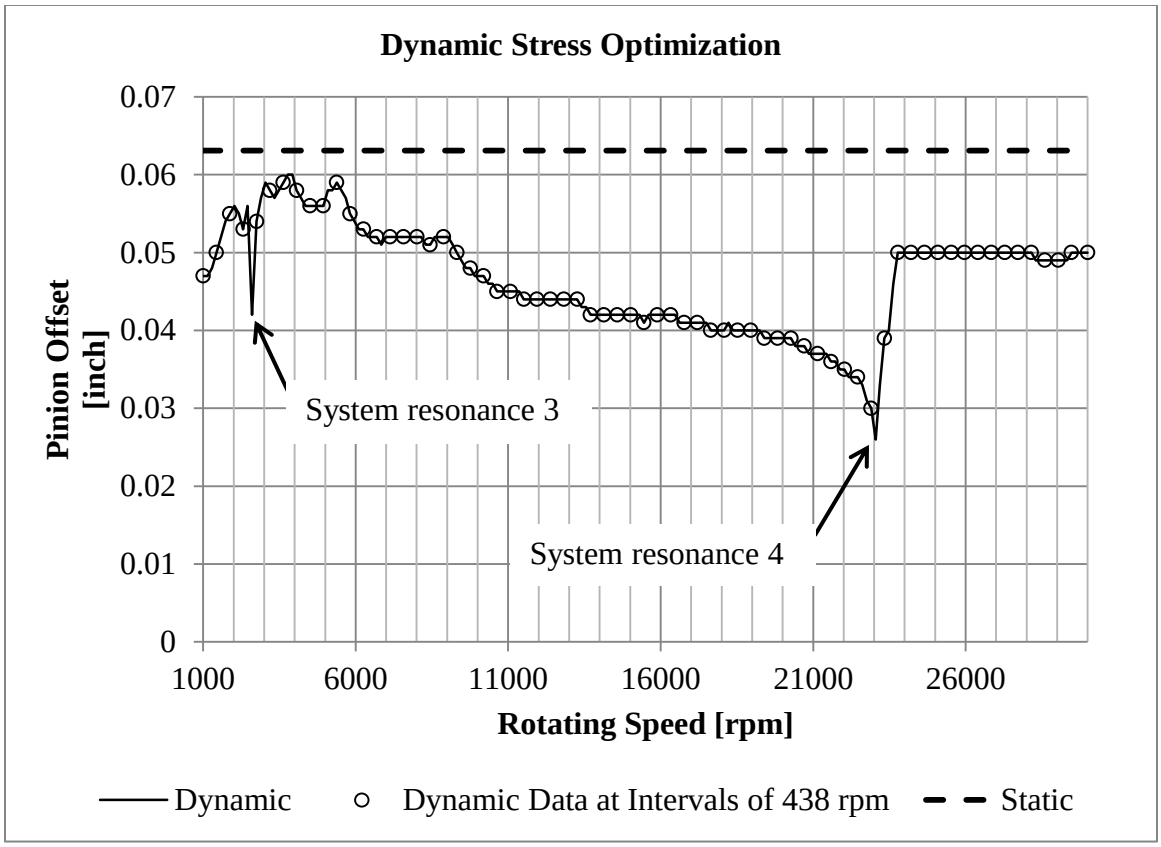

Figure 29. Dynamic stress equalization, the pinion offset [inch], e_1, where both dynamic and static stress for pinion and gear are approximately equal for a given rotational speed [rpm]. The solid line represents the pinion offset and rotational speed where the dynamic root tooth stress is balanced, and data points are shown at intervals of 438 rpm for clarity. Actual data intervals are 146 rpm. The dashed line represents the pinion offset and rotational speed where root tooth static stress is balanced.

The optimization process shows that the pinion offset should be lower than that of the static optimization process, between 0.026 and 0.06 inches. Between 1,500 and 9,000 rpm, the optimal pinion offset is closest for balancing the maximum root tooth stress dynamically and statically. Past 9,000 rpm, the pinion offset decreases relatively smoothly towards the largest system resonance. As the speed increases, the dynamic effects also increase, and figure 29 shows that the pinion offset be reduced, or pinion tooth shortened, and the gear offset increased, or gear tooth lengthened. The sudden

drops in pinion offset optimization occur due to system resonances. However, even though the gear assembly may be optimized for this region, and the maximum dynamic stresses equalized, operating near the resonance is not recommended. The general shape within figure 29 agrees with figure 30 from Lin et al. (1996). Though the optimization shown by figure 29 shows the pinion offset should be reduced, not increased, as described by Lin et al. This difference in pinion offset optimization may be due to the dimensional differences of the design problem considered (pp. 3-6). As far as a design consideration, sections of figure 29 show, for a range of rotational speeds, what the optimum offset is in terms of pinion offset.

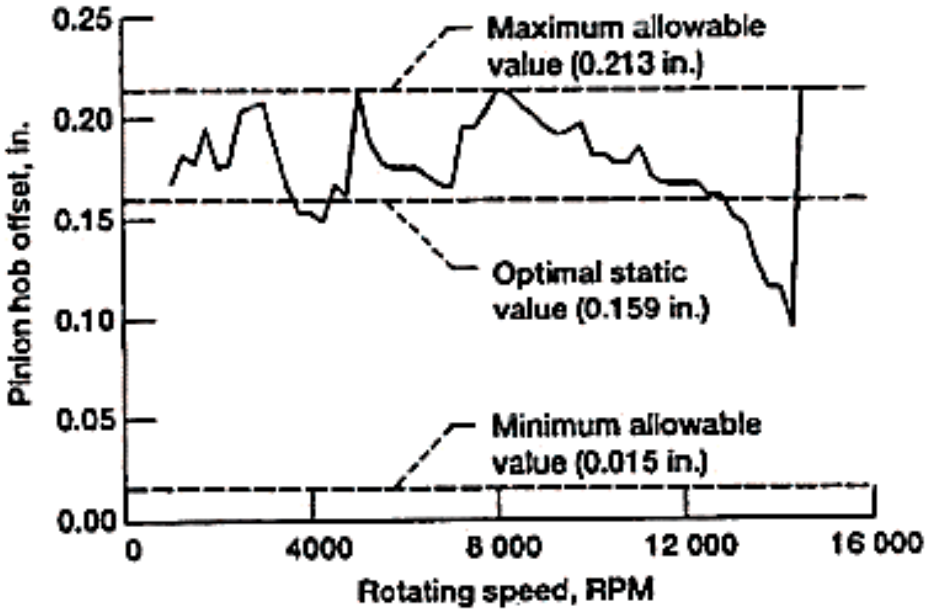

Figure 30. "Determining pinion hob offset to balance dynamic tooth strength of pinion and gear at different speeds" (Lin et al., 1996, p. 5).

3.5. Root Fillet Radius as Cut by Pinion Cutter

The radius of curvature at the root of the tooth is the region of interest in this study. Since the stress being considered is the stress at the root of the tooth, the radius of curvature at that location directly influences the stress by its shape. In essence, the larger the radius of curvature is, the lower the stress is, and vice versa.

According to Colbourne (1987), "the minimum radius of curvature in the gear tooth fillet, when the gear is cut by a pinion cutter, is larger than when the gear is cut by the hob" (p. 240). This means that the stress at the root of the tooth would result in a higher, more conservative stress design when cut by a hob. According to Colbourne, the minimum radius is at the bottom of the fillet. In an example provided by the author, the radius of curvature for a gear cut by pinion cutter is 1.235 times greater than the radius of curvature cut by a hob cutter. Though Colbourne states that the maximum stress exists over a large portion of the fillet, the author generalizes that the maximum stress in the fillet is more likely to occur towards the top of that fillet. However, Colbourne suggests a trial by error or graphical approach: find the stress "at a number of points along the fillet, and chose the [maximum] value" (Colbourne, 1987, pp. 239-240, 251-252).

As shown in chapter 2 section 5, Lin and Liou (1998, pp. 43-44) describe an approach established by Heywood (1952) and continued by Cornell (1981, pp. 447-459) for calculating the location of maximum stress. Figure 19 outlines this methodology, and the stress resulting from this location is given by equation 117 (Lin & Liou, 1998, pp. 43-44). This equation is used in the DANST program (Oswald et al., 1996). According to Oswald, Rebbechi, Zakrajsek, Townsend, and Lin (1991) in the DANST program the "tooth root geometry [was] created by a standard hob" (p. 6).

The radius of curvature used in the dynamic model, the radius cut by a hob where the stress is at a maximum, is plotted against the range of the radii of curvature that would be cut by a pinion cutter for pinion and gear in figures 31 and 32. The figures agree with the statement by Colbourne (1987), that the radius of curvature for that cut by a hob is less than that cut by a pinion cutter (pp. 239-240).

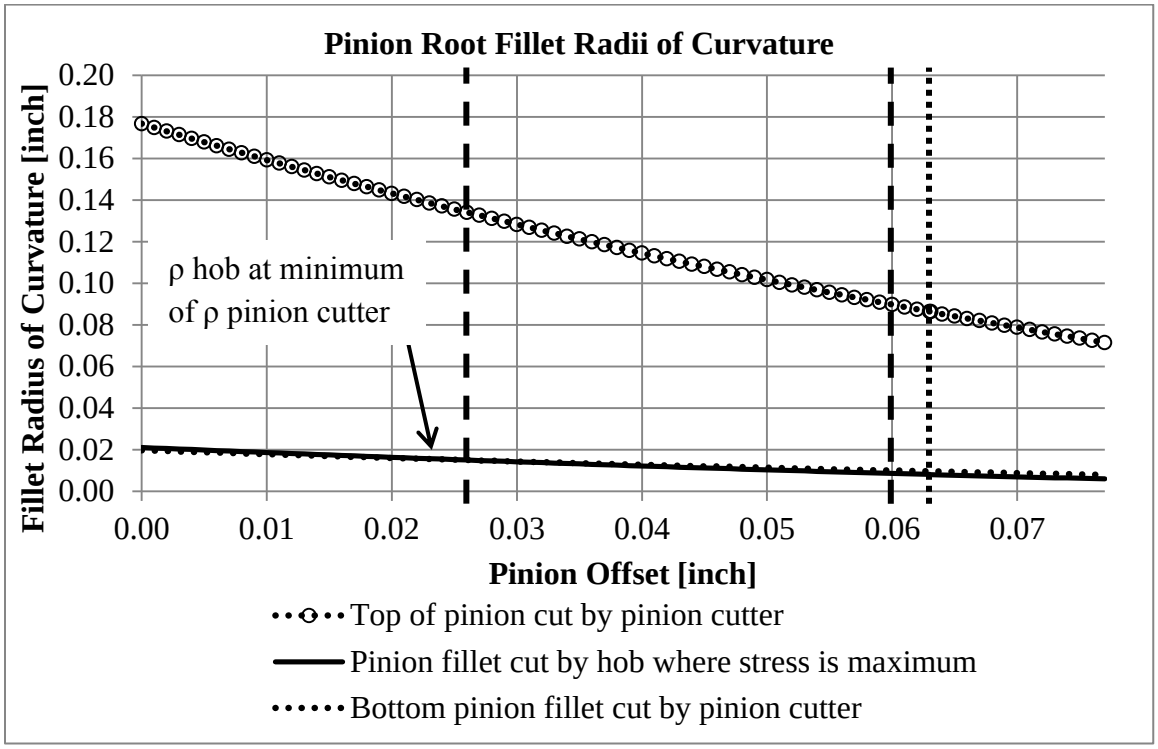

Figure 31. Comparison of fillet radius of curvature for pinion at the bottom and the top of the fillet when cut by pinion cutter to the fillet radius of curvature when cut by hob cutter where the stress due to moment is at a maximum. The top data set shows the number of data points used. Dashed lines show the range of dynamic optimization (heavy dash) and the static optimization (light dash).

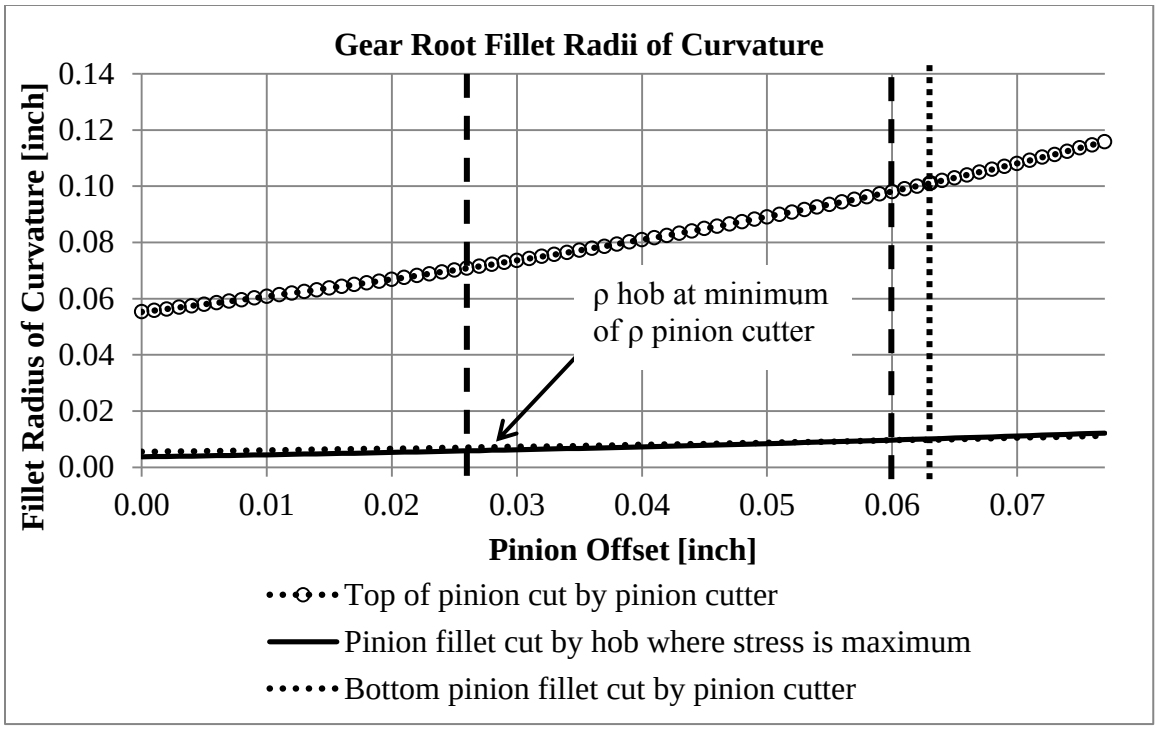

Figure 32. Comparison of fillet radius of curvature for pinion at the bottom and the top of the fillet when cut by pinion cutter to the fillet radius of curvature when cut by hob cutter where the stress due to moment is at a maximum. The top data set shows the number of data points used. Dashed lines show the range of dynamic optimization (heavy dash) and the static optimization (light dash).

Based upon the literature and the data from figures 31 and 32, using the radius of curvature cut by a hob as found from the DANST program is a conservative, safe assumption. Thus, the dynamic model uses this assumption and approximates r_f in equation 117 as cut by a hob cutter.

Chapter 4

Conclusion

This study represents an extension of the work performed by Lin et al. (1996). The dynamic model within DANST program can model a design of spur gears set at an extended center distance that are cut by pinion cutter. This dynamic model minimizes the difference in stress at the root of the teeth, where the stress is caused by the moment created by the tangential component of the tooth load (Mabie et al., 1983). The results provided by the model agree well with the literature, and highlight the importance of dynamic modeling in gear design. Several conclusions can be drawn from the results and discussion.

1. The dynamic affects serve to amplify the stresses within the gear system.

2. In terms of minimizing the stress at the root of the tooth, the dynamic optimization of the system may be different than that of the static optimization.

3. For dynamic minimization of the stress difference at the root of the teeth, the offset of the pinion cutter on the pinion needs to be reduced and the offset of the pinion cutter on the gear needs to be increased. This results in shorter pinion teeth and longer gear teeth.

4. The assumption for fillet radii cut by a hob, instead of a pinion cutter, results in a safer, more conservative design.

These conclusions are based upon a series of assumptions and limitations in the dynamic model.

1. Since a gear design involves multiple parameters, some parameters must be chosen, fixed, or approximated. Thus, the problem statement given in chapter 3 is for a

specific design provided by various sources in the literature. Certain assumptions are required, such as using plane strain (Cornell & Westervelt, 1978; Lin & Liou, 1998; MacDonald, 2007), standard tooth profile (Rogers et al., 1990), no undercutting (Lin et al., 1996; Rogers et al., 1990), approximate damping coefficients (Lin & Liou, 1998), and non-transverse motion (Lin & Liou, 1998). Though a series of supported, conservative assumptions are made in r_f (Colbourne, 1987, p. 237; Lin & Liou, 1998) and r_{cT} (Colbourne, 1987, pp. 133-136), actual manufacturing techniques provide different results that are not as conservative.

2. The dynamic stress being balanced in this study is that due to moment caused by the tangential load (Mabie et al., 1983). However, other stress categories exist, such as the stress at the tooth contact point, as can be seen in figure 38 in appendix D. Moreover, though equal tooth strength is beneficial for component life, the designer should always design for gear wear and fatigue.

3. As shown in chapter 3, the actual location of primary and parametric resonance is greatly dependent upon the gear model and design. Resonance interference as found in this study should be of concern to the designer. Moreover, the designer should understand that dynamic effects may continue outside of the rotational speed ranges considered in this study.

4. As shown in chapter 1 in the literature review, a series of past tests have been performed to verify the accuracy of the DANST program (Oswald & Townsend et al., 1996; Oswald et al., 1993; Oswald et al., 1991). However, the designer should be aware that specific testing or inspection should be performed for any design based upon this dynamic, analytical model.

It is important to note that dimensions play a key aspect in this design, from the rotational speed to the size and tooth number of the gear. Each design being different, it is important to perform design checks against the general trends shown in this study. With an optimized design and balanced stresses, the resulting gear system will have less wear and damage, and will have a longer service life.

Bibliography

American Gear Manufacturers Association. (1974, August). *AGMA Standard 201.02, ANSI Standard System Tooth Proportions for Coarse - Pitch Involute Spur Gears*. Alexandria, VA: American Gear Manufacturers Association.

Boyd, L. S., & Pike, J. A. (1987). Gear Dynamic Analysis Program (GEARDYN) [Computer software]. HSER-10853, NAS3-24614, NASA CR-179563, and NASA CR-165514. Windsor Locks, CT: Hamilton Standard.

Brauer, J. (2004). "A General Finite Element Model of Involute Gears." *Finite Elements in Analysis and Design, 40*, 1857–1872. Stockholm, Sweden: Elsevier

Buckingham, E. (1931). "Dynamic Load on Gear Teeth." *Report of Special Research Committee on the Strength of Spur Gear Teeth*. New York, NY: ASME.

Buckingham, E. (1949). *Analytical Mechanics of Gears*. New York, NY: Dover Publication, Inc.

Cloutier, J. L., & Tordion, G. V. (1962, June). "Dynamic Loads on Precision Spur Gear Teeth According to the Theory of Variable Elasticity." *University Laval, Laboratoire d'lements des Machines*, Report Number EM-3.

Colbourne, J. R. (1987). *The Geometry of Involute Gears*. New York, NY: Springer-Verlag.

Cornell, R. (1981). "Compliance and Stress Sensitivity of Spur Gear Teeth." *ASME Journal of Mechanical Design, 103*(2), 447-459.

Cornell, R. W., & Westervelt, J. (1978, January). "Dynamic Tooth Load and Stressing for High Contact Ratio Spur Gears." *Journal of Mechanical Design, 100*(1), 69-76.

Dudley, D. W. (1984). *Handbook of Practical Gear Design*. New York, NY: McGraw-Hill.

Green, R. N., & Mabie, H. H. (1980a, May). "Determination of Pinion-Cutter Offsets Required to Produce Nonstandard Spur Gears with Teeth of Equal Strength." *Mechanism and Machine Theory, 15*(6), 491-506. Great Britain: Pergamon Press.

Green, R. N., & Mabie, H. H. (1980b, May). "Determination of Static Tooth Stresses in Nonstandard Spur Gears Cut by Pinion Cutter." *Mechanism and Machine Theory, 15*(6), 507-514. Great Britain: Pergamon Press.

Gregory, R. W., Harris, S. L., & Munro, R. G. (1964). "Dynamic Behavior of Spur Gears." *Proceedings of the Institution of Mechanical Engineers, 178*(8), 261-266.

Hamad, B. M., & Seireg, A. (1980). "Simulation of Whirl Interaction in Pinion-Gear System Supported on Oil Film Bearings." *Journal of Engineering for Power, Transactions of ASME, 102*, 508-510.

Hahn, W. F. (1969). "Study of Instantaneous Load to Which Gear Teeth are Subjected." Ph.D. Dissertation, University of Illinois, 1969.

Heywood, R. B. (1952). *Designing by Photoelasticity*. Chapman and Hall, Ltd.

Iida, H., Tamura, A., Kikuchi, K., & Agata, H. (1980). "Coupled Torsional-Flexural Vibration of a Shaft in a Geared System of Rotors." *Bulletin of Japanese Society of Mechanical Engineers, 23*, 2111-2117.

Iwatsubo, N., Arii, S., & Kawai, R. (1984a). "Coupled Lateral-Torsional Vibrations of Rotor Systems Trained by Gears, 1. Analysis by Transfer Matrix Method." *Bulletin of the Japanese Society of Mechanical Engineers, 27*, 271-277.

Iwatsubo, N., Arii, S., & Kawai, R. (1984b). "Coupled Lateral-Torsional Vibrations of Rotor Systems." *Proceedings of the Third International Conference on Vibrations in Rotating Machinery, Institution of Mechanical Engineers*, pp. 59-66.

Kasuba, R., & Evans, J. W. (1981, April). "An Extended Model for Determining Dynamic Load in Spur Gearing." *ASME Journal of Mechanical Design, 103*, 398-409.

Kahraman, A., Ozguven, H. N., Houser, D. R., Zakrajsek, J. J., Oswald, F. B., Townsend, D. P., & Coy, J. J. (1990). GRD [Computer software]. NASA TM-102349.

Kubo, A. (1981). *Estimation of Gear Performance, Proceedings of the International Symposium on Gearing and Power Transmissions*. Japan Society of Mechanical Engineers, 201-206. Tokyo, Japan.

Lee, C. H. (2009). Non-Linear Contact Analysis of Meshing Gears. Master's Defense. California Polytechnic State University, 2009.

Lim, T. C., & Singh, R. (1989). *A Review of Gear Housing Dynamics and Acoustics Literature*. NASA CR-185148. Washington, DC: National Aeronautics and Space Administration and U.S. Army Research Laboratory.

Lin, H. H., Huston, R. L., & Coy, J. J. (1987, December). *On Dynamic Loads in Parallel Shaft Transmissions, II—Parameter Study*. NASA TM-100181. Washington, DC: National Aeronautics and Space Administration and U.S. Army Research Laboratory.

Lin, H. H., & Liou, C. H. (1998, January). *A Parametric Study of Spur Gear Dynamics*. NASA/CR--1998-206598 and ARL-CR-419. Washington, DC: National Aeronautics and Space Administration and U.S. Army Research Laboratory.

Lin, H. H., Liou, C. H., Oswald, F. B., & Townsend, D. P. (1996). "Balancing Dynamic Strength of Spur Gears Operated at Extended Center Distance." *Prepared for the Seventh International Power Transmission and Gearing Conference*. NASA TM-107222. San Diego, CA: National Aeronautics and Space Administration and U.S. Army Research Laboratory.

Mabie, H. H., Walsh, E. J., & Bateman, V. I. (1983). "Determination of Hob Offset Required to Generate Nonstandard Spur Gears with Teeth of Equal Strength." *Mechanism and Machine Theory*, *18*(3), 181-192. Great Britain: Pergamon Press.

Mabie, H. H., & Reinholtz, C. F. (1987). *Mechanisms and Dynamics of Machinery* (4th Ed.). Wiley.

MacDonald, B. J. (2007). *Practical Stress with Finite Elements*. Dublin, Ireland: Glasnevin Publishing.

Microsoft Corporation. (1995). Microsoft Developer Studio: Fortran PowerStation 4.0. [Computer software]. Redmond, WA: Microsoft Corporation.

Nafeh, A. H., & Mook, D. T. *Nonlinear Oscillations*. Wiley, 1979, chapter 5.

Oswald, F. B., Lin, H. H., & Delgado, I. R. (1996a). Dynamic Analysis of Spur Gear Transmissions (DANST) [Computer Software]. Washington, DC: National Aeronautics and Space Administration and U.S. Army Research Laboratory.

Oswald, F. B., Lin, H. H., & Delgado, I. R. (1996b, August). *Dynamic Analysis of Spur Gear Transmissions (DANST), PC Version 3.00 User Manual*. NASA TM-107291. Washington, DC: National Aeronautics and Space Administration and U.S. Army Research Laboratory.

Oswald, F. B., Lin, H. H., Liou, C. H., & Valco, M. J. (1993). *Dynamic Analysis of Spur Gears Using Computer Program DANST*. NASA TM-106211. Prepared for the 29th Joint Propulsion Conference and Exhibit cosponsored by the AIAA, SAE, ASME, and ASEE. Monterey, CA: National Aeronautics and Space Administration and U.S. Army Research Laboratory.

Oswald, F. B., Rebbechi, B., Zakrajsek, J. J., Townsend, D. P., & Lin, H. H. (1991, September). *Comparison of Analysis and Experiment for Dynamics of Low-Contact-Ratio Spur Gears*, NASA TM-103232. ASME 13th Biennial Conference on Mechanical Vibration and Noise. Miami, FL: National Aeronautics and Space Administration and U.S. Army Research Laboratory.

Oswald, F. B., Townsend, D. P., Rebbechi, B., & Lin, H. H. (1996, October). *Dynamic Forces in Spur Gears—Measurement, Prediction, and Code Validation*. Seventh International Power Transmission and Gearing Conference sponsored by the American Society of Mechanical Engineers. San Diego, CA: National Aeronautics and Space Administration and U.S. Army Research Laboratory.

Richardson, H. H. (1958). "Static and Dynamic Load, Stresses, and Deflection Cycles in Spur Gear Systems." Doctoral dissertation report, Massachusetts Institute of Technology.

Rogers, C. A., Mabie, H. H., & Reinholtz, C. F. (1990). "Design of Spur Gears Generated with Pinion Cutters." *Mechanism and Machine Theory*, *25*(6), 623-634. Great Britain: Pergamon Press.

Tavakoli, M. S., & Houser, D. R. (1985, December). "Optimum Profile Modifications for the Minimization of Static Transmission Errors of Spur Gears." *ASME Journal of Mechanisms, Transmissions, and Automation in Design*, *107*, 529-535.

Tupin, W. A. (1953, October). "Dynamic Loads on Gear Teeth." *Machine Design*, p. 203.

Van der Zijp, J. (2009). ABAQUS/CAE 6.9-EF1 [Computer software]. Providence, RI: Dassault Systemes Simulia Corporation.

Wang, K. L., & Cheng, H. S. (1981, January). "A Numerical Solution to the Dynamic Load, Film Thickness, and Surface Temperature in Spur Gears." *ASME Journal of Mechanical Design*, 177-187.

Wang, S. M. (1968). Static and Dynamic Response of Torsional Systems. Ph.D. Dissertation, University of Cincinnati, 1968.

Appendix A

Static Code as Written in FORTRAN

The following code has been modified so as to fit appropriately in this document. Certain formatting, indentation, tabs, and spacing, must be removed for accurate program execution. The code is meant to be run in FORTRAN-90 (Microsoft, 1995, computer software).

```
!----------!
      PROGRAM STATC
!
!-----This is the rough draft program intended to
!     and built upon the work of Green and Mabie
!
!-----This particular can give a
!     range of values of stress factors for a domain
!     of offset values of "delta" C.
!
!-----"p" represents prime in the following calculations
!
      INTEGER DecB, N1I, N2I, NcI
      REAL Ad1, Ad2, ALPHA1, ALPHA2, BETA1, BETA2, B, B0, Btemp, C
      REAL CdstEx, Cp, Cratio, Cstddist, Cstd(2), D1, D2, Dc
      REAL Ded1, Ded2, Do1p, Do2p, E(2), estar1, estar2, etotal
      REAL FaceW, Fnf1, Fnf2, Ftf1, H1
      REAL H2, Ht, I1, I2, invPHIc, invPHId1, invPHId2, invPHIg1
      REAL invPHIg2, invPSI1, invPSI2, k, Loadin, Mp, N(2)
      REAL Nc, P, Pb, PHIc, PHIcD, PHId1, PHId2, PHIg1
      REAL PHIg2, PHIo, PHIoD, Pi, PSI1, PSI2, Ro1p, Ro2p
      REAL R(2), Rb(2), Rd1p, Rd2p, Rg(2)
      REAL Rbc, Rc, Roc, Rp1, Rp2, RPM1, RPM2, RPMi, S1, S2, Stress1
      REAL Stress2, Ta1, Ta2, Td1, Td2, Tc, Tg1, Tg2, Tp1, Tp2
      REAL THETA1, THETA2, Torq, Xa1, Xa2, Xd1, Xd2
      CHARACTER OUTF*12
!-----Placeholders for optimizing Pinion Cutter Edge Radius
      INTEGER M
      REAL An, Bn, Diff, GAMMAhc, PHIhc, Rhc
      REAL SgnFct, THETAhc, TOL, Rcp, Rct, RctMax, Ycp
!-----Placeholders for calculating tooth fillet radius
      INTEGER i
      REAL ALPHAB(2), ALPHAT(2)
      REAL BETAcB(2), BETAcT(2), BETAgB(2), BETAgT(2)
      REAL Cc
      REAL Ec, ETApB(2), ETApT(2), ETAB(2), ETAT(2)
      REAL INVPHIcp
      REAL PHIB(2), PHIcp, PHImesh, PHIT(2), Ps
      REAL RBot(2), RHOfB(2), RHOfT(2), Rpcc, RT(2), R0
      REAL SpB(2), SpT(2), SB(2), ST(2)
      REAL THETAcp, THETArB(2), THETArT(2), Tsg(2)
      REAL Xcp
```

```
      REAL ZETApB(2), ZETApT(2), ZETAB(2), ZETAT(2)
!
!-----Data input
!
      PRINT*, 'Input pinion cutter radius, in:'
      READ*, Rc
      Dc = Rc*2.0
      PRINT*, 'Input diametral pitch:'
      READ*, P
      PRINT*, 'Input number of pinion (gear 1) teeth:'
      READ*, N(1)
      PRINT*, 'Input number of gear (gear 2) teeth:'
      READ*, N(2)
      PRINT*, 'Input operating center distance, in:'
      READ*, Cp
      PRINT*, 'Input face width, in:'
      READ*, FaceW
      k = 1.0
      Pi = ACOS(-1.0)
      PRINT*, 'Input cutting pressure angle, deg:'
      READ*, PHIcD
      PHIc = PHIcD*Pi/180.0
      PRINT*, 'Input torq, in-lb:'
      READ*, Torq
      ![2 and 9]
      PRINT*, 'Input initial gear velocity, RPM:'
      READ*, RPM1
      PRINT*, 'Input final gear velocity, RPM:'
      READ*, RPM2
      RPMi = 1+(RPM2-RPM1)/200.0 ![7]
!
!-----Data input for offset
!
      Cstddist = (N(1)+N(2))/(2.0*P) ![2]
      CdstEx = Cp - Cstddist
      PHIo = ACOS(Cstddist*COS(PHIc)/Cp)
      PHIoD = PHIo*180.0/Pi ![2 and 6]
!
      PRINT*, 'Input pinion (gear 1) offset, in:'
      READ*, E(1)
      PRINT*, 'Input gear (gear 2) offset, in:'
      READ*, E(2)
      Ec = 0.0 !Pinion "profile shift", calculation not in force ![1]
!
      PRINT*, 'Output File Name ?'
      READ(*,'(a)') OUTF
      OPEN(11,file=OUTF,status='unknown')
      OPEN(UNIT=12, FILE='IntFile.TXT', STATUS='OLD')
!
!-----Preliminary calculations
!
!     "Required Dimensions of the standard gears
!      and cutter" [3]
!
 20   Nc = Dc*P ![3]
      etotal = E(1) + E(2) ![2]
      Cstd(1) = (N(1)+Nc)/(2.0*P)
```

```
      Cstd(2) = (N(2)+Nc)/(2.0*P)
      Pb = (Pi/P)*COS(PHIc)
      Tc = Pi/(2.0*P)
      R(1) = (N(1))/(2.0*P)
      R(2) = (N(2))/(2.0*P)
      Rbc = Rc*COS(PHIc)
      Rb(1) = R(1)*COS(PHIc)
      Rb(2) = R(2)*COS(PHIc) ![3]
      Cratio = 0.25
      C = Cratio/P ![6]
      Roc = Rc + k/P + C ![2]
!
!-----"Proportions of nonstandard gears" [3]
!
!-----Calculation of PHIg2
!     Calculation of E(2), gear offset, based upon beginning knowledge
      of backlash [3, 9, and 4]
!
      PHIg1 = ACOS(((N(1)+Nc)*Pb)/(2.0*Pi*(Cstd(1)+E(1))))
      ![3]
 30   PRINT*
      PRINT*, 'Do you know the gear assembly backlash?'
      PRINT*, 'Enter 0 for yes or 1 for no'
      PRINT*, '**Input of backlash will override value for gear (E(2))
         offset**'
      READ*, DecB
      IF (DecB.EQ.0) THEN
            PRINT*
            PRINT*, 'Enter Backlash value: '
            READ*, B
            PRINT*, 'Calculating gear (E(2)) offset.'
      Btemp = ( (2.0*Nc*(TAN(PHIc)-PHIc))-((Nc+N(1))*(TAN(PHIg1)-
         PHIg1))+((N(1)+N(2))*(TAN(PHIo)-PHIo))-((B*P*Cstddist)/(Cp))
         )/(Nc+N(2))
            PHIg2 = SOLINV(Btemp)
            E(2) = ( (N(2)+Nc)*Pb )/( 2.0*Pi*COS(PHIg2) )-Cstd(2)
            ![3 and 9]
            etotal = E(1) + E(2)
            ![2]
      ELSEIF (DecB.EQ.1) THEN
            PRINT*
            PRINT*, 'Resuming calculation with backlash unknown'
            PRINT*, 'gear (E(2)) offset remains unchanged'
            PHIg2 = ACOS(((N(2)+Nc)*Pb)/(2.0*Pi*(Cstd(2)+E(2))))
            ![3]
      ELSE !(DecB.NE.1.OR.2)
            PRINT*
      PRINT*, 'Incorrect decision value entered, asking question
         again.'
            PRINT*
            GOTO 30
      ENDIF
      Rg(1) = N(1)/(N(1)+Nc)*(Cstd(1)+E(1))
      Rg(2) = N(2)/(N(2)+Nc)*(Cstd(2)+E(2)) ![3]
!
!-----"Minimum offset that will prevent undercutting" [2]
!
```

```
      estar1 = sqrt(Roc**2.0-Rb(1)**2.0+Rb(1)*((N(1)+Nc)/Pi)*Pb)-
         Cstd(1)
      estar2 = sqrt(Roc**2.0-Rb(2)**2.0+Rb(2)*((N(2)+Nc)/Pi)*Pb)-
         Cstd(2) ![2]
      IF (E(1).LT.estar1) THEN
            PRINT*, 'Offset for pinion (gear 1) exceeds minimum offset'
            PRINT*, 'Resetting pinion (gear 1) offset to minimum'
            PRINT*
            E(1) = estar1
            GOTO 20 !Jump back to reset preliminary calculations
      ENDIF
      IF (E(2).LT.estar2) THEN
            PRINT*, 'Offset for gear (gear 2) exceeds minimum offset'
            PRINT*, 'Resetting gear (gear 2) offset to minimum'
            PRINT*
            E(2) = estar2
            GOTO 20 !Jump back to reset preliminary calculations
      ENDIF
!
!-----"Involute functions of cutter pressure
!      angle and of generating pressure angles" [3]
!
      invPHIc = TAN(PHIc) - PHIc
      invPHIg1 = TAN(PHIg1) - PHIg1
      invPHIg2 = TAN(PHIg2) - PHIg2 ![3]
!
!-----"Tooth thickness of the pinion and gear on their
!      respective generating pitch circles" [3]
!
      Tg1 = (Pb-Tc*COS(PHIc)-2.0*Rbc*(invPHIc-invPHIg1))/(COS(PHIg1))
      Tg2 = (Pb-Tc*COS(PHIc)-2.0*Rbc*(invPHIc-invPHIg2))/(COS(PHIg2))
      ![3]
!
!-----"Outside radii, depth of cut, and dedendum radii" [3]
!
      Ro1p = Cp-R(2)-E(2)+k/P
      Ro2p = Cp-R(1)-E(1)+k/P
      Do1p = Ro1p*2.0
      Do2p = Ro2p*2.0
      Ht = Ro1p+Ro2p-Cp+C
      Rd1p = Ro1p-Ht
      Rd2p = Ro2p-Ht ![3]
!
!-----"Stress factor for the pinion" [3]
!
      PSI1 = ACOS(Rb(1)/Ro1p)
      invPSI1 = TAN(PSI1) - PSI1
      ALPHA1 = Tg1/(2.0*Rg(1))+invPHIg1-invPSI1
      BETA1 = PSI1-ALPHA1
      IF (Rb(1).LE.Rd1p) THEN !Case 1
            PHId1 = ACOS(Rg(1)/Rd1p*COS(PHIg1))
            invPHId1 = TAN(PHId1)-PHId1
            THETA1 = Tg1/(2.0*Rg(1))+invPHIg1-invPHId1
            Xa1 = Ro1p*COS(ALPHA1)
            Xd1 = Rd1p*COS(THETA1)
            D1 = Xa1 - Xd1
            H1 = 2.0*Rd1p*SIN(THETA1)
```

```
            S1 = (6.0*D1*COS(BETA1))/H1**2.0
      ELSE !(Rb(1).GT.Rd1p) Case 2
            THETA1 = (Tg1)/(2.0*Rg(1))+invPHIg1
            Xa1 = Ro1p*COS(ALPHA1)
            Xd1 = Rd1p*COS(THETA1)
            D1 = Xa1-Xd1
            H1 = 2.0*Rd1p*SIN(THETA1)
            S1 = (6.0*D1*COS(BETA1))/(H1**2.0)
      ENDIF ![3]
      Ta1 = 2.0*ALPHA1*Ro1p
      Td1 = 2.0*Rd1p*THETA1 ![2]
      Rp1 = Rb(1)/COS(PHIo)
      Ad1 = Ro1p - Rp1
      Ded1 = Rp1 - Rd1p ![2 and 6]
!
!-----"Stress factor for the gear' [3]
!
      PSI2 = ACOS(Rb(2)/Ro2p)
      invPSI2 = TAN(PSI2)-PSI2
      ALPHA2 = (Tg2)/(2.0*Rg(2))+invPHIg2-invPSI2
      BETA2 = PSI2-ALPHA2
      IF (Rb(2).LE.Rd2p) THEN !Case 1
            PHId2 = ACOS(Rg(2)/Rd2p*COS(PHIg2))
            invPHId2 = TAN(PHId2)-PHId2
            THETA2 = Tg2/(2.0*Rg(2))+invPHIg2-invPHId2
            Xa2 = Ro2p*COS(ALPHA2)
            Xd2 = Rd2p*COS(THETA2)
            D2 = Xa2 - Xd2
            H2 = 2.0*Rd2p*SIN(THETA2)
            S2 = (6.0*D2*COS(BETA2))/H2**2.0
      ELSE !(Rb(2).GT.Rd2p) Case 2
            THETA2 = (Tg2)/(2.0*Rg(2))+invPHIg2
            Xa2 = Ro2p*COS(ALPHA2)
            Xd2 = Rd2p*COS(THETA2)
            D2 = Xa2-Xd2
            H2 = 2.0*Rd2p*SIN(THETA2)
            S2 = (6.0*D2*COS(BETA2))/(H2**2.0)
      ENDIF ![3]
      Ta2 = 2.0*ALPHA2*Ro2p
      Td2 = 2.0*Rd2p*THETA2 ![2]
      Rp2 = Rb(2)/COS(PHIo)
      Ad2 = Ro2p - Rp2
      Ded2 = Rp2 - Rd2p ![2 and 6]
!
!-----Calculating tooth thickness (t') of a gear on a running
!     pitch circle [2]
!
      Tp1 = (Pb-Tc*COS(PHIc)-2.0*Rbc*(invPHIc-
         invPHIg1))/(COS(PHIo))+(2.0*Rb(1)*(invPHIg1-(TAN(PHIo)-
         PHIo)))/(COS(PHIo))
      Tp2 = (Pb-Tc*COS(PHIc)-2.0*Rbc*(invPHIc-
         invPHIg2))/(COS(PHIo))+(2.0*Rb(2)*(invPHIg2-(TAN(PHIo)-
         PHIo)))/(COS(PHIo))
      ![2]
!
!-----Calculating additional values for comparison
!     to dynamic analysis [5 and 6]
```

```
!
      Ftf1 = Torq/Rb(1)
      Fnf1 = Ftf1/COS(BETA1)
      Stress1 = S1*Fnf1/FaceW
      Fnf2 = Ftf1/COS(BETA2)
      Stress2 = S2*Fnf2/FaceW ![5 and 6]
      Loadin = Ftf1/FaceW !Static Tooth Load per inch
!
!-----Calculating backlash [9]
!
      B = Cp/(P*Cstddist)*(2.0*Nc*invPHIc-(Nc+N(1))*invPHIg1-
         (Nc+N(2))*invPHIg2+(N(1)+N(2))*(TAN(PHIo)-PHIo))
      B0 = 0.0 !AN INPUT TO THE DANST PROGRAM ADDS TO INHERENT BACKLASH
      ![9]
!
!-----Calculating contact ratio [9]
!
      Mp = N(1)*SQRT((Cp-R(2)-E(2)+k/P)**2.0-Rb(1)**2.0)/(2.0*Pi*Rb(1))
         + N(1)*SQRT((Cp-R(1)-E(1)+k/P)**2.0-Rb(2)**2.0)/(2.0*Pi*Rb(1))
         - (N(1)*Cp*SIN(PHIo))/(2.0*Pi*Rb(1))
      ![9]
!
!-----Calculating pinion (Gear 1) and gear (Gear 2) inertia [8]
!
      I1 = (Pi*Rp1**4.0*FaceW*0.284)/(2.0*386.4)
      I2 = (Pi*Rp2**4.0*FaceW*0.284)/(2.0*386.4) ![8]
!
!-----Calculating MAXIMUM cutter tooth tip geometry [1, 2, and 3]
!
      M = 0
      An = 0.0
      Bn = Tc
      TOL = 10.0**(-5.0)
      Diff = Bn-An
 40   IF (M.LE.100.AND.Diff.GT.TOL) THEN
            RctMax = (An+Bn)/2.0
            !Calculate dimension value
            Rcp = Roc - RctMax
            PHIhc = ATAN((SQRT(Rcp**2.0-Rbc**2.0)+RctMax)/(Rbc))
            Rhc = Rbc/COS(PHIhc)
            THETAhc = Tc/(2.0*Rc)+(TAN(PHIc)-PHIc)-(TAN(PHIhc)-PHIhc)
            GAMMAhc = PHIhc - THETAhc
            Ycp = Rhc*SIN(THETAhc) - RctMax*COS(GAMMAhc)
            IF (Ycp.EQ.0.0) THEN
                  PRINT*, 'Exact numerical solution found.'
                  GO TO 41
            ENDIF
            SgnFct = Ycp / ABS(Ycp)
            IF (SgnFct.GT.0.0) THEN
                  An = RctMax
            ELSEIF (SgnFct.LT.0.0) THEN
                  Bn = RctMax
            ELSE !(SgnFct.EQ.0.0)
                  PRINT*, 'PROGRAM ERROR AT PINION CUTTER EDGE
                     CALCULATION,'
                  PRINT*, 'INCORRECT SIGN FUNCTION.'
                  STOP
```

```
            ENDIF
            Diff = Bn-An
            M = M+1
            GO TO 40
      ENDIF
 41   PRINT* ![1, 2, and 3]
!
!-----Calculating tooth fillet radius [1]
!
 50   WRITE(*,'(1X,A,F6.4,A)') 'The MAXIMUM tooth cutter tip radius is:
         ', RctMax, ' in'
      PRINT*
      PRINT*, 'What value do you wish to use for Rct?'
      PRINT*, 'Enter a value from 0.0 up to Rct'
      READ*, Rct
      IF (Rct.LT.0.0.OR.Rct.GT.RctMAX) THEN
            PRINT*, 'Rct value chosen is outside the acceptable limit'
            PRINT*
            GOTO 50
      ENDIF
      Rcp = Roc - Rct !Perform similar calculations as previous section
      PHIhc = ATAN( (SQRT(Rcp**2.0-Rbc**2.0)+Rct)/(Rbc) )
      Rhc = Rbc/COS(PHIhc)
      THETAhc = Tc/(2.0*Rc)+(TAN(PHIc)-PHIc)-(TAN(PHIhc)-PHIhc)
      GAMMAhc = PHIhc - THETAhc
      Xcp = Rhc*COS(THETAhc) - Rct*SIN(GAMMAhc)
      Ycp = Rhc*SIN(THETAhc) - Rct*COS(GAMMAhc)
      THETAcp = ATAN(Ycp/Xcp)
      Ps = Pi/P
      DO 55 i=1,2
            Tsg(i) = 0.5*Pi*1.0/P + 2.0*E(i)*TAN(PHIc)
            INVPHIcp = ( TAN(PHIc)-PHIc ) - 1/(2.0*Cstd(i)) * (Ps-
               Tsg(i)-Tc)
            PHIcp = SOLINV(INVPHIcp)
            PHImesh = PHIcp
            Cc = (Rb(i)+Rbc) / COS(PHImesh)
            Rpcc = ( Nc*Cc )/( N(i)+Nc )
            R0 = ( N(i)*Nc*Cc )/( N(i)+Nc )**2.0
!
!-----------Top of fillet
!
            ALPHAT(i) = ACOS( Rbc/Rcp ) - PHImesh
            ZETApT(i) = Rpcc - Rcp*COS(ALPHAT(i))
            ETApT(i) = -1.0*Rcp*SIN(ALPHAT(i))
            SpT(i) = -1.0*SQRT( (ZETApT(i))**2.0+(ETApT(i))**2.0 )
            ST(i) = SpT(i) - Rct
            ZETAT(i) = (ST(i)/SpT(i))*ZETApT(i)
            ETAT(i) = (ST(i)/SpT(i))*ETApT(i)
            BETAcT(i) = ALPHAT(i) - THETAcp
            BETAgT(i) = -1.0/R(i) * ( Rc*BETAcT(i)+0.5*Ps )
            RT(i) = SQRT( (Rg(i)+ZETAT(i))**2.0+(ETAT(i))**2.0 )
            THETArT(i) = ATAN( ETAT(i)/(Rg(i)+ZETAT(i)) ) - BETAgT(i)
            PHIT(i) = ATAN(ZETAT(i)/ETAT(i))
            RHOfT(i) = Rct + ( Rct+ST(i) )**2.0 / ( R0*SIN(PHIT(i))-
               (Rct+ST(i)) )
!
!-----------Bottom of fillet
```

```
!
            ALPHAB(i) = 0.0
            ZETApB(i) = Rpcc - Rcp*COS(ALPHAB(i))
            ETApB(i) = -1.0*Rcp*SIN(ALPHAB(i))
            SpB(i) = -1.0*SQRT( (ZETApB(i))**2.0+(ETApB(i))**2.0 )
            SB(i) = SpB(i) - Rct
            ZETAB(i) = (SB(i)/SpB(i))*ZETApB(i)
            ETAB(i) = (SB(i)/SpB(i))*ETApB(i)
            BETAcB(i) = ALPHAB(i) - THETAcp
            BETAgB(i) = -1.0/R(i) * ( Rc*BETAcB(i)+0.5*Ps )
            RBot(i) = SQRT( (Rg(i)+ZETAB(i))**2.0+(ETAB(i))**2.0 )
            THETArB(i) = ATAN( ETAB(i)/(Rg(i)+ZETAB(i)) ) - BETAgB(1)
            PHIB(i) = Pi/2.0
            RHOfB(i) = Rct + ( Rct+SB(i) )**2.0 / ( R0*SIN(PHIB(i))-
               (Rct+SB(i)) )
55    CONTINUE ![1]
!
!-----End of calculations
!
!-----Print error messages
!
      IF (Ta1.LE.0.0.OR.Ta2.LE.0.0) THEN
            PRINT*
            PRINT*, 'ERROR: Negative addendum tooth thickness'
            PRINT*, '       > Pinion or gear teeth are pointed'
            PRINT*
            STOP
      ENDIF
      IF (B.LT.-0.00005) THEN
            PRINT*
            PRINT*, 'ERROR: Gear assembly inherent backlash is less
               than zero'
            PRINT*, '       > Interference will occur'
            PRINT*
            STOP
      ENDIF
!
!-----Output [2, 3, and 6]
!
      PRINT*,                  '          GEAR SET SUMMARY'
      PRINT*,                  '-------------------------------------'
      PRINT*
      WRITE(*,'(1X,A,F10.4)')  'Diametral Pitch:            ', P
      WRITE(*,'(1X,A,F10.4,A)')'Radius of Cutter:           ',
                               Rc, ' in'
      WRITE(*,'(1X,A,F10.4)')  'Number of Teeth in Cutter:  ', Nc
      WRITE(*,'(1X,A,F10.4,A)')'Standard Pressure Angle:    ',
                               PHIcD, ' deg'
      WRITE(*,'(1X,A,F10.4,A)')'Operating Pressure Angle:   ',
                               PHIoD, ' deg'
      WRITE(*,'(1X,A,F10.4,A)')'Pinion Cutter Tooth Tip Radius:',
                               Rct, ' in'
      WRITE(*,'(1X,A,F10.4,A)')'Standard Center Distance:',
                               Cstddist, ' in'
      WRITE(*,'(1X,A,F10.4,A)')'Operating Center Distance:  ',
                               Cp, ' in'
      WRITE(*,'(1X,A,F10.4,A)')'Total Offset:               ',
```

```
                          etotal, ' in'
WRITE(*,'(1X,A,F10.4)')   'Standard Tooth Type:        ', k
WRITE(*,'(1X,A,F10.4,A)')'Backlash:                    ', B, ' in'
WRITE(*,'(1X,A,F10.4,A)')'Face Width:                  ',
                          FaceW, ' in'
WRITE(*,'(1X,A,F10.4,A)')'Torque:                      ',
                          Torq, ' in*lb'
WRITE(*,'(1X,A,F10.4,A)')'Starting Speed:              ',
                          RPM1, ' rpm'
WRITE(*,'(1X,A,F10.4,A)')'Ending Speed:                ',
                          RPM2, ' rpm'
WRITE(*,'(1X,A,F10.4,A)')'Tooth Load (fillet):         ',
                          Loadin, ' lb/in'
WRITE(*,'(1X,A,F10.4)')   'Contact Ratio:              ', Mp
PRINT*
PRINT*,                                'Pinion     Gear'
PRINT*
WRITE(*,'(1X,A,F11.4,4X,F11.4)')   'Teeth Number:          ',
                                   N(1), N(2)
WRITE(*,'(1X,A,F11.4,4X,F11.4,A)')'Addendum:               ',
                                   Ad1, Ad2, ' in'
WRITE(*,'(1X,A,F11.4,4X,F11.4,A)')'Dedendum:               ',
                                   Ded1, Ded2, ' in'
WRITE(*,'(1X,A,F11.4,4X,F11.4,A)')'Clearance               ',
                                   C, C, ' in'
WRITE(*,'(1X,A,F11.4,4X,F11.4,A)')'Addendum Radius:        ',
                                   Ro1p, Ro2p, ' in'
WRITE(*,'(1X,A,F11.4,4X,F11.4,A)')'Operating Pitch Radius:',
                                   Rp1, Rp2, ' in'
WRITE(*,'(1X,A,F11.4,4X,F11.4,A)')'Base Radius:            ',
                                   Rb(1), Rb(2), ' in'
WRITE(*,'(1X,A,F11.4,4X,F11.4,A)')'Dedendum Radius:        ',
                                   Rd1p, Rd2p, ' in'
WRITE(*,'(1X,A,F11.4,4X,F11.4,A)')'Generating Pitch Rad.: ',
                                   Rg(1), Rg(2), ' in'
WRITE(*,'(1X,A,F11.4,4X,F11.4,A)')'Addendum Tooth Thick.: ',
                                   Ta1, Ta2, ' in'
WRITE(*,'(1X,A,F11.4,4X,F11.4,A)')'Generating Pitch Thick:',
                                   Tg1, Tg2, ' in'
WRITE(*,'(1X,A,F11.4,4X,F11.4,A)')'Operating Pitch Thick.:',
                                   Tp1, Tp2, ' in'
WRITE(*,'(1X,A,F11.4,4X,F11.4,A)')'Op. Dedend. Tooth Th.: ',
                                   Td1, Td2, ' in'
WRITE(*,'(1X,A,F11.4,4X,F11.4,A)')'Gear Inertia:           ',
                                   I1, I2, ' lb*in*s^2'
WRITE(*,'(1X,A,F11.4,4X,F11.4,A)')'Offset:                 ',
                                   E(1), E(2), ' in'
WRITE(*,'(1X,A,F11.4,4X,F11.4,A)')'Stress Factor:          ',
                                   S1, S2, ' /in'
WRITE(*,'(1X,A,F11.4,4X,F11.4,A)')'Fillet (Tooth) Stress: ',
                                   Stress1, Stress2, ' psi'
WRITE(*,'(1X,A,F11.4,4X,F11.4,A)')'Standard Pitch Radius: ',
                                   R(1), R(2), ' in'
WRITE(*,'(1X,A,F11.4,4X,F11.4,A)')'Top Filt Curvature Rad:',
                                   RHOfT(1), RHOfT(2), ' in'
WRITE(*,'(1X,A,F11.4,4X,F11.4,A)')'Btm Filt Curvature Rad:',
                                   RHOfB(1), RHOfB(2), ' in'
```

```
      PRINT*
      PRINT*, '**ALWAYS CHECK AND COMPARE STATIC AND DYNAMIC OUTPUT**'
!-----Print to file 11, user named file
      WRITE(11,'(A)')           '          GEAR SET SUMMARY'
      WRITE(11,'(A)')           '-------------------------------------'
      WRITE(11,'(A)')           ' '
      WRITE(11,'(1X,A,F10.4)')  'Diametral Pitch:           ', P
      WRITE(11,'(1X,A,F10.4,A)')'Radius of Cutter:          ',
                                Rc, ' in'
      WRITE(11,'(1X,A,F10.4)')  'Number of Teeth in Cutter: ', Nc
      WRITE(11,'(1X,A,F10.4,A)')'Standard Pressure Angle:   ',
                                PHIcD, ' deg'
      WRITE(11,'(1X,A,F10.4,A)')'Operating Pressure Angle:  ',
                                PHIoD, ' deg'
      WRITE(11,'(1X,A,F10.4,A)')'Pinion Cutter Tooth Tip Radius:     ',
                                Rct, ' in'
      WRITE(11,'(1X,A,F10.4,A)')'Standard Center Distance:  ',
                                Cstddist, ' in'
      WRITE(11,'(1X,A,F10.4,A)')'Operating Center Distance: ',
                                Cp, ' in'
      WRITE(11,'(1X,A,F10.4,A)')'Total Offset:              ',
                                etotal, ' in'
      WRITE(11,'(1X,A,F10.4)')  'Standard Tooth Type:       ', k
      WRITE(11,'(1X,A,F10.4,A)')'Backlash:                  ', B, ' in'
      WRITE(11,'(1X,A,F10.4,A)')'Face Width:                ',
                                FaceW, ' in'
      WRITE(11,'(1X,A,F10.4,A)')'Torque:                    ',
                                Torq, ' in*lb'
      WRITE(11,'(1X,A,F10.4,A)')'Starting Speed:            ',
                                RPM1, ' rpm'
      WRITE(11,'(1X,A,F10.4,A)')'Ending Speed:              ',
                                RPM2, ' rpm'
      WRITE(11,'(1X,A,F10.4,A)')'Tooth Load (fillet):       ',
                                Loadin, ' lb/in'
      WRITE(11,'(1X,A,F10.4)')  'Contact Ratio:             ',
                                Mp
      WRITE(11,'(A)')                   ' '
      WRITE(11,'(A)')                   'Pinion      Gear'
      WRITE(11,'(A)')                   ' '
      WRITE(11,'(1X,A,F11.4,4X,F11.4)')  'Teeth Number:          ',
                                         N(1), N(2)
      WRITE(11,'(1X,A,F11.4,4X,F11.4,A)')'Addendum:              ',
                                         Ad1, Ad2, ' in'
      WRITE(11,'(1X,A,F11.4,4X,F11.4,A)')'Dedendum:              ',
                                         Ded1, Ded2, ' in'
      WRITE(11,'(1X,A,F11.4,4X,F11.4,A)')'Clearance              ',
                                         C, C, ' in'
      WRITE(11,'(1X,A,F11.4,4X,F11.4,A)')'Addendum Radius:       ',
                                         Ro1p, Ro2p, ' in'
      WRITE(11,'(1X,A,F11.4,4X,F11.4,A)')'Operating Pitch Radius:',
                                         Rp1, Rp2, ' in'
      WRITE(11,'(1X,A,F11.4,4X,F11.4,A)')'Base Radius:           ',
                                         Rb(1), Rb(2), ' in'
      WRITE(11,'(1X,A,F11.4,4X,F11.4,A)')'Dedendum Radius:       ',
                                         Rd1p, Rd2p, ' in'
      WRITE(11,'(1X,A,F11.4,4X,F11.4,A)')'Generating Pitch Rad.: ',
                                         Rg(1), Rg(2), ' in'
```

```
      WRITE(11,'(1X,A,F11.4,4X,F11.4,A)')'Addendum Tooth Thick.: ',
                                         Ta1, Ta2, ' in'
      WRITE(11,'(1X,A,F11.4,4X,F11.4,A)')'Generating Pitch Thick:',
                                         Tg1, Tg2, ' in'
      WRITE(11,'(1X,A,F11.4,4X,F11.4,A)')'Operating Pitch Thick.:',
                                         Tp1, Tp2, ' in'
      WRITE(11,'(1X,A,F11.4,4X,F11.4,A)')'Op. Dedend. Tooth Th.: ',
                                         Td1, Td2, ' in'
      WRITE(11,'(1X,A,F11.4,4X,F11.4,A)')'Gear Inertia:          ',
                                         I1, I2, ' lb*in*s^2'
      WRITE(11,'(1X,A,F11.4,4X,F11.4,A)')'Offset:                ',
                                         E(1), E(2), ' in'
      WRITE(11,'(1X,A,F11.4,4X,F11.4,A)')'Stress Factor:         ',
                                         S1, S2, ' /in'
      WRITE(11,'(1X,A,F11.4,4X,F11.4,A)')'Fillet (Tooth) Stress: ',
                                         Stress1, Stress2, ' psi'
      WRITE(11,'(1X,A,F11.4,4X,F11.4,A)')'Standard Pitch Radius: ',
                                         R(1), R(2), ' in'
      WRITE(11,'(1X,A,F11.4,4X,F11.4,A)')'Top Filt Curvature Rad:',
                                         RHOfT(1), RHOfT(2), ' in'
      WRITE(11,'(1X,A,F11.4,4X,F11.4,A)')'Btm Filt Curvature Rad:',
                                         RHOfB(1), RHOfB(2), ' in'
!
!-----Print to file 12: "IntFile.TXT" ![7]
!
      NcI = INT(Nc)
      N1I = INT(N(1))
      N2I = INT(N(2))
      WRITE(12,'(A)')               'Intermediate File
                                    ! Job Identification'
      WRITE(12,'(A)')               '===> Cutter Geometry'
      WRITE(12,'(A,F6.4,A)')        '2       ', E(1), '
                                    ! Hob offset code (0=None, 1=Offset
                                    2=Cutter); Offset Amount'
      WRITE(12,'(F4.1,4X,F4.1,A)')  P, PHIcD, '
                                    ! Diametral Pitch, Pressure Angle
                                    (deg)'
      WRITE(12,'(I2,A)')            NcI, '
                                    ! Number of cutter teeth (Shaper
                                    cutter)'
      WRITE(12,'(A)')               '1.000      1.000
                                    ! Cutter Addendum Ratio (A/DP)'
      WRITE(12,'(A)')               '0.0  0.0
                                    ! Cutter edge radius ratio
                                    (RCEG/DP)'
      WRITE(12,'(A)')               '===> Gear Geometry'
      WRITE(12,'(I2,7X,I2,A)')      N1I, N2I, '
                                    ! Number of teeth'
      WRITE(12,'(F6.4,4X,F6.4,A)')  Do1p, Do2p, '
                                    ! Outside Diameters'
      WRITE(12,'(F4.2,4X,F4.2,A)')  Cratio, Cratio,'
                                    ! Tooth Clearance Ratios (C/DP)'
      WRITE(12,'(F4.2,4X,F6.4,A)')  FaceW, B0, '
                                    ! Face Width (in), Backlash (in)'
      WRITE(12,'(A)')               '===> Center dist., Std. or spread
                                    cntr.'
      WRITE(12,'(A)')               '1
```

```
                                ! Center Distance Code (0=Standard
                                1=Extended CD)'
WRITE(12,'(F5.3, A)')           CdstEx , '
                                ! Center Distance Extension (in)'
WRITE(12,'(A)')                 '===> Gear Material Data'
WRITE(12,'(A)')                 '30.E6     30.E6
                                ! Youngs Modulus'
WRITE(12,'(A)')                 '0.3       0.3
                                ! Poissons Ratio'
WRITE(12,'(A)')                 '===> Operating Parameters'
WRITE(12,'(F6.2,A)')            Torq, '
                                ! Input Torque (lb-in)'
WRITE(12,'(F6.0,4X,F6.0,A)')    RPM1, RPM2, '
                                ! Starting Speed, Ending Speed
                                (rpm)'
WRITE(12,'(F6.0,A)')            RPMi, '
                                ! Speed Increment (rpm)'
WRITE(12,'(A)')                 '1
                                ! Lubrication Code (1=Buckingham,
                                2=EHD)'
WRITE(12,'(A)')                 '1
                                ! Damping Code (0=No Damping,
                                1=Damping & Friction)'
WRITE(12,'(A)')                 '0.1
                                ! Gear Mesh Damping Coefficient'
WRITE(12,'(A)')                 '===> Inertia and Stiffness Data'
WRITE(12,'(A)')                 '0.100      0.124
                                ! Input and Output Inertia'
WRITE(12,'(F7.5,1X,F7.5,A)')    I1, I2, '
                                ! Gear-1 and Gear-2 Inertia'
WRITE(12,'(A)')                 '150000.    150000.
                                ! Input and Output Shaft Torsional
                                Stiffness'
WRITE(12,'(A)')                 '===> Solution & Modif. Codes
                                (See Notes)'
WRITE(12,'(A)')                 '2
                                ! Solution Code (1|2
                                static,dynamic,negative=rigid)'
WRITE(12,'(A)')                 '0
                                ! Modification Code (-1 to 4
                                conv,none,lin,para1/2,digi)'
WRITE(12,'(A)')                 '0    0
                                ! Modification Length (Start) on
                                Gear 1 & 2'
WRITE(12,'(A)')                 '0    0
                                ! Amount of Modification on Gear 1
                                & 2'
WRITE(12,'(A)')    '===> Plot Control Codes (See Notes)'
WRITE(12,'(A)')    ' 0          ! Profile Modification Chart'
WRITE(12,'(A)')    ' 0          ! Tooth Deflection Curves'
WRITE(12,'(A)')    ' 0          ! Static Transmission Error'
WRITE(12,'(A)')    ' 0          ! Dynamic Transmission Error'
WRITE(12,'(A)')    ' 0          ! Static Tooth Load'
WRITE(12,'(A)')    ' 0          ! Dynamic & Static Tooth Load'
WRITE(12,'(A)')    ' 0          ! Static Tooth Stiffness'
WRITE(12,'(A)')    ' 0          ! FFT of Static Transmission Error'
WRITE(12,'(A)')    ' 0          ! FFT of Dynamic Tooth Load'
```

```
      WRITE(12,'(A)')   ' 0         ! Friction Coefficient'
      WRITE(12,'(A)')   ' 0         ! Friction Torque'
      WRITE(12,'(A)')   ' 0         ! Dynamic Stress'
      WRITE(12,'(A)')   ' 0         ! Dynamic Factor Speed Survey'
      WRITE(12,'(A)')   '===> Printer-Plot Output Device Code'
      WRITE(12,'(A)')   ' 0         ! 0=VGA, 1=EPSON FX-8*, 2=HP LJ,
                                    3=Post Script File, 4=Auto CAD
                                    File'
      WRITE(12,'(A)')   '*** Notes:'
      WRITE(12,'(A)')   '   >>> Solution Control Code - - - -'
      WRITE(12,'(A)')   '      1=Static Analysis   2=Dynamic Analysis'
      WRITE(12,'(A)')   '      Negative (-1 or -2) --> Suppress
                                   Extended Tooth Contact'
      WRITE(12,'(A)')   '   >>> Modification code (-1 to 4) - - - -'
      WRITE(12,'(A)')   '     -1=Conventional Relief    0=Involute, No
                                   Mod. 1=Linear Modification'
      WRITE(12,'(A)')   '      2=Parabolic Type 1 Mod.  3=Parabolic
                                   Type 2 Mod.  4=Digitized Mod.'
      WRITE(12,'(A)')   '   >>> Plot Control Code (0 to 3) - - - -'
      WRITE(12,'(A)')   '      0=no output   1=Printer Plot   2=Plot
                                   File 3=Both Plot & Plot File'
      PRINT*
      PRINT*, 'End of program STATIC.'
      END
!
!----------!
!==========!
!
      REAL FUNCTION SOLINV(Soltn)
!
!     This function contains the
!     half interval method
!     It solves the involute function
!     (invA = Soltn, solve for 'A')
!
      INTEGER i
      REAL An, Bn, TOL, Diff, Mo, FctMo, SgnFct, Soltn
!
      i = 0
      An = 0.0
      Bn = 3.14/2
      TOL = 10.0**(-5.0)
      Diff = Bn-An
 10   IF (i.LE.100.AND.Diff.GT.TOL) THEN
            Mo = (An+Bn)/2.0
            !Function
            FctMo = TAN(Mo)-Mo
            IF (FctMo.EQ.Soltn) THEN
                  PRINT*, 'Exact numerical solution found.'
                  GO TO 20
            ENDIF
            SgnFct = (FctMo-Soltn) / ABS(FctMo-Soltn)
            IF (SgnFct.GT.0.0) THEN
                  Bn = Mo
            ELSEIF (SgnFct.LT.0.0) THEN
                  An = Mo
            ELSE !(SgnFct.EQ.0.0)
```

```
                  PRINT*, 'PROGRAM ERROR, INCORRECT SIGN FUNCTION.'
                  STOP
            ENDIF
            Diff = Bn-An
            i = i+1
            GO TO 10
      ENDIF
 20   SOLINV = Mo
      RETURN
      END
!
!==========!
!::::::::::!
!
!     WORKS CITED
!
!     1.    Colbourne, J. R. (1987).  The Geometry of
!           Involute Gears.  New York: Springer-Verlag.
!     2.    Green, R. N. and Mabie, H. H. (1980a, May).
!           "Determination of Pinion-Cutter Offsets Required
!           to Produce Nonstandard Spur Gears with Teeth of
!           Equal Strength."  Mechanism and Machine Theory,
!           15(6), 491-506.  Great Britain: Pergamon Press.
!     3.    Green, R. N. and Mabie, H. H. (1980b, May).
!           "Determination of Static Tooth Stresses in
!           Nonstandard Spur Gears Cut by Pinion Cutter."
!           Mechanism and Machine Theory, 15(6), 507-514.
!           Great Britain: Pergamon Press.
!     4.    Lin, H. H., Liou, C. H., Oswald, F. B.,
!           and Townsend, D. P. (1996).  "Balancing
!           Dynamic Strength of Spur Gears Operated at
!           Extended Center Distance."  Prepared for the
!           Seventh International Power Transmission and
!           Gearing Conference.  NASA TM-107222.
!           San Diego, CA: National Aeronautics and
!           Space Administration and U.S. Army Research
!           Laboratory.
!     5.    Mabie, H. H. and Reinholtz, C. F. (1987).
!           Mechanisms and Dynamics of Machinery (4th Ed.).
!           Wiley.
!     6.    Oswald, F. B., Lin, H. H., and Delgado, I. R.
!           (1996).  Dynamic Analysis of Spur Gear
!           Transmissions (DANST) [Computer Software].
!           Washington, D.C.: National Aeronautics and
!           Space Administration and U.S. Army Research
!           Laboratory.
!     7.    Oswald, F. B., Lin, H. H., and Delgado, I. R.
!           (1996, August).  Dynamic Analysis of Spur
!           Gear Transmissions (DANST), PC Version 3.00
!           User Manual.  NASA TM-107291.  Washington, D.C.:
!           National Aeronautics and Space Administration
!           and U.S. Army Research Laboratory.
!     8.    Oswald, F. B., Lin, H. H., Liou, C. H.,
!           and Valco, M. J. (1993).  Dynamic Analysis of
!           Spur Gears Using Computer Program DANST.
!           NASA TM-106211.  Prepared for the 29th Joint
!           Propulsion Conference and Exhibit cosponsored
```

!   by the AIAA, SAE, ASME, and ASEE.
!   Monterey, California.
!   9.   Rogers, C. A., Mabie, H. H., and Reinholtz, C. F.
!   (1990). "Design of Spur Gears Generated
!   with Pinion Cutters." Mechanism and Machine
!   Theory, 25(6), 623-634. Great Britain:
!   Pergamon Press.
!
!:::::::::::!

Appendix B

Example Output of Static Program

GEAR SET SUMMARY

Diametral Pitch:	10.0000	
Radius of Cutter:	2.0000	in
Number of Teeth in Cutter:	40.0000	
Standard Pressure Angle:	20.0000	deg
Operating Pressure Angle:	24.5802	deg
Pinion Cutter Tooth Tip Radius:	.0000	in
Standard Center Distance:	3.0000	in
Operating Center Distance:	3.1000	in
Total Offset:	.1050	in
Standard Tooth Type:	1.0000	
Backlash:	.0000	in
Face Width:	1.0000	in
Torque:	480.0000	in*lb
Starting Speed:	6000.0000	rpm
Ending Speed:	6000.0000	rpm
Tooth Load (fillet):	510.8053	lb/in
Contact Ratio:	1.3698	

	Pinion	Gear	
Teeth Number:	20.0000	40.0000	
Addendum:	.1248	.0702	in
Dedendum:	.0952	.1498	in
Clearance	.0250	.0250	in
Addendum Radius:	1.1581	2.1369	in
Operating Pitch Radius:	1.0333	2.0667	in
Base Radius:	.9397	1.8794	in
Dedendum Radius:	.9381	1.9169	in
Generating Pitch Rad.:	1.0210	2.0210	in
Addendum Tooth Thick.:	.0510	.0725	in
Generating Pitch Thick:	.1940	.1747	in
Operating Pitch Thick.:	.1854	.1392	in
Op. Dedend. Tooth Th.:	.2216	.2279	in
Gear Inertia:	.0013	.0211	lb*in*s^2
Offset:	.0631	.0419	in
Stress Factor:	22.8868	22.8889	/in
Fillet (Tooth) Stress:	14186.2600	13174.6900	psi
Standard Pitch Radius:	1.0000	2.0000	in
Top Filt Curvature Rad:	.0863	.1012	in
Btm Filt Curvature Rad:	.0096	.0099	in

Appendix C

Example Output for Dynamic Program Input

The following is an example of the static program output for input into the DANST program. The following code has been modified so as to fit appropriately in this document. Certain formatting, indentation, tabs, and spacing, must be removed for accurate program execution.

```
Intermediate File                                ! Job Identification
===> Cutter Geometry
2        .0631          ! Hob offset code (0=None, 1=Offset 2=Cutter);
Offset Amount
10.0    20.0            ! Diametral Pitch, Pressure Angle (deg)
40                      ! Number of cutter teeth (Shaper cutter)
1.000 1.000             ! Cutter Addendum Ratio (A/DP)
0.0   0.0               ! Cutter edge radius ratio (RCEG/DP)
===> Gear Geometry
20       40             ! Number of teeth
2.3161    4.2738        ! Outside Diameters
 .25     .25            ! Tooth Clearance Ratios (C/DP)
1.00     .0000          ! Face Width (in), Backlash (in)
===> Center dist., Std. or spread cntr.
1                       ! Center Distance Code (0=Standard 1=Extended
                          CD)
 .100                   ! Center Distance Extension (in)
===> Gear Material Data
30.E6     30.E6         ! Youngs Modulus
0.3       0.3           ! Poissons Ratio
===> Operating Parameters
480.00                  ! Input Torque (lb-in)
 1000.    30000.        ! Starting Speed, Ending Speed (rpm)
  146.                  ! Speed Increment (rpm)
1                       ! Lubrication Code (1=Buckingham, 2=EHD)
1                       ! Damping Code (0=No Damping, 1=Damping &
Friction)
0.1                     ! Gear Mesh Damping Coefficient
===> Inertia and Stiffness Data
0.100 0.124             ! Input and Output Inertia
 .00132  .02106         ! Gear-1 and Gear-2 Inertia
150000.     150000.     ! Input and Output Shaft Torsional Stiffness
===> Solution & Modif. Codes (See Notes)
2                       ! Solution Code (1|2
static,dynamic,negative=rigid)
0                       ! Modification Code (-1 to 4
conv,none,lin,para1/2,digi)
0     0                 ! Modification Length (Start) on Gear 1 & 2
0     0                 ! Amount of Modification on Gear 1 & 2
===> Plot Control Codes (See Notes)
 0                      ! Profile Modification Chart
 0                      ! Tooth Deflection Curves
```

```
 0                     ! Static Transmission Error
 0                     ! Dynamic Transmission Error
 0                     ! Static Tooth Load
 0                     ! Dynamic & Static Tooth Load
 0                     ! Static Tooth Stiffness
 0                     ! FFT of Static Transmission Error
 0                     ! FFT of Dynamic Tooth Load
 0                     ! Friction Coefficient
 0                     ! Friction Torque
 0                     ! Dynamic Stress
 0                     ! Dynamic Factor Speed Survey
===> Printer-Plot Output Device Code
 0       ! 0=VGA, 1=EPSON FX-8*, 2=HP LJ, 3=Post Script File, 4=Auto
           CAD File
*** Notes:
   >>> Solution Control Code - - - -
      1=Static Analysis   2=Dynamic Analysis
      Negative (-1 or -2) --> Suppress Extended Tooth Contact
   >>> Modification code (-1 to 4) - - - -
     -1=Conventional Relief 0=Involute, No Mod. 1=Linear Modification
      2=Parabolic Type 1 Mod. 3=Parabolic Type 2 Mod. 4=Digitized Mod.
   >>> Plot Control Code (0 to 3) - - - -
      0=no output 1=Printer Plot 2=Plot File 3=Both Plot & Plot File
```

Appendix D

Finite Element Model

D.4.1. Overview and Model Type

Finite element modeling, as defined by Macdonald (2007), "divides the domain of interest into a finite number of simple sub-domains and uses [varying] concepts to construct an approximation of the solution over the collection of sub-domains." The author further elaborates that the finite element method is encapsulated by equation 120, which relates force, {F}, to stiffness, [K], and displacement, {U}. However, for a "dynamic analysis and nonlinear analysis," velocity, $\{\dot{U}\}$, and acceleration, $\{\ddot{U}\}$, must be taken into account with consideration of the mass, [M], and damping, [C] within the system. This is encapsulated by equation 121 (pp. 4, 73-75). A further description can be found in the literature.

$$\{F\} = [K] * \{U\} \qquad \text{EQ. 120}$$

$$\{F\} = [M] * \{\ddot{U}\} + [C] * \{\dot{U}\} + [K] * \{U\} \qquad \text{EQ. 121}$$

As can be seen by the relationships described through equations 120 and 121, a finite element model can be described statically or dynamically. Dynamically, a model can be solved implicitly or explicitly. Macdonald (2007) describes the implicit solution in the following manner:

> The current nodal displacement . . . is a function of time derivatives of . . . nodal acceleration and velocity . . . which are also unknown. Consequently the implicit method iterates . . . a solution for the nodal displacements and its time derivatives

> in order to solve the equation. This requires . . . solving simultaneous equations and hence inverting the large system of matrices. (p. 246)

The implicit solution method completely solves equation 121 in several stages for current and future "steps." Consequently, this type of solution is more precise than the explicit solution method. However, dynamic contact conditions, which are found in the current model, can destabilize the solution process (Macdonald, 2007, pp. 243-245).

Macdonald (2007) describes the strength of the explicit model as following "Newton's Second Law, F = ma." The explicit solution method solves equation 121 based upon current and past steps. However, the explicit solution is not as precise as the implicit solution, and precise measurements are required for the current model. The explicit "solution time is essentially based upon the size of the smallest element in the mesh;" thus, smaller element mesh would require more computational power (pp. 245-247). Macdonald (2007) describes the explicit solution in the following manner:

> The current nodal displacement is a function of the nodal displacement, velocity, and accelerations from the previous time step. Since this information is already known a diagonal mass matrix can be used and the global equation is a system of linear algebraic equations which can be solved without using simultaneous equations." (p. 246)

Unfortunately, both dynamic solution methods are still computationally expensive, the implicit solution more so than the explicit solution. As found by Lee (2009), a quasi-static procedure can be used to simplify the dynamic model.

> Quasi-Static is a condition that refers to forces or displacements which vary or change slowly with time. A force is considered to vary slowly if the frequency of variation is much lower than the lowest natural frequency of the system. (p. 30)

In essence, the quasi-static model considers the dynamic model is a series of sub models. In terms of the spur gear dynamic model, the pinion and gear can be rotated through a mesh cycle, simulating the motion of the assembly (Lee, 2009, pp. 29-31) The

statements made by Lee (2009, pp. 29-31) agree, in part, with those of MacDonald (2007). According to Macdonald, a static solution does not consider dynamic effects and assumes the "load and boundary conditions remain constant over the course of the solution or change relatively slowly" (pp. 236-239).

At 6,000 rpm, the dynamic effects, according to the DANST program, are minimal and the speed is far away from the natural frequencies. Moreover, with the dynamic load factor calculated by the DANST program, general dynamic effects can be taken into account by a static model. In order to minimize changing load and boundary conditions, the quasi-static gear assembly model is broken down into a series of individual frames at a specific rotation. For this finite element model and analysis, ABAQUS/CAE 6.9-EF1 is used. As the stress within the gear tooth is a combination of many different components, Von Mises stress, as calculated within ABAQUS, is used during the course of this study (Van der Zijp, 2009, ABAQUS program). With the dynamic load factor as described by Lin and Liou (1998), the quasi-static, finite element model is built in several sub models providing an alternative, simplified model to the dynamic solution (pp. 45-48).

D.4.2. Model Construction

The information provided in chapter 3, section 2, and table 1 provides the basis for the finite element model. In order to simplify the model, a specific pinion and gear offset is chosen, 0.0631 inches and 0.0419 inches, respectively, values which are from the works of Green and Mabie (1980b, p. 508). The rotational speed is set at 6000 rpm, as given by the example files from DANST manual (Oswald et al., 1996b, p. 5).

The output created by the static model following the works of Green and Mabie (1980a, p. 506; 1980b, pp. 507-514), supplies several dimensions. In order to create the involute profile, an assumption is made that the curve is a continuous arc. This assumption is made, in part, from figure 3 (Mabie & Reinholtz, 1987, p. 133). Knowing the tooth thickness, t_a, is a curve along a circle with a certain radii, R_a, an involute curve can be created from equation 123, see figure 33.

Since $t_a = R_a * \theta_a = R_a * (2 * \gamma_a)$ where γ_a is in radians EQ. 122

Then $\gamma_a = \frac{180}{\pi} * \left(\frac{t_a}{2 * R_a}\right)$ EQ. 123

The fillet radius is found through equations 39 through 66 in chapter 2 section 3 as described by Colbourne (1987, pp. 39-40, 120-121, 133-136, 151, 221-223, 235-237). Since the radius of curvature at the top of the fillet is much larger than that at the bottom of the fillet, the latter is used in the finite element model (Colbourne, 1987, pp. 239-240).

The pinion and gear are three-dimensional parts; however, the dimensions of the tooth, such as its thickness and height, are much less than thickness of the spur gear, a face width of 1.0 inch. Since the perpendicular thickness dimensions is much greater, the plane strain assumption can be used, according to MacDonald (2007). Based upon this assumption, the pinion and gear can be modeled as a two-dimensional instance (pp. 116-118).

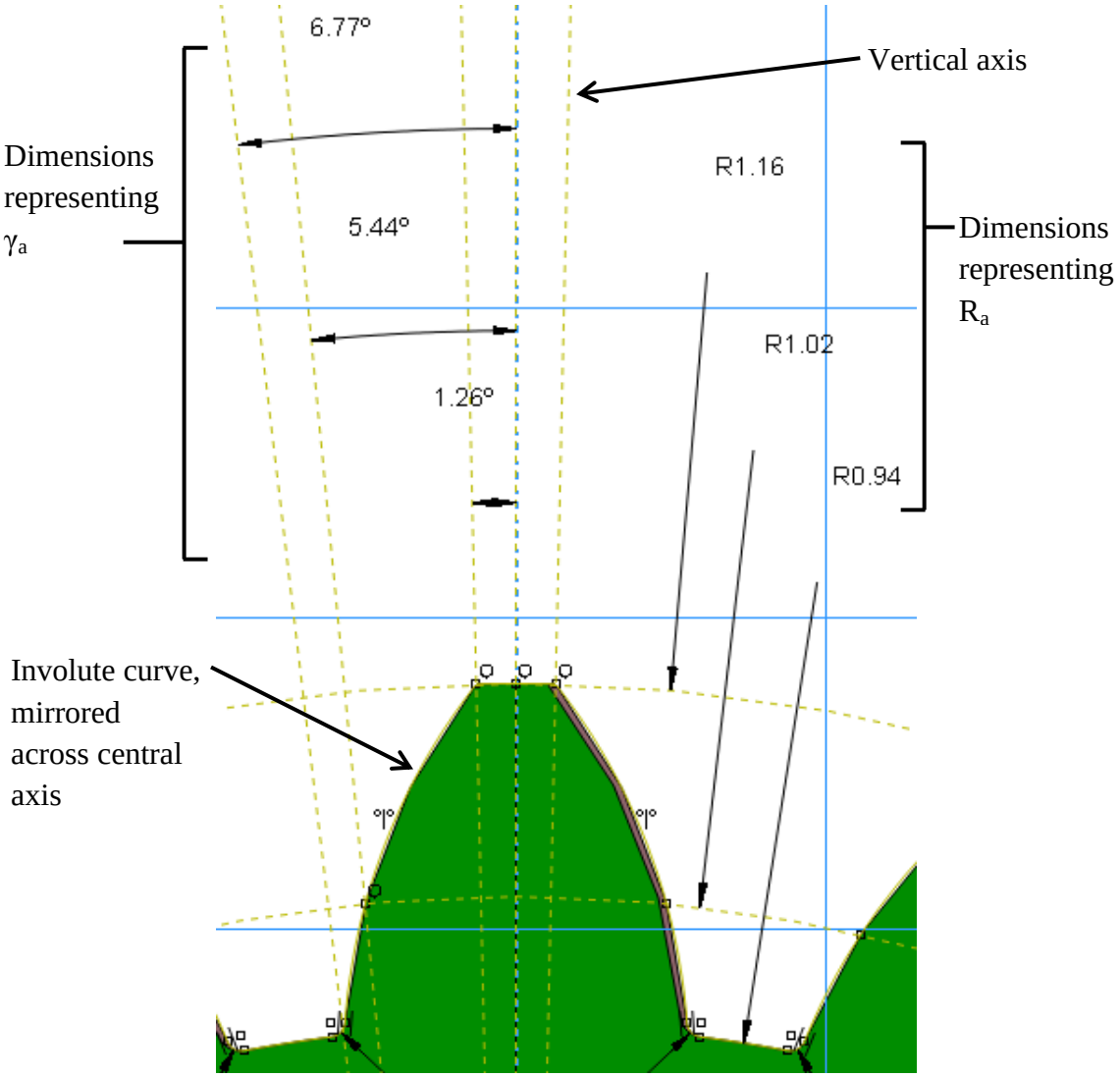

Figure 33. Base dimension sketch in ABAQUS program (Van der Zijp, 2009).

A spur gear contains cyclic geometry, being the base is a circle and the teeth are arranged in circular pattern upon that base. Macdonald (2007) described individual features, such as the teeth, can be removed if they are "far away from expected stress concentrations or load paths" (pp. 188-191). In a preliminary study, a de-featured model consisting of only one tooth for a spur gear with point loads at the tip is created and compared to a full model with a point load at the tip of one tooth. These preliminary

studies show a stress difference of 0.1%. Moreover, the results of the preliminary study indicate that a distance of one full tooth away from the tooth carrying load is sufficient. Additional studies showing similar results support the following concept that the gear tooth acts against a larger, and comparatively rigid, body. The percent difference between the full body and de-featured model body is 2.8%. Thus, teeth not carrying load can be de-featured and the finite element model is simplified.

The boundary conditions of the pinion and gear are related to the center bore, key, and shaft that run through the center of each. Modeling the center boundary condition of the pinion and gear as a point would, in essence, create a point load and complicate other parts of the finite element model, such as creating distortion within the element mesh with. Thus, a center hole is made in the pinion and gear, and the boundary condition is built upon this central key. The assumption that a model having a distance of one full tooth away from the loaded teeth is accurate is also part of the boundary condition. With the central hole and pie shaped region of the model, as seen in figure 35, a rigid body tie interaction is created between the edge lines and the central vertex of the pinion or gear. As shown in section 1 of this appendix, describing the quasi-static model, the pinion vertex is modeled as pinned and the gear vertex is modeled as fixed. Thus, this creates a pinned body for the pinion, which is under load, and a fixed body for the gear, which experiences the load.

The second interaction, which is standard surface-to-surface contact, is the contact between two separate surfaces or assembly instances, the pinion and gear (Van der Zijp, 2009, ABAQUS program). The contact is described as having finite sliding, which, according to Lee (2009), allows for the continual adjustment between changing master

and slave surfaces (p. 46). In order to simplify the finite element model, the surface property is modeled as frictionless and damping is not included. An intermediate study shows that a coefficient of friction up to 1.0 leads to a maximum difference in stress of 3.1%. Also, the model assumes lubrication. The master surface is chosen to be the gear, and the slave surface is chosen to be the pinion, as is shown in figure 36. In order to initiate the model, a negligible overlap is required, which is approximately one quarter of an element in length. This being the case, adjustment allowance is allowed within the ABAQUS finite element model; however, this means that the slave surface or assembly, the pinion, is moved (Van der Zijp, 2009, ABAQUS program). Since the pinion is modeled as pinned, this reduces residual stresses.

The partitioning and mesh of the model is based upon the work of Brauer (2004). This mesh mapping and partitioning favors the shape and symmetry of the tooth profile, root, and body, as can be seen in figure 34. The mesh mapping also indicates general regions of interest (pp. 1868-1871). The primary region of interest in this study is at the fillet at the base of the tooth. As explained by Colbourne (1987), the stresses at the base of the tooth are cause by the moment produced by the tangential part of the applied force and the smaller compressive force produced by the radial part of the applied force. Though the unloaded side of the tooth that is in compression will have a greater stress at the tooth root, the side of the tooth that is in tension is of greater concern to the engineer. This is because the "tensile stress . . . is found to cause fatigue cracks" (pp. 248-249). Thus, the region of interest is the root of the tooth that is in tension, the side where contact occurs.

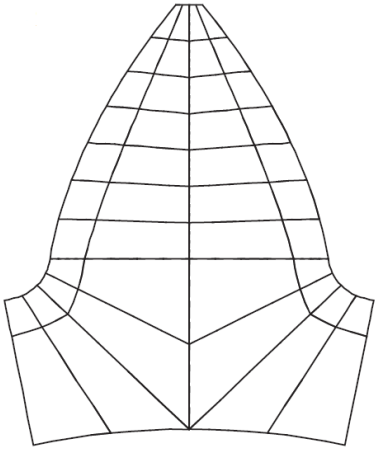

Figure 34. Preliminary mesh model by Brauer (2004, p. 1870).

The finite element model pinion and gear instances are constructed based upon the dimensional input of zero backlash, which means there is neither space nor interference between the teeth. Due to the approximations provided by the ABAQUS mesh modeling software and the geometric instance input, minor interference occurs between the teeth of the pinion and gear (Van der Zijp, 2009, ABAQUS program). This is overcome by adding an offset on the pinion tooth equal to the interference, 0.004 inches, where the pinion tooth where contact does not occur.

Further refinement in the model includes the choice of an element orientation, distribution, bias, and type. As indicated by figure 34, bias should be oriented towards the edge (Brauer, 2004). The element type is confined to tetrahedral or quadrilateral. The Structured Technique, Minimize Mesh Transition Algorithm is chosen in ABAQUS to aid in reducing the element distortion. For model simplicity, the standard element library, linear element type, and reduced integration techniques are used with the plane strain assumption already discussed. The resulting element is a 4-node bilinear plane

strain quadrilateral, reduced integration, hourglass control. The resulting mesh is shown through a convergence study in the following section (Van der Zijp, 2009, ABAQUS program).

Load is applied to the finite element model as a moment placed upon the central vertex of the pinion. The dynamic model created by DANST outputs a dynamic load factor of 1.173. Thus, a static torque of 480 in-lb would become 563.04 in-lb for a dynamic finite element model. This load path follows the pinion, through the contact condition, into the gear and gear body. The resulting solution displays the stress as described in section 1 of this appendix.

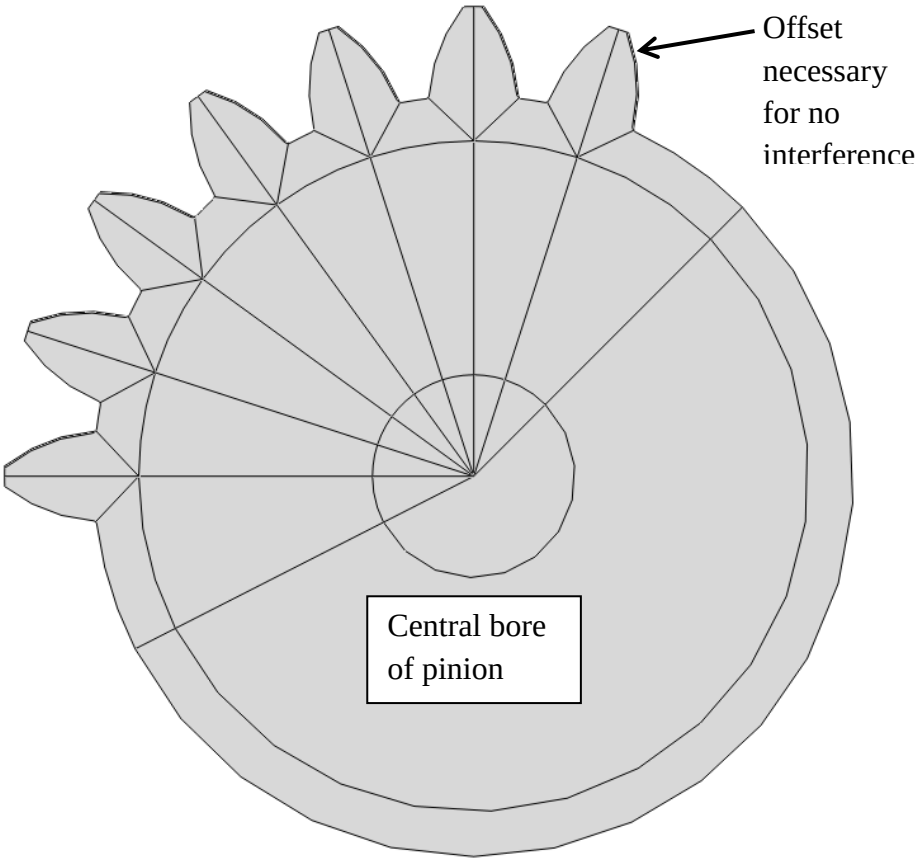

Figure 35. Instance partitions, pinion is shown. Note that the model is de-featured to only certain, key teeth (Van der Zijp, 2009, ABAQUS program).

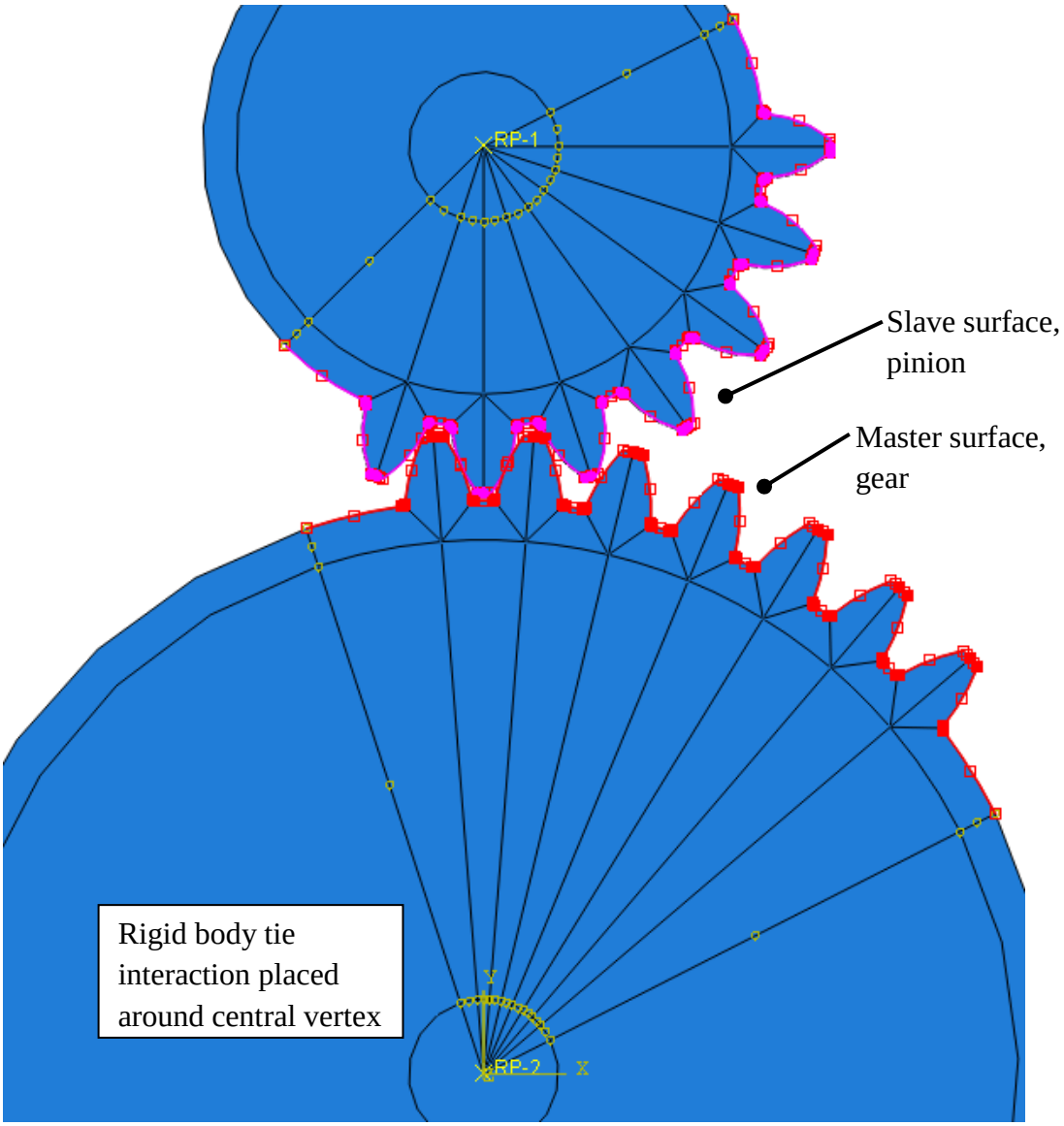

Figure 36. Interactions between pinion (top) and gear (bottom). The red highlight indicates the master surface, and the purple highlight indicates the slave surface. Rigid body tie constraints are also shown for both pinion and gear (Van der Zijp, 2009, ABAQUS program).

D.4.3. Mesh Convergence Study

As stated in the previous section, the region of interest exists at the tooth fillet on the side where contact occurs. Additionally, the mesh convergence study requires a standard with which to be compared, before the quasi-static model is run. To create this

standard, the general finite element model is first compared to the static assumptions made by Rogers, Mabie, and Reinholtz (1990). Multiple tooth contact is ignored, and the pinion and gear are rotated such that full load is applied at the tip. For the pinion, this results in a stress of 14,186 psi at the root of the tooth and 13,175 psi for that of the gear (p. 629). Based upon a series of preliminary models, and the partitioning by Brauer (2004), the following partitioning and element bias patterns are set as shown in figure 37 and tables 4 and 5.

Using the element bias and spacing on figure 37, a mesh convergence study is performed. To reduce computational requirements, the instance opposite to the instance under study is set to the lowest global element size, 0.013 inches. For example, for table 4, which is a convergence study of the pinion, the gear element size is set at the minimum while the pinion mesh is optimized.

The element size and bias chosen are shown in underline in tables 4 and 5. These mesh dimensions are then applied to the quasi-static finite element model, where the pinion and gear are rotated through a full mesh cycle where the factored, dynamic load is applied.

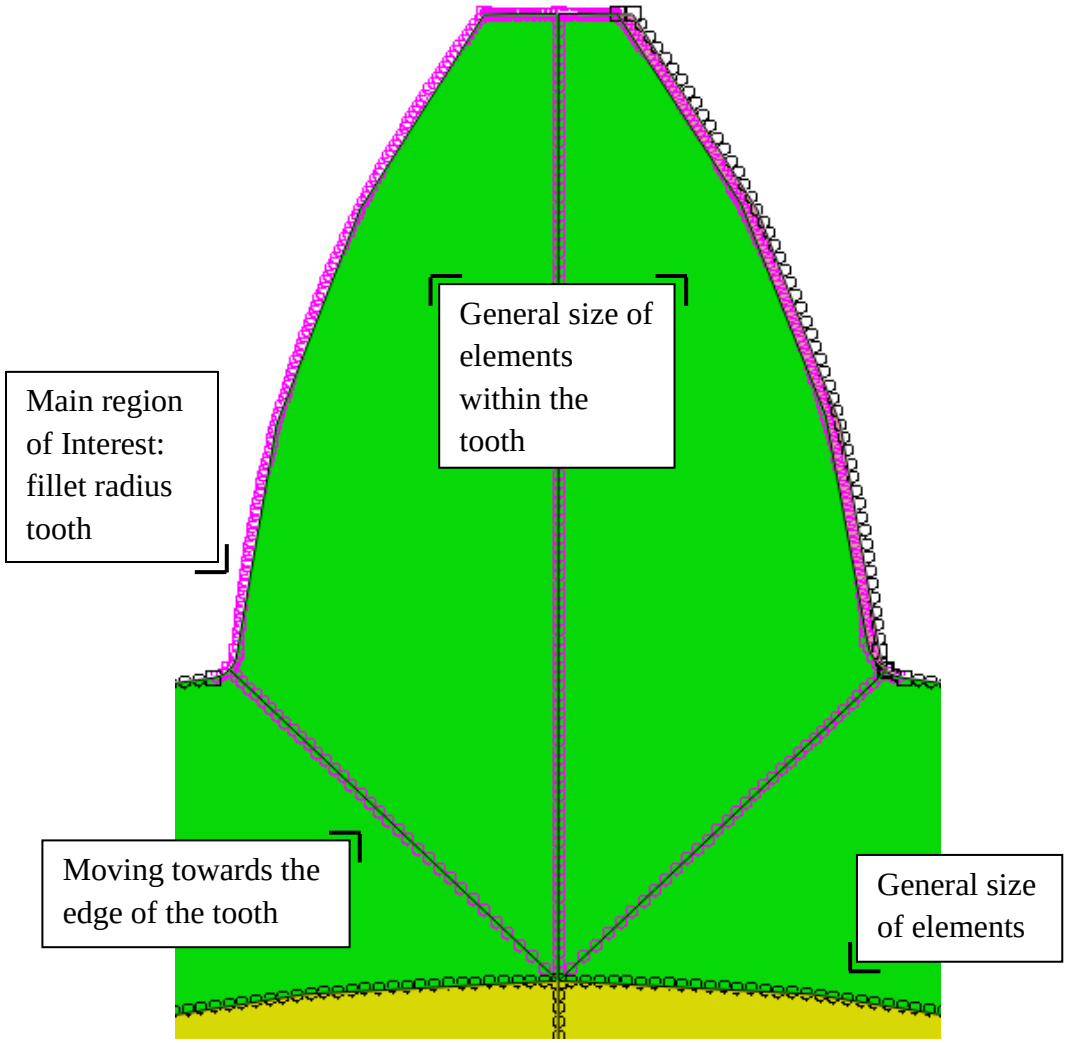

Figure 37. Image of element size and bias. This image is the result of the mesh convergence study for the pinion as shown in table 4 (Van der Zijp, 2009, ABAQUS program).

Table 4. Mesh convergence study of the pinion

Pinion					
Moving towards the edge of the tooth	General size of elements	General size of elements within the tooth	Main region of Interest: fillet radius	Von Mises stress, not averaged	Percent Difference
Bias, Number of elements per given length	General element size	Number of elements along tooth height	Number of elements along fillet	Loaded Tooth Side [psi]	%
2, 10	0.0130	30	1	9093	-35.9%
2, 15	0.0113	45	2	10820	-23.7%
2, 20	0.0097	60	2	12052	-15.0%
2, 25	0.0080	75	3	13150	-7.3%
2, 30	0.0063	90	3	13809	-2.7%
2, 35	0.0047	105	4	14474	2.0%

Table 5. Mesh convergence study of the gear

Gear					
Moving towards the edge of the tooth	General size of elements	General size of elements within the tooth	Main region of Interest: fillet radius	Von Mises stress, not averaged	Percent Difference
Bias, Number of elements per given length	General element size	Number of elements along tooth height	Number of elements along fillet	Loaded Tooth Side [psi]	%
2, 10	0.0130	30	1	10506	-20.3%
2, 15	0.0113	45	2	12763	-3.1%
2, 20	0.0097	60	2	14311	8.6%

D.4.4. Results and Discussion

From the model description and construction, the pinion and gear are rotated through a complete cycle of tooth pair interaction. Shown in figure 39 is the stress at the root of the tooth due to bending [ksi] against the rotation of the pinion [inch]. Figure 38

shows the stress contour. As discussed previously, the stress method used is Von Mises stress, with no averaging within the elements (Van der Zijp, 2009, ABAQUS program). Since the ratio of gear to pinion is 2:1, the corresponding gear rotation of the gear is half that of the pinion, but in the opposite direction.

As shown in figure 39, the maximum stress of the pinion and gear due to bending of the applied load at the base of the tooth is 19 ksi and 12 ksi respectively. According to the corresponding dynamic model performed in DANST, the stress for the pinion and gear is 19 ksi each. The finite element model provides a good comparison for the pinion stress, but the difference of the gear stress is approximately 37%.

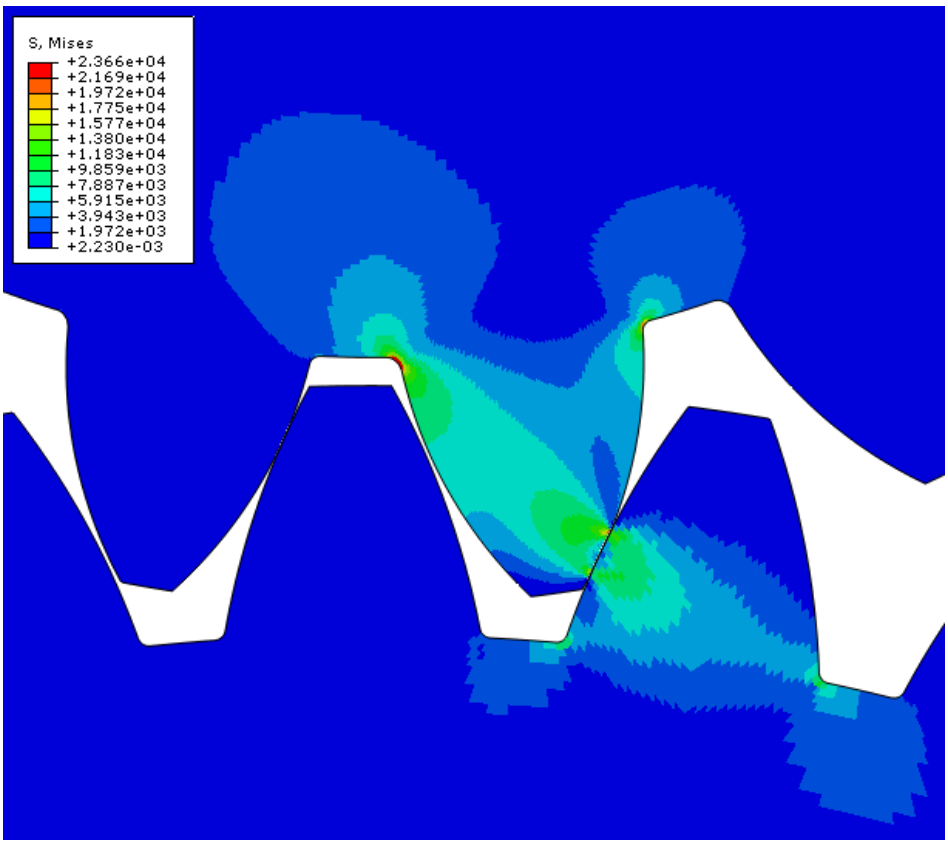

Figure 38. Stress contour map (Van der Zijp, 2009, ABAQUS program).

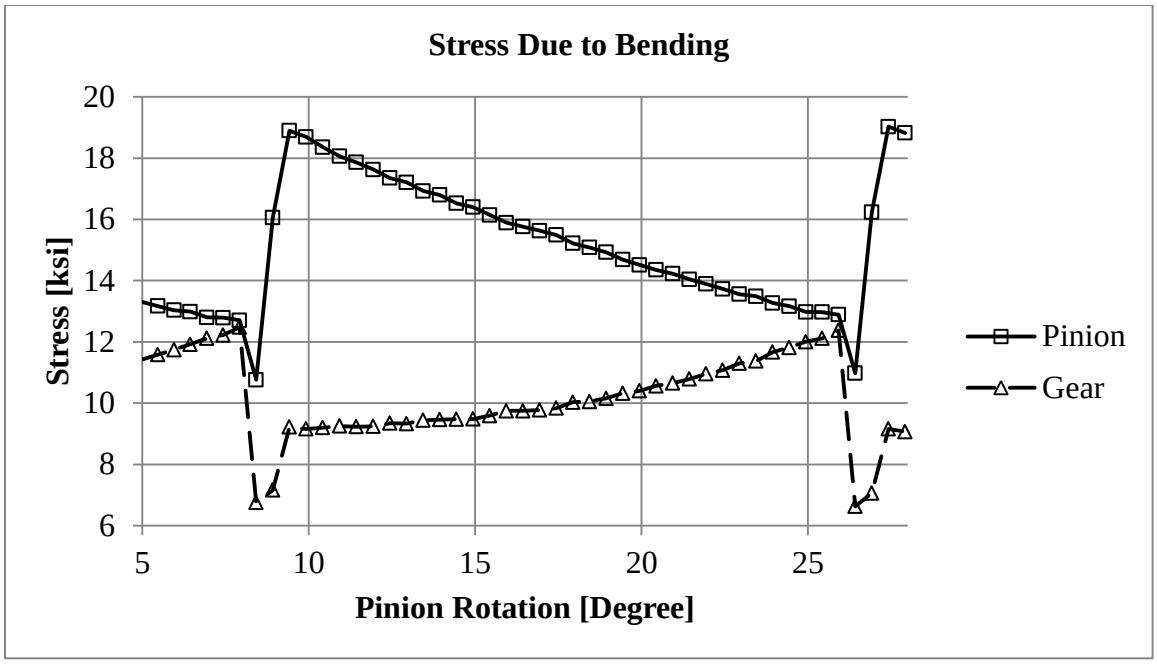

Figure 39. Stress [ksi] against pinion rotation [degree] of pinion and gear.

Several factors may be contributing to these errors: dimensional simplification, the contact between the teeth, and mesh stiffness. Several dimensions were assumed during the creation of the model. The fillet radius, as explained in the previous section, is approximated by using the radius at the bottom of the fillet according to equation 66. However, equation 66 can take into account any change in radius along the fillet. Moreover, as shown by Colbourne (1987, pp. 239-240) and equation 117 (Cornell, 1981; Heywood; Lin & Liou, 1998), the fillet radius can change over the course of the fillet. Since the radius of curvature directly influences stress concentration, the assumption made may not be adequate. Second, the involute was assumed to be a continuous arc from the outer radius, R_{0g}', to the dedendum radius, R_{dg}', excluding the fillet which is added subsequently. This assumption may be an oversimplification.

As explained and derived in chapter 2, the stiffness of the system is related to the deflection and deformation globally and locally. The deformation is affected if the system is not adequately modeled at the contact regions, in transferring the load from the teeth to the gear body, or in the gear body due to the related constraints. Moreover, contact is nonlinear, which may require a more complex model than the one in this study. Changes in deformation due to stiffness may permit or prevent tooth contact to early or late during the mesh cycle. Also, assuming that the system can be defined as linear elastic may not be adequate.

Several items pertain to contact within the ABAQUS program, involving friction, damping, and sliding, all of which have been omitted for simplicity in the finite element model. Moreover, to create a stable model, a marginally small piece of each instance must overlap, since the model is load controlled. The resulting contact is either one or a pair of point loads, and concentrated loads can create model instability (Van der Zijp, 2009, ABAQUS program).